Cdc73 Protects Notch-Induced Leukemia Cells From DNA Damage and Mitochondrial Stress

by

Ashley F. Melnick

A dissertation submitted in partial fulfillment
of the requirements for the degree of
Doctor of Philosophy
(Cellular and Molecular Biology)
in the University of Michigan
2023

Doctoral Committee:

Associate Professor Mark Y. Chiang, Chair
Associate Professor Alan Boyle
Associate Professor Qing Li
Associate Professor Andrew Muntean
Assistant Professor Russell Ryan

Ashley F. Melnick

amelnic@umich.edu

ORCID iD: 0000-0001-5880-3072

Dedication

I dedicate this thesis to myself, my supportive husband Austin, my compassionate sister Jenna, my encouraging parents Joy and Charles, my loyal friends, my incredible lab mates, my inspirational mentors at Michigan State University, and my encouraging Ph.D. mentor, Mark Chiang. I could not have completed this Ph.D. without the endless love and support you all provided me with. I hope someday I can payback the support you all have given me, in the same ways you have supported me. I will always hold you all close to my heart.

Acknowledgements

Reflecting on the last 5 years of my Ph.D. has made me realize how much I have valued the different communities I have been a part of throughout my educational journey. Each community has supported me in diverse ways to help me get where I am today, completing a PhD in cellular and molecular biology. Most people outside of academia will look at a Ph.D. degree and only think of the value and praise of the education and degree, respectively. Here, I would like to highlight that a Ph.D. is way more than just a degree… it is a metaphor for how it takes the blends of entire communities to advance the field of science, both within academia and outside. In this acknowledgement, I would like to highlight those both within my immediate scientific community and many external, who helped me achieve this degree and monumental milestone in my life.

First, I would like to thank my mentor, Dr. Mark Chiang. When I first met Mark, it was at the PIBS match-a-thon event in 2018. I often wonder how I got matched with Mark, as cancer research was not on my radar, and I certainly did not indicate cancer biology on my interest form. However, I consider being matched with Mark one of the greatest miracles that happened to me that year. Out of the 10 or more PI's that I met with that day, Mark was the only one who could communicate his research calmly and clearly over the persistent buzzing of 100 other people. I ended up accepting a half rotation in his lab and quickly felt like I had found my home. I cannot express how much it means to have a mentor who adapts their teaching style to best support their students. While I came in with no T-cell knowledge, I have always recognized and

appreciated Mark's patience with me from the beginning, as I navigated a brand-new field, new ways to analyze data, new experiments, and a new lab environment.

Next, I would like to recognize all my lab mates, past and present, of the Chiang lab. My first lab manager, Amparo, immediately took me under her wing when I joined the lab and onboarded me on everything mouse related in a crash session for 3 months before she left. I cannot say enough positive sentiments about Anna—she is the smartest and kindest person I have ever met. Anna was a senior MSTP student in the lab at the time I started. Always knowing the answer to both my large scientific questions and small, Anna taught me everything I needed to know in the lab about T-cell development, ChIP, leukemia, and toxicities of current treatments. She graciously continued to answer my technical ChIP questions long after she graduated without hesitation. Alice, until this day, continues to be the most helpful and giving person I have ever worked with. Her willingness to constantly assist and answer questions daily is unmatched by anyone I know. I will miss my daily chit-chats with Alice about life and non-lab related news as my desk neighbor. I would like the extend a huge thank you to past Chiang lab members Cher, Ambre, Jahnavi, Geethika, Nicole, and Bella for your help and friendship over the years. I would like to thank my current lab members Karena, Carea, Elizabeth and Zeel for your generous support and making the lab a fun place to be every day. I would like to extend an extra special shout out to Shannon, the exceptionally talented undergraduate student who worked under my supervision for almost the entirety of my PhD and contributed a ton of time and work towards my project. I want to thank Shannon for allowing me to be a mentor to her over the years. Since she started in the lab as a freshman, she has encouraged me to be a more patient teacher and think more deeply about the research and experiments I was doing. I cannot wait to see her succeed in her own Ph.D. someday.

Experimentally, I would like to thank Anna for her contributions to the ChIP-seq experiments, Nick for his help with bioinformatic analysis related to Anna's data, Elizabeth for help with bioinformatic analysis and figure making for my ChIP-seq, Bru-seq, and Bru-UV-seq data, Brian for help with Bru-seq and Bru-UV seq data analysis, and Michelle for help with executing the Bru experiments. Thank you to Nicole for help with human cell line and PDX work, Alice for help with all mouse harvests and data analysis, Shannon for help with inhibitor assays and Ets1 work, Carea and Karena for help with mouse maintenance and harvests, Geethika for help with figure making, Andrea for teaching me metaphase assays, and Surinder for teaching me how to perform a seahorse assay.

I would like to thank my dissertation committee: Dr. Alan Boyle, Dr. Qing Li, Dr. Andy Muntean, and Dr. Russell Ryan. Their comments and questions at committee meetings helped keep my project moving forward in the right direction and has encouraged me to learn many new assays and techniques that can be applied outside the scope of T-cell research. I would also like to thank them for help when it came to grants, abstracts, and conferences. I truly appreciate the endless support they have given me.

There have been many labs outside of my own that have helped me tremendously, from teaching me entire protocols, to lending me last minute reagents, and letting me borrow equipment. Thank you to the Dr. Russell Ryan lab, particularly Rohan, Alec, and Athalee who have always been essential to my ChIP-seq endeavors and finding lo-bind plasticware. Thank you to the Dr. Qing Li lab, particularly Morgan and Koral who have helped me with many flow-based assays and troubleshooting when the Fortessa went down. I'd also like to thank Dr. Surinder Kumar and Dr. David Lombard for teaching me how to preform and optimize a Seahorse assay, Dr. Andy Muntean's lab for help with Cdc73 and Paf1c related questions, Dr.

Mats Ljungman's lab, particularly Brain Magnuson and Michelle Paulson, for help with the Bru and Bru-seq experiments and Dr. Shannon Carty's lab, particularly Luis who always helped me troubleshoot my metabolic assays. I also wanted to thank external collaborators including Dr. Andrew Weng for the PDX's and T-ALL cell lines, the University of Michigan flow cytometry core for training me and allowing me to use equipment, and the University of Michigan advanced genomics core for helping me process my sequencing samples.

Next, I would like to thank the Molecular and Integrative Physiology program, for which I was a part of for my initial year at Michigan before I transferred to the Cellular and Molecular Biology (CMB) Program, and the CMB program for their support over the years, specifically Dr. Dan Michael, Dr. Roberta Fuller, Dr. Manoj Puthenveedu, Dr. Ben Allen, Lauren Perl, and Carolyn Walsh. In addition, I would like to thank the PIBS program at University of Michigan and the OGPS for providing many professional development opportunities. I would also like to thank my previous mentors during my master's degree at Michigan State University including Dr. Chen Chen, Dr. Steven Bursian, Barb Sweeney, and Janet Ireland. My MSU mentors have kept in touch with me throughout my PhD and had always encouraged me to take the next step in my educational journey.

I would like to take a minute to acknowledge the various funding sources that helped me complete this research including PIBS, the CMB T-32 grant, Rackham for pre- and post-candidate research grants and travel funding, the NCI Ruth L. Kirschstein F31 for funding me for three years, the American Society of Hematology, Alex's Lemonade Stand, and The Rally Foundation.

Last but certainly not least, I would like to thank my family and friends for which I truly could not have gotten through my PhD without. I want to thank my entire family including my

sister Jenna, my parents Joy and Charles, and my in-laws Kathie, Alan, Lauren, Garrett, and Grandma Schuld, for always supporting my academic endeavors despite not always understanding exactly what I do. I would like to give a special thanks to the friends I have made through Rackham Student Government including Olivia and Claire. They are some of the hardest working ladies I have ever met and made my personal time outside of my PhD research something I continue to look forward to. I am incredibly grateful to have met one of my first and closest friends at the University of Michigan, Johanna. She was always the first to hear about my successes and struggles in my PhD and in life and has been essential to both my happiness and laughter, and my healing and moving forward in my PhD journey. I truly believe I was placed at the University of Michigan to have met her. I will continue to cherish this friendship for the rest of my life.

Finally, I would like to thank my incredible, loving, supportive husband, Austin, who has been my rock throughout my entire academic experience. He has always been my biggest cheerleader and was, even when I got into the University of Michigan, despite being a die-hard Michigan State alumnus. I am so grateful to share a life with someone like him, who gives his love and support so selflessly, and encourages me every day to be the best version of myself. Him and our loving dog Leo have been both my emotional support resources and my biggest fans, supporting me though the good times and the bad. They always knew how to put a smile on my face at the end of each day. I seriously could not have done it without them.

Table of Contents

List of Tables

List of Figures

Abstract

Activated Notch signaling is highly prevalent in T-cell acute lymphoblastic leukemia (T-ALL) and accounts for about 60% of mutations in this disease. Since Notch has essential functions in normal tissue homeostasis, pan-Notch inhibitors used in clinical trials exhibited toxic effects to the patients receiving them. To find alternative ways to target Notch signals, we investigated Cell division cycle 73 (Cdc73), which is a Notch cofactor and component of the RNA polymerase-associated factor complex (Paf1c) transcriptional machinery. Transcriptional control is believed to be an attractive target in advancing T-ALL therapies. In this setting, we confirmed previous work done in a breast cancer cell line, showing that CDC73 interacts with NOTCH1 in T-ALL cell lines. However, we found that this interaction in T-ALL was context-dependent and is facilitated by the transcription factor ETS1. Using mouse models, we found that Cdc73 is important for Notch-induced T-cell development and T-ALL maintenance. Mechanistically, we identified that Cdc73, Ets1, and Notch intersect with chromatin at promoters and enhancers to activate gene expression programs that promote DNA repair and oxidative phosphorylation in the context of T-ALL. Consistently, deletion of *Cdc73* induced DNA damage and impaired mitochondrial function. My project shows that Cdc73 induces these pathways through its canonical functions in regulating mRNA synthesis but can also activate oncogenes non-canonically through regulation of enhancers. This study suggests that *Cdc73* might promote context-dependent gene expression programs that was eventually intersected by Notch to mitigate the genotoxic and metabolic stresses of supraphysiological Notch signaling. We also

provide mechanistic support for testing inhibitors of DNA repair, oxidative phosphorylation, and transcriptional machinery as an alternative anti-leukemic therapy. In theory, inhibiting Cdc73 regulated pathways that intersect with Notch at chromatin might constitute a safer strategy to weaken Notch signals without directly targeting the entire Notch complex.

Chapter 1 Introduction

1.1 T-ALL Subgroups and Biomarkers

T-ALL can be broken up into A-type and B-type abnormalities (Van Vlierberghe et al.). Type-A abnormalities cause the up-regulation of oncogenes that code for transcription factors important for T-cell development, maturation, differentiation, and hematopoiesis. 70% of T-ALL cases can be accounted for by Type-A abnormalities, characterized by the classified subgroups *TAL/LMO, HOXA, TLX3, TLX1*, *NKX2-1/2-2, and MEF2C* (Homminga et al. ; La Starza et al. ; Liu et al. ; Soulier et al. ; Ferrando et al. 2002). Type-B abnormalities include genes that encode for different proteins including epigenetic factors, ribosomal proteins, tyrosine kinases and proteins involved in signaling pathways (Bardelli et al.). Below I will go into detail about each subtype and the biomarkers currently associated with their corresponding diagnosis.

1.1.1 TAL/LMO subtype

Overexpression of the *TAL1* genes characterizes 30-45% of pediatric T-ALL cases and 10-15% of adult T-ALL cases, caused by the activation of transcription factors *TAL1/TAL2* and/or the LIM-only domain family members *LMO1/LMO2/LMO3* where their proteins are commonly co-deregulated (La Starza et al. ; Mansour et al. ; Rahman et al. ; Ferrando et al. 2002). Additionally, leukemogenic activity by *TAL and LMO* lead to the altered expression of downstream targets such as *MYB, GATA3*, and *RUNX1 (Sanda et al.)*. The immunopheotype of this T-ALL subtype generally leads to arrest in mature T-cell development as represented by CD8 biomarkers and relatively low incidences of *NOTCH1* mutations (~40%), but is commonly associated with *PTEN*

inactivation (19%) and *MYC* translocations (10%) (La Starza et al. ; La Starza et al. ; Milani et al.). While this T-ALL subtype is not outlined in this dissertation, we have projects ongoing in our lab utilizing *LMO2* transgenic mice to understand how *Cdc73* plays a role in regulating *LMO2* driven T-ALLs.

1.1.2 HOXA, MEF2C and BCL11b subtype

HOXA, MEF2C, and *BCL11b* are genes associated with early T-cell precursor- (ETP) ALL and immature T-ALL. All ETP-ALL cases are characterized by at least one stem cell or myeloid marker such as CD34 or CD117 and CD13, CD33, HLA-DR, CD11b, or CD65, respectively. All ETP cases also express low levels of CD5 and no expression of CD4/CD8 (Coustan-Smith et al.). *BCL2* is an anti-apoptotic protein that ETP-ALL subtypes rely on (Ferrando et al. 2002). Inhibitors of *BCL2*, such as venetoclax, are being tested in clinical trials and have been shown to be a putative target in immature T-ALL but not mature T-ALL due to its anti-leukemic activity and synergistic effects when combined with chemotherapy or steroids (Peirs et al.). ETP-ALL cases tend to exhibit heterogeneous genomic profiles, with mutations in genes important for RAS signaling, hematopoietic development, and histone modifications. About half of the ETP-ALL cases fall into the *HOXA, MEF2C,* and *BCL11b* oncogenic subtypes and the rest are unknown. Conversely, less than half *HOXA* subtypes fall into the ETP-ALL category (Bardelli et al.). Since this project was mainly focused on Notch-induced T-ALL, our studies in this dissertation do not investigate Cdc73 in the context of ETP-ALL.

1.1.3 TLX1, NKX2-1, and TLX3 subtype

The *TLX1, NKX2-1,* and *TLX3* subtype can be characterized by the expression of *CD1a*, DN3-DP T-cell development arrest and overexpression of *TLX1 or NKX2.1* (Ferrando et al.

2002). Additionally, this subtype has a high prevalence of mutations in *NOTCH1* (96.2% and 92.9% respectively) (Liu et al.). In pediatric cases specifically, mutations in *NKX2.1* often have associated deletions of the gene *LEF1*, a DNA binding transcription factor that functions in the WNT signaling pathway (La Starza et al. ; Liu et al.).

In summary, T-ALL treatments should be approached with the subgroups in mind. With Notch being highly expressed in a large subset of groups with high indices of mutations in T-ALL patients (60%), our studies focused exclusively on Notch-induced T-ALL. It is possible that some treatments and methods of targeting oncogenic Notch could be expanded into other subsets, however, for the purpose of this dissertation, we only use models where Notch is induced to drive T-ALL.

1.2 Notch pathway activation in T-ALL

Activation of the Notch signaling pathway is highly conserved in mammalian cells where it plays essential roles in the development and homeostasis of diverse tissues, including multiple stages of T-cell fate specification and development (Artavanis-Tsakonas et al. ; Siebel and Lendahl 2017). Notch1 is one of four total paralogues of the Notch receptor and is activated via ligands or by mutations. Under normal physiological conditions, the extracellular domain of the Notch receptor interacts with its ligand (JAGGED, DLL) on an adjacent cell, triggering gamma-secretase catalyzed cleavage events. Subsequently, gamma secretase cleaves Notch, releasing intracellular Notch (ICN) and allowing it to translocate to the nucleus where it engages DNA-binding factor RBPJ and MAML. This binding event drives the transcription of several Notch target genes**,** activating a transcriptional program that promotes cellular growth, development, and homeostasis (Kopan 2012).

1.2.1 Notch1 mutations in T-ALL

~60% of T-cell acute lymphoblastic leukemia (T-ALL) cases have activating *NOTCH1* mutations, making *NOTCH1* the most prevalent oncogene in this cancer (Weng et al. 2004). In early T-cell precursor- (ETP) ALL, however, *NOTCH1* mutations occur less frequently than in conventional T-ALL, with Notch mutations occurring 11-36% of the time in ETP-ALL versus 50-62% in conventional T-ALL (Coustan-Smith et al.).

Gain of function *NOTCH1* mutations can be broken up into two types, ligand-independent and ligand-dependent activation. In T-ALL, ligand-independent cleavage is triggered by mutations in the negative regulatory region (NRR) and juxtamembrane extracellular region (JME). NOTCH1 can have mutations caused by single amino acid substitutions or in-frame insertions (Gordon et al. ; Gordon et al. ; Sanchez-Irizarry et al.). Mutation inducing, ligand-independent changes expose the S2 cleavage site which leads to the transcriptionally active form of Notch1, intracellular Notch1 (ICN1).

Ligand-dependent activation is caused by the cleavage of NOTCH1/2 in mature lymphoid neoplasms. These mutations are caused by nonsense mutations or short insertions or deletions that are dispersed throughout the c-terminal PEST domain, leading to premature STOP codons (McCarter et al. 2018). These mutations lead to the removal of degron sites, typically phosphorylated by serine or threonine kinases that get recognized by E3 ubiquitin ligases and eventually targeted for degradation (Chiang et al. ; Fryer et al. ; Li et al. ; Thompson et al.). With these mutations, ICN1 half-life is extended (McCarter et al. 2018). Mutations in *FBXW7* have also been shown to lead to alterations in *NOTCH1* by coding for a ubiquitin protein responsible for the degradation of *NOTCH1* (O'Neil et al. ; Thompson et al.).

NOTCH1 mutations can also arise as initiating events as early as prenatally or as late stage events during disease progression or relapse (Eguchi-Ishimae et al.). Therefore, it is

important to continue developing treatments for *NOTCH1* activated T-ALL, though the challenge still lies in the ability to specifically target only oncogenic Notch signals without targeting the essential function of Notch in normal tissue homeostasis.

1.2.2 Abnormal Notch Signaling

Abnormal Notch activation in T-ALL was first discovered as a chromosomal translocation t(7;9)(q34;q34.3), putting the Notch1 gene adjacent to the T-cell receptor locus (McCarter et al. 2018). Later on, another chromosomal translocation t(9;14)(q34;q11) was discovered, though more rare than the original translocation (Suzuki S Fau - Nagel et al.). Both translocations lead to a constitutively active Notch1 phonotype (Ellisen et al.). Later on, many other studies confirmed this acquired, recurrent, gain-of-function mutation of Notch1 in human pediatric T-ALLs and extended them to adult T-ALLs ((Weng et al. 2004; Asnafi et al. 2009; Mansour et al. 2009; Clappier et al. 2010; Kox et al. 2010; Jenkinson et al. 2013; Trinquand et al. 2013). Other gain of function NOTCH mutations were later identified in other types of mature lymphoid neoplasms arising from mature B-cells and T-cells circulating in the lymph nodes, spleens and other organs involved in adaptive immunity (McCarter et al. 2018).

1.2.3 Notch inhibitors

The frequent dysregulation of NOTCH1 in cancer patients inspired the clinical testing of pan-Notch inhibitors such as gamma-secretase inhibitors (GSI). However, these early clinical trials reported serious toxicities with continuous dosing of GSI, such as diarrhea and skin cancers, because GSIs inhibit Notch activation in both normal and cancer cells. This is important because Notch signaling is crucial for normal tissue homeostasis and tumor suppression (Krop et al. 2012; Tolcher et al. 2012). Notch functions in a context dependent manner and pan-Notch

inhibition may lead to undesirable consequences. Therefore, identifying transcription factors that interact with oncogenic Notch signaling is important to potentially mitigate these toxicities associated with global Notch inhibition.

In summary, Notch signaling plays a prominent role in T-ALL and in normal tissue homeostasis. Targeting Notch via global inhibition as a treatment for T-ALL has shown to have undesirable side effects in the patients receiving these treatments. Therefore, work by our lab and others have focused on how to target only oncogenic Notch signals, by researching co-factors that intersect with Notch.

1.3 Other pathways activated in T-ALL and targeted inhibition

1.3.1 IL7R/JAK/STAT signaling in T-ALL

About 10% of all T-ALL cases are gain-of-function mutations in the interleukin receptor 7 (IL7R), causing the JAK/STAT pathway to be constitutively active (Zenatti et al.). The commitment, proliferation and survival of early T-cell progenitors is reliant on proper IL-7R signaling (Mazzucchelli and Durum). Activation of IL7R causes *JAK1* and *JAK3* phosphorylation, thereby recruiting and activating *STAT5*, a transcriptional regulator, which becomes phosphorylated, homodimerizes, and migrates to the nucleus where it acts as a transcription factor (Mazzucchelli and Durum).

The *JAK/STAT* pathway is thought to be an actionable target in the treatment of T-ALL. *JAK/STAT* inhibitors, such as ruxolitinib, have shown promising results in a murine xenograft model of ETP-ALL (Maude et al.). Further, combining ruxolitinib with dexamethasone overcame IL7-induced glucocorticoid resistance in human T-ALL samples (Delgado-Martin et al.). *PIM1* is a downstream target of the *JAK/STAT* pathway that has also become an actionable target in T-ALL treatment, with both *in vitro* and *in vivo* studies demonstrating that pan-*PIM*

inhibitors combined with glucocorticoids or chemotherapy is a beneficial treatment for this T-ALL (De Smedt et al. ; Padi et al.).

IL-7R, which is upstream of STAT5 in the *JAK/STAT* pathway (Spits ; Ribeiro et al. 2018), is also being studied an actionable target in the treatment of T-ALL. In a recent study, researchers showed that one third of primary T-ALLs cultured in the presence of IL-7R were resistant to glucocorticoids (GCs) (Meyer et al. 2020). Resistance to (GCs) is a strong indicator of a negative prognosis in T-ALL patients (Gao and Liu 2018). The study concluded that IL-7R can mediate the intrinsic and physiologic response of GC resistance in normal T-cell development that is retained in T-ALL progression (Meyer et al. 2020). Importantly, they show that using targeted inhibitors of the IL-7R, *JAK/STAT*, and *STAT5* pathway, they can reverse this GC resistance (Meyer et al. 2020).

1.3.2 ABL1/Src-family kinases

6% of pediatric T-ALL cases have constitutive activation of *ABL1 (Liu et al.).* T-ALLs with mutations in *ABL1* are sensitive to tyrosine kinase inhibition, such as with the drugs imatinib and dasatinib (Moorman et al.). *LCK*, a protein of the SRC family, has been associated with the functional consequences of *ABL* activation and is required for the proliferation of cells (De Keersmaecker et al.). Dependency on *LCK* also extends into pediatric ETP-ALL patients (Serafin et al.).

1.3.3 PI3K/AKT signaling

Deletions and/or loss of function mutations in *PTEN* are linked to resistance in *NOTCH1* inhibition in T-ALL cell lines (Palomero et al.). Inactivating mutations of *PTEN* are seen in about 10-15% of cases and commonly linked to abnormalities in the *TAL/LMO2* subgroup about 20% of

the time (La Starza et al.). Glucocorticoid resistance is linked to any alteration of *PI3K/AKT* signaling, however *PI3K/AKT* inhibitors and steroids have shown a synergistic cytotoxic effect, suggesting that T-ALLs with genetic mutations in *PI3K/AKT* can benefit from targeted therapies (Follini et al. ; Silveira et al.).

Targeting the *P16/INK4A or PI3K* pathway is a potential T-ALL treatment option that works by targeting the cell cycle to prevent dysregulated cell cycle progression. This can be done by targeting the gene *P16/INK4A*, a tumor suppressor gene that acts as a negative regulator of cyclin-CDK complexes (Belver and Ferrando 2016). Another option is targeting the *P13K* pathway by restoring the tumor suppressor *PTEN*. Constitutive activation of the *PI3K* pathway happens when *PTEN* is lost, which drives cellular proliferation, growth, metabolism, and overall survival in the T-ALL pathway (Palomero et al.). Blocking the *PI3K* pathway pharmacologically by inhibition of *PI3K gamma* and *PI3K delta* have promising antileukemic effects in preclinical models (Subramaniam et al. 2012).

1.3.4 mTOR signaling

Targeting the mTOR pathway is another approach towards selective oncogenic Notch inhibition in T-ALL. This pathway is a key cellular network that connects cell growth and survival pathways with energy sensing and nutrient availability (Szwed et al. 2021). In T-ALL, elevated expression of the gene *MTOR* is correlated with failure of patient response to induction chemotherapy (Khanna et al. 2018). Additionally, primary cells from T-ALL patients frequently exhibit increased levels of reactive oxidative species (ROS), and leukemic T-cells are vulnerable to further increasing this ROS production (Silic-Benussi et al. 2009; Silic-Benussi et al. 2010; Silva et al. 2011).

mTORC1 and mTORC2 are two protein complexes that regulate different downstream pathways and possess unique sensitivities to inhibitors (Szwed et al. 2021). Preclinical trials that inhibited the mTOR pathway in T-ALL cells showed promising results, where T-ALL cells with inhibited mTOR underwent apoptosis, paving the way for clinical trials (Evangelisti et al. 2018). A more recent study published in 2022 looked at the mechanistic links between mTOR and ROS homeostasis in glucocorticoid (GC)-resistant T-ALL. They found that in response to mTOR inhibition, GC-resistant T-ALL cells possessed increased levels of ROS production, decreased NADPH levels, and reduced levels of gluco-6-phosphate which is a product of the Pentose Phosphate Pathway (PPP). This ultimately led to the death of T-ALL cells (Silic-Benussi et al. 2022). Together, these studies suggest an alternative way to selectively target drivers of T-ALL via the mTOR pathway.

1.3.5 RAS/MAPK signaling

40% of relapsed T-ALL cases can be attributed to *RAS/MAPK* activation (Liu et al.). Activation of this pathway in T-ALL can be due to common mutations in *KRAS/NRAS* or *BRAF*, gain of function mutations occurring upstream of *FLT3*, or aberrations in negative regulators including *PTPN11* and *NF1* (Balgobind et al. ; De Smedt et al.). *MEK1/2* inhibitors such as selumetinib and trametinib have proven to be a safe alternative in phase 2 ALL clinical trials (Irving et al. ; Lonetti et al. ; Oshima et al.). ETP-ALL and *HOXA* subgroups tend to exhibit strong enrichment in *RAS/MAPK* activation, however activation has also been seen with *TLX1*, *TLX3*, *NKX2.1*, and *NKX2.2* and to a much lesser extent, the *TAL/LMO* subgroup (Liu et al.).

In summary, there are multiple pathways that are activated in Notch-induced T-ALL. Some of these pathways might be good places to research further to understand how we might be

able to only inhibit oncogenic Notch signals. In this dissertation, we have identified some potential targets that fall under regulation of these major pathways.

1.4 T-ALL diagnostic methods

1.4.1 Gene expression as a method of T-ALL diagnosis

There has been an increase in using targeted sequencing diagnostic measures to approach treating T-ALL and ALL in general (Wu and Li 2018). These methods include exome sequencing, transcriptome analysis, and whole genome sequencing (WGS). Exome sequencing is a popular and cost-effective way to identify sequence mutations and genetic mutations in ALL by capturing and sequencing coding exons, promoter domains, and non-coding domains in the genome (De Keersmaecker et al. 2013). However, this method is not able to identify deletions, insertions, and structural rearrangements (Zhang et al. 2012). Transcriptome analysis identifies protein-coding transcripts and small non-coding transcript changes in enhancer regions that generally play a large role in the development of leukemia (Trimarchi et al. 2014). Whole exome sequencing, commonly referred to as exome sequencing, can identify high frequency variants and compares them to a non-tumor genome to identify somatic variants (Huether et al. 2014; Mühlbacher et al. 2014). While this method tends to be the most precise and widely accepted diagnostic technique, it fails to identify promoter regions, GC-rich regions, and complex genomic sequences (Wu and Li 2018). In this dissertation, while I do not usre sequencing to determine T-ALL diagnosis directly, I use RNA-seq to understand changes in transcription and how that can effect the regulation of specific genes that might drive the T-ALL phenotype.

1.5 T-ALL treatments in adults and pediatrics

1.5.1 Targeting NOTCH1 as a treatment for T-ALL

While once classified as a highly aggressive subtype of acute lymphoblastic leukemia (ALL), children and adults diagnosed with T-ALL now have greatly improved outcomes due to new therapies and treatment regimens (Bassan et al.). While *NOTCH1* cannot be used as a prognostic biomarker, targeting the *NOTCH1* pathway is a common and agreed upon target in T-ALL therapies. This includes the use of gamma-secretase and ADAM (Disintegrin Metalloproteases) inhibitors, monoclonal antibodies, and small molecules that block the activity of NOTCH transcription factors (Zheng et al.). More recently, targeting *SKP2*, an E3 ubiquitin ligase regulated by *NOTCH1*, was shown to prevent T-ALL proliferation in both *in vitro* and *in vivo* models (Rodriguez et al.). While not tested in human trials just yet, sarco-endoplasmic reticulum Ca2+-ATPase (SERCA) inhibitors have been tested *in vitro* and in PDX models to successfully suppress oncogenic *NOTCH1* signaling (Marchesini et al.).

1.5.2 GSIs alone are insufficient to treat Notch-induced T-ALL

GSIs alone have been used in clinical trials to treat T-ALL but are not the safest to use due to gastrointestinal toxicities (Paganin and Ferrando ; Wei et al.). Attempts to decrease intestinal toxicity have been in the works in pre-clinical trials including using a combination of GSIs and glucocorticoids or withaferin A, rapamycin, and vorinostat in combination with GSIs (Paganin and Ferrando ; Samon et al. ; Sanchez-Martin et al.). Together this suggests that using GSIs alone are insufficient in treating Notch-induced T-ALL, however in combination with other drugs, might be an effective alternative option.

1.5.3 Transcriptional inhibition of P300

It has been well established in the literature that P300 acts as a transcriptional co-activator of Notch (Oswald et al. 2001; Wallberg et al. 2002). In a more recently published

paper, the authors found that binding of intracellular Notch3 and activated Notch1to the *NOTCH3* gene locus increased recruitment of H3K27ac modifiers JMJD3 and P300 (Tottone et al. 2019). This binding sustained *NOTCH3* expression. When JMJD4 and P300 were inhibited using specific inhibitors, its decreased expression of *NOTCH3*, *NOTCH1*, and related Notch-target genes such as *DELTEX1* and *MYC* (Tottone et al. 2019*)*. This inhibition also interfered with cell viability in both Notch1 and Notch3 dependent T-cells. This suggests that targeting P300 might be an effective way to suppress supraphysiological Notch signaling.

1.5.4 Transcriptional inhibition of BRD4

Bromodomain-containing protein 4 (BRD4) is a BET family protein, important for the binding of acetylated lysine residues to histone H3. It provides a platform for the assembly of super-enhancer complexes important for driving transcriptional regulation and expression of specific oncogenes, such as Myc, and anti-apoptotic proteins, such as Bcl-2 (Zuber et al. 2011; Lovén et al. 2013; Filippakopoulos and Knapp 2014). *BRD4* is important for regulation of targets downstream of *NOTCH1* and was recently shown to regulate the expression of *CD44*. Using a proteolysis targeting chimera (PROTAC) ARV-825, the researchers were able to degrade BRD4, showing that you can dismantle the NOTCH1-MYC-CD44 complex (Piya et al. 2022). Degrading BRD4 prolonged the survival of mice using both a *NOTCH1* mutated PDX model and a genetic ΔPTEN mouse model. Additionally, their proteomic analysis revealed that degrading BRD4 in their PDX model also reduced the number of leukemia initiating cells (LICs), downregulated the NOTCH1-MYC-CD44 axis, and the cell cycle, apoptosis, and PI3K/Akt pathways. In their secondary transplant PDX model, they saw delayed development of leukemia and extended mouse survival in mice that were treated with the BRD4 degrader (Piya et al.

2022). This makes BRD4 a promising target to continue studying for the treatment of Notch-induced T-ALL.

1.5.5 Transcriptional inhibition of the RNA Pol II complex

CDK9 is an important regulator of RNA Pol II directed transcription. It works by phosphorylating the C-terminal domain of the largest RNA Pol II subunit. It also can bind super-enhancers by forming complexes with BRD4, mentioned previously (Ott et al. 2012). Inhibitors of CDK9, such as NVP-2, LDC067, and BAY1143752, have already proven successful in the treatment of AML (Albert et al. 2014; Narita et al. 2017; Olson et al. 2018).

Alvocidib is another CDK9 inhibitor that possesses anti-tumor activity by inhibiting RNA Pol II phosphorylation and suppressing super-enhancer mediated gene expression specific to tumors. A recent study showed that Alvocidib successfully inhibited the proliferation of adult t-cell leukemia/lymphoma (ATL) cells lines and tumor cells derived from patients with ATL. Additionally, they identified *IRF4*, an important transcription factor in T-cells, was being regulated by a super-enhancer (Sakamoto et al. 2022). This supports data from others that has suggested *IRF4* plays an important role in ATL progression and survival (Nakagawa et al. 2018; Rauch et al. 2020). This study concluded that Alvocidib is a reliable target to continue studying in the treatment of ATL, that effectively suppressed ATL in a mouse xenograft model.

CDK7 inhibitors have also been used as anticancer drugs and is essential the cell cycle. When CDK7-mediated phosphorylation of RNA polymerase II (Pol II) happens at active promoters, it allows transcription to occur (Sava et al. 2020). CDK7 has been shown to exhibit high levels of expression in many cancers, including T-ALL, suggesting a higher dependence on CDK7 than other normal cell types. Due to this, CDK7 was identified as a therapeutic target for treatment of this disease. Like CDK9 inhibitors, CDK7 inhibitors in phase II clinical trials

include Alvocidib, Seliciclib, and in phase I clinical trials, SNS-032 (Sava et al. 2020). In T-ALL specifically, THZ1, a covalent CDK7 inhibitor, is being tested in non-clinical settings (Kwiatkowski et al. 2014).

1.5.6 Pharmacogenetics in T-ALL treatments

Pharmacogenetics has been an increasingly popular method of treating T-ALL and ALL in general. While the initial approach is to still use non-genetic methods, pharmacogenetics allows for a better understanding of the genetic inconsistencies across patients, leading to improved efficacy of drug treatments slowing down the progression of the disease (Cheok et al. ; Relling and Ramsey 2013). For example, in a case study looking at ALL, the group was able to identify common germline genetic polymorphisms and associate them with increased odds of ALL relapses. *GSTM1* deletion was one gene they identified with high risk of relapse (Rocha et al. 2005). By combining genetics, transcriptomics, metabolomics, proteomics, bioinformatics, and clinical data, we can start to better understand how certain pathways and genes work in the context of T-ALL to provide better treatments and care to patients.

1.5.7 FDA approved targeted therapies in T-ALL

There are many therapies being tested to treat T-ALL and several that have been FDA approved. To name a few, the first example is a JAK1/2 inhibitor called Ruxolitinib. This drug blocks that JAK/STAT signaling regardless of the presence of mutations (Verstovsek et al. 2010). In the context of T-ALL, it works best in patients who exhibit IL7-responsive T-ALL and ETP-ALL (Maude et al. 2015).

Antibody based therapies are another group of FDA approved therapies for T-ALL treatment. The anti-CD38 monoclonal antibody called daratumumab was approved in 2015 for

multiple myeloma and is being tested as a promising target for T-ALL. CD38 is robustly expressed in T-ALL and ETP-ALL blasts during diagnosis, chemotherapy treatment and at relapse (Bride et al. 2018). In a small clinical test of 2 patients with T-ALL, daratumumab treatment allowed the patients to achieve MRD-negative remission. This drug is also in clinical trial for pediatric and young adult ALL patients with use of standard chemotherapy (NCT03384654).

In summary, there are many treatment options in research and clinical testing phases for both pediatric and adult T-ALL. In this dissertation, the data generated supports further investigation into drugs that might regulate DNA repair and oxidative phosphorylation pathways and their roles in the maintenance of T-ALL.

1.6 The Polymerase Associated Factor complex (Paf1c)

1.6.1 The Paf1c in Yeast and Drosophila

The polymerase-associated factor 1 complex (Paf1C) can be linked to the Notch pathway in early studies using a *Drosophila* model. When ICN translocates to the nucleus, it binds to transcription factors called the "CSL" family which include the transcription factors Suppressor of Hairless (Su(H)) in *Drosophila,* LAG-1 in *C. elegans*, and CBF1 in vertebrates (Christensen et al. ; Fortini and Artavanis-Tsakonas ; Hsieh et al. ; Jarriault et al.). From here, CSL and ICN activate *Notch* target genes including Enhancer of split/HES genes (Artavanis-Tsakonas et al.). Activity of this pathway is highly dependent on other interactions with proteins and post-translational modifications.

Original studies investigating the Notch signaling pathway in the *Drosophila* model and yeast models identified many genes responsible for regulation of the *Notch1* pathway (Justice and Jan ; Panin and Irvine). A different study identified a RING finger protein necessary for the

transcription of *Notch* target genes in a *Drosophila* model called *Bre1*, which is a direct cofactor of the Paf1c. It is also conserved across mammals, *C. elegans*, *Arabidopsis*, and yeast. *Bre1* is responsible for the monoubiquitination of histone H2B and indirectly regulates methylation of histone 3, and lysine 4 and 79 (H3K4/79) (Bray et al. 2005). In *Saccharomyces cerevisiae*, this methylation is catalyzed by a complex of proteins called Set1 (COMPASS) and Dot1p (Shilatifard).

The Paf1c indirectly regulates histone methylation by regulating histone H2B monoubiquitination and interaction of COMPASS with RNA Polymerase II (RNA Pol II) (Krogan et al.). Studies of mutating Bre1 in yeast lead to decreased growth and decreased transcription of inducible genes (Wood et al.). Interestingly, *Drosophila* with mutations in *Bre1*, a direct Paf1C cofactor, displayed a "notched" wing phenotype and impaired transcription of Notch target genes (Bray et al. 2005).

The Paf1c is composed of five subunits, including Cdc73, Paf1, Rtf1, Leo1, and Ctr9. *Rtf1* is required for the ubiquitination of H2B by *Rad6* and the recruitment of COMPASS to elongating RNA Pol II (Krogan et al. ; Shilatifard). *Rtf1* has been shown to colocalize with actively transcribing RNA Pol II in a similar manner to *CDC73* and *Paf1c* (Adelman et al.). Drosophila with mutations in *Rtf1* also (a Paf1C subunit) showed "notched" wings in and impaired transcription of Notch target genes (Tenney et al. 2006).

1.6.2 Canonical functions of the Paf1c

The canonical function of the Paf1c is to act as a scaffold that physically links mRNA transcriptional machinery (e.g. RNA polymerase II or Pol II) to chromatin modifying enzymes, promoting the deposition of histone marks associated with transcriptional activation such as H2BK120ub, H3K4me, H3K79me, and H3K36me, and mRNA synthesis from initiation and

elongation to termination and processing (Jaehning 2010; Van Oss et al. 2017; Francette et al. 2021). The Paf1C is associated with active chromatin at gene bodies or promoters but is not a universal inducer of transcription.

Cdc73 is a scaffold subunit of the Paf1C, promoting mRNA synthesis of ~15-20% of the most highly expressed genes (Penheiter et al. 2005; Yu et al. 2015). Cdc73, or Parafibromin, was first identified as a product of the *HRPT2* (*hyperparathyroidism-jaw tumor type 2*) gene (Carpten et al. 2002a). It is associated with a loss-of-function mutation linked with hyperparathyroidism-jaw tumor syndrome (Carpten et al. 2002a).

1.6.3 Non-canonical functions of the Paf1c

The PAF1C has non-canonical functions at enhancers, regulating eRNA synthesis, H3K27ac deposition, and looping to promoters (Chen et al. 2017; Ding et al. 2021). For example, in colon cancer cells, Chen et al. discovered that PAF1 occupies and restrains the hyperactivation of only a subset of enhancers. Additionally, enhancers that were activated because of PAF1 loss allowed RNA Pol II to be released from its paused state at the promoters of nearby PAF1 target genes. Consequently, knockout of PAF1-regulated enhancers weakened the release of paused RNA Pol II at PAF1 target genes without interfering with pausing at its equivalent promoters. This study showed that some enhancers can modify gene expression by controlling the release of paused Pol II in a PAF1-dependent manner (Chen et al. 2017).

CDC73 was also previously shown to interact with NOTCH1 in breast cancer cells (Kikuchi et al. 2016). This study highlighted the eloquent power Cdc73 has in coordinating signals from a multitude of transcriptional networks, including Wnt, Notch, and hedgehog signaling and emphasized its unique role in regulating only a subset of target genes independent of the PAF

complex (Kikuchi et al. 2016). Nonetheless, the precise link between CDC73 and NOTCH1 and its relevance in Notch-driven cancers remains unclear.

Investigating the role of CDC73 in the context of Notch1 transcriptional machinery is attractive since T-ALL cells are known to be "addicted" to certain components of transcriptional machinery, once considered too toxic to inhibit given its vital functions in normal cell homeostasis (Bradner et al. 2017). In this context, we proposed and experimentally tested the role of CDC73 in Notch-induced T-ALL. Our results show that CDC73 intersects Notch-regulated pathways, particularly in DNA repair and oxidative phosphorylation, and suggest CDC73 as a potential therapeutic target in this cancer.

1.6.4 The Paf1c as a tumor suppressor

Mutations in HRPT2, another name for Cdc73, are also associated with sporadic parathyroid cancers, denoting its other role as a tumor suppressor (Howell et al. 2003; Shattuck et al. 2003). In this context, mutations in HRPT are associated with HPT-JT syndrome, a disease characterized by hyperthyroidism ossifying fibromas, and solid tumors (Weinstein and Simonds 2003). It encodes for a protein called Parafibromin (Carpten et al. 2002b). In additional support of this, other mutations in the human PAF1c have been linked to various genomic instabilities, leading to cancers, such as deletion of Ctr9, a PAF1c member, leading to pancreatic cancer (Chaudhary et al. 2007). Notch has also been identified as tumor suppressor found in myeloid neoplasms, with associated cancers arising from monocytes, a mature myeloid cell important for innate immunity. These data support a role for Cdc73 as a tumor suppressor. The data from our studies for which I describe in chapters 2-4, however, supports a role for Cdc73 as an oncogene.

1.6.5 Controversies in PAF1c as an activator and repressor of transcription and enhancer activity

The Paf1c has been shown to act as both an activator and repressor of transcription. For example, Paf1C-associated marks, such as H3K36me3 and H3K79me2/3, can be found at highly active enhancers (Zentner et al. 2011; Godfrey et al. 2019). In several papers by Chen et al., they showed that the PAF1c can facilitate promoter proximal pausing by localizing to transcriptional enhancers where it can block the overactivation of several genes in a colon cancer cell line. Their analysis revealed that the PAF1c can function in this way at both active promoters and enhancers. Also, RNA Pol II generally occupied active promoter regions more frequently whereas PAF1c occupied both enhancers and promoter regions almost equally (Chen et al. 2017). They conclude that the PAF1c can restrain activation of enhancers affecting the release of paused Pol II. This supports their model that the PAF1c represses enhancer activity to downregulate eRNA transcription by maintaining the paused state of RNA Pol II at enhancers and promoters.

Conversely, Ding et al. show that he Paf1c positively regulates enhancer activity by occupying and functioning at super enhancers in mESCs. They show a positive correlation between Paf1c binding and the strength of enhancer activity, marking highly active enhancers (Ding et al. 2021). They go on to support a model where Paf1c binding can stimulate eRNA transcription at enhancers.

Taken together, this conflicting data suggests that the Paf1c might function in different ways depending on the cell type and context, which could be even more pronounced when comparing primary cells to cancer cells. The data we have generated in our studies suggests that Cdc73 can both repress and activate eRNAs in T-ALL in general, however it appears to activate T-ALL driver genes specifically, which I discuss more in chapters 3 and 4, when binding at enhancer regions.

Chapter 2 Cdc73 is Important For Notch-Induced T-Cell Development and Leukemia[1]

2.1 CDC73 interacts with NOTCH1 and ETS1 in T-ALL cells

My project investigated the possibility of targeting transcriptional regulators that intersect with the Notch pathway given leukemia associated *NOTCH1* alleles are inherently weak transactivators (Chiang et al. 2008). In *Drosophila* studies, transcriptional cofactors create the cell-specific chromatin context that helps Notch activate its enhancers (Bray 2016; Falo-Sanjuan and Bray 2019; Aster 2020). Proteomic studies by our lab and others have shown that the core Notch complex can interact with transcriptional regulators that co-bind its response elements in T-ALL (Yatim et al. 2012; Lin et al. 2013; Pinnell et al. 2015) and in other cellular contexts (Borggrefe and Liefke 2012; Bray and Gomez-Lamarca 2018). In theory, inhibiting these "Notch cofactors" might interfere with oncogenic Notch signals without disrupting essential Notch functions.

One target of NOTCH1 is *MYC,* an oncogene that shares several overlapping genes with NOTCH1 important for cellular proliferation (Herranz et al. 2014). NOTCH and MYC interact via a regulatory circuit, where NOTCH1 controls the T-cell specific distal enhancer of MYC, called the N-ME (Herranz et al. 2014). This enhancer is essential for Notch-induced T-cell development and leukemogenesis (Herranz et al. 2014).

[1] Adapted from Cdc73 protects Notch-induced T-cell leukemia cells from DNA damage and mitochondrial stress Ashley F. Melnick, Anna C. McCarter, Shannon Liang, Yiran Liu, Qing Wang, Nicole A. Dean, Elizabeth Choe, Nicholas Kunnath, Geethika Bodanapu, Carea Mullin, Fatema Akter, Karena Lin, Brian Magnuson, Surinder Kumar, David B. Lombard, Andrew G. Muntean, Mats Ljungman, JoAnn Sekiguchi, Russell J.H. Ryan, Mark Y. Chiang. bioRxiv 2023.01.22.525059; doi: https://doi.org/10.1101/2023.01.22.525059. The data from this chapter was completed with the help from those listed in the acknowledgements section of this manuscript.

Previous studies showed that CDC73 and associated factors interact with NOTCH1 and enhance Notch target gene expression (Bray et al. 2005; Tenney et al. 2006; Kikuchi et al. 2016). We previously showed that the transcription factor ETS1 nucleates multiple transcription factors at chromatin, including NOTCH1 (McCarter et al. 2020b). We wondered if CDC73 had a stronger interaction with ETS1 than NOTCH1. In support of a role for CDC73 in T-ALL and to confirm and investigate these interactions, we performed co-immunoprecipitation (co-IP) assays. We were able to detect endogenous interactions between NOTCH1, ETS1, and CDC73 in T-ALL cells but were unable to detect NOTCH1 with reciprocal pulldown with CDC73 (Fig. 1A-C). This suggests that CDC73 might interact more closely with ETS1 than Notch.

In support of this data, we performed CDC73 ChIP-Seq in control and ETS1 knockdown THP-6 cells to define the genomic locations of CDC73-associated complexes and then integrated these datasets with our previously published RNA-Seq and ChIP-Seq datasets (McCarter et al. 2020b). Consistent with a previous report of PAF1 in myeloid leukemia cells (Yu et al. 2015), the strongest CDC73 signals were associated with the most highly transcribed genes (Fig. 1D) and active chromatin (Fig. 1E). In support of our co-IP data, our ChIP-Seq data showed that CDC73 peaks overlapped more frequently with ETS1 peaks at 56% than Notch/RBPJ peaks at 40% (Fig. 1F). A majority of RBPJ peaks overlapped with CDC73 peaks in the presence of ETS1 (86%). Additionally, our motif analysis showed that CDC73 peaks were more frequently associated with ETS motifs than any other motif (Fig. 1G).

When we knocked down ETS1, this led to the general downregulation of CDC73 peaks that overlapped with dynamic ETS1 peaks, which are defined as ETS1 peaks that are significantly diminished by ETS1 knockdown (Fig. 1H-I) relative to all CDC73 peaks. Together, this data confirms previous work from others that NOTCH1 does interact with CDC73, but we advance the

field by showing that the interaction between CDC73 and NOTCH1 appears to be context-dependent and at least partially dependent on ETS1.

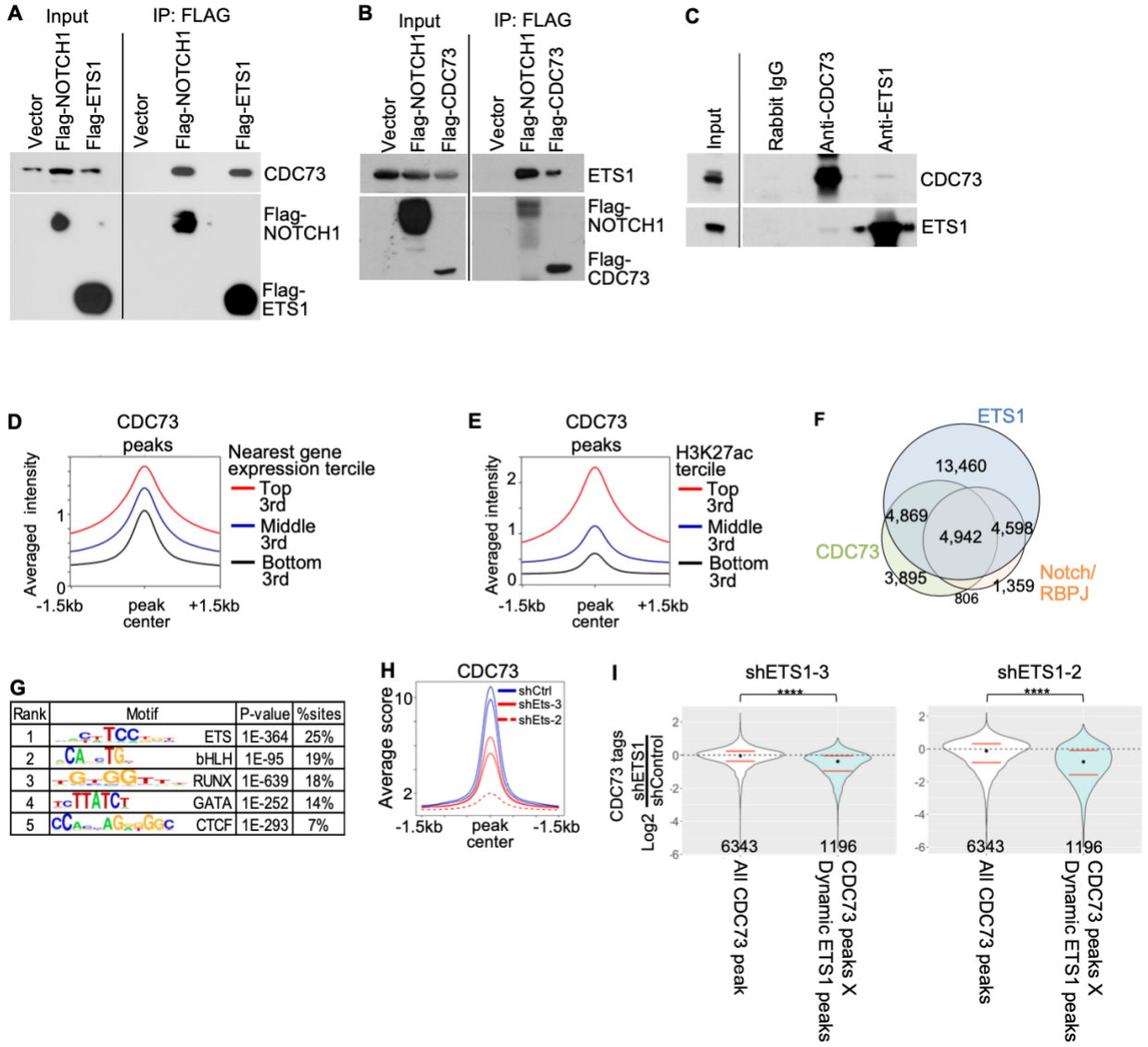

Figure 1 CDC73 interacts with NOTCH1 and ETS1 in T-ALL cells

Co-IP with Flag-NOTCH1 and Flag-ETS1 showing interactions between NOTCH1 or ETS1 with CDC73 in CEM T-ALL cells treated with benzonase. B) Co-IP with Flag-CDC73 showing interaction of ETS1 with CDC73 in 8946 T-ALL cells treated with benzonase. C) Endogenous co-IP showing interaction between ETS1 and CDC73 in THP-6 T-ALL cells treated with benzonase. D-E) Metagene plots of averaged CDC73 ChIP-Seq tags of two THP-6 bioreplicates at ATAC-Seq peaks ranked by tercile mean FPKM expression of nearest genes (D; N=4) or tercile mean H3K27ac tags (E; N=2) (McCarter et al. 2020). F) Venn diagram showing overlap of ETS1, CDC73, and Notch/RBPJ ChIP-Seq peaks in THP-6 cells. G) De novo motif analysis of merged CDC73 ChIP-Seq peaks in THP-6 cells from (McCarter et al. 2020). H) Metagene plot of averaged CDC73 ChIP- Seq peaks that overlap with dynamic ETS1 peaks in human THP-6 cells transduced with either control shRNA (solid blue line; N=2) or shETS1-3 (solid red line; N=2) or shETS1-2 (dotted red line; N=2). Dynamic ETS1 peaks were defined as ETS1 peaks that diminish with FDR<0.1 upon knockdown with two independent shETS1 (McCarter et al. 2020). I) Violin plots showing the CDC73 ChIP-Seq

Log2FC for all CDC73 peaks and CDC73 peaks that overlap with dynamic ETS1 peaks in context of ETS1 knockdown with shETS1-3 (left) or shETS1-2 (right).

2.2 Cdc73 is important for Notch-dependent T-cell development

During Murine T-cell development, highly proliferative T-cells proceeds in the thymus through a series of stages from the double-negative (DN) $CD4^-CD8^-$ "pre-T-cell" stages (DN1-DN4) to the immature single positive (ISP) and $CD4^+CD8^+$ double-positive (DP) stages, and then to the single-positive (SP) $CD4^+$ or $CD8^+$ stages. Pre-T-cells are important because they can transform into T-ALL cells (Pui et al. 2008; Berquam-Vrieze et al. 2011; Tatarek et al. 2011). Notch1 and Ets1 are essential for the transition between the DN stage to the DP stage (Wolfer et al. 2002; Eyquem et al. 2004; Tanigaki et al. 2004; Maillard et al. 2006a). Broadly relevant, oncogenic TFs like Notch1, Myc, and Myb are "hijacked" from their normal physiological roles in promoting pre-T-cell proliferation (Wolfer et al. 2002; Lieu et al. 2004; Tanigaki et al. 2004; Dose et al. 2006; Maillard et al. 2006b). Consequently, TFs that drive pre-T-cell proliferation are often broadly essential for maintaining T-ALL cells of diverse oncogenomic subsets.

To investigate the importance of Cdc73 for Notch functions in T-cells, we first studied its effect in T-cell development, which is driven primarily by Notch signals (Hosokawa and Rothenberg 2021). We first wondered if Cdc73 was being expressed at all stages of T-cell development or specific stages, and if so, what stage had the highest expression. We found that like Notch1 and Ets1, Cdc73 and other Paf1C members including Paf1, Leo1, Ctr9, Rft1, and Wrd61, are expressed throughout T-cell development in both murine and human T-cells, starting from the multipotent progenitor (MPP4) stages through the CD8 DP stages (Fig. 2A-B). Cdc73 specifically seemed to increase in expression levels at the DP stages and later. Together, this confirmed that Cdc73 was being expressed throughout all stages of T-cell development.

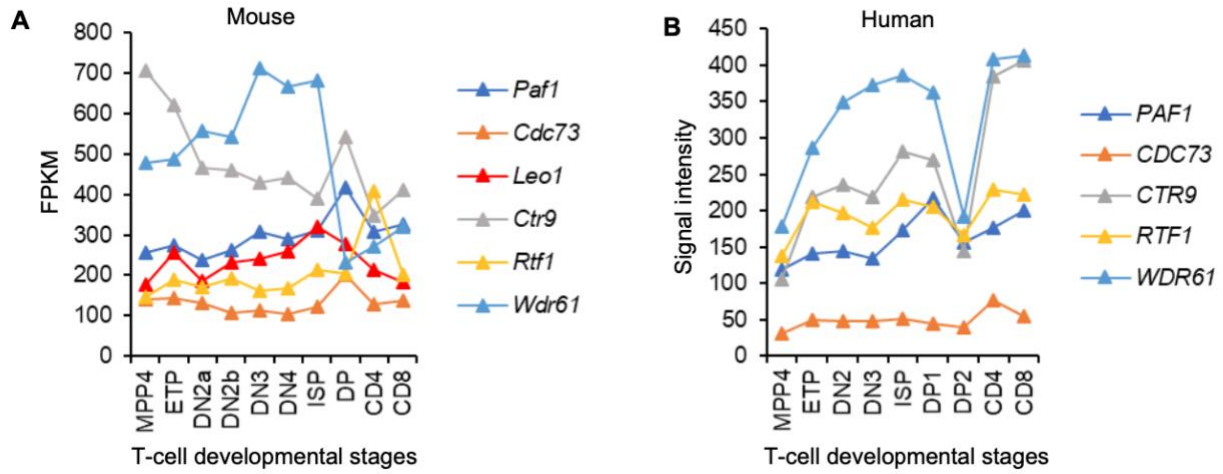

Figure 2 CDC73 is expressed throughout T-cell development

A) Expression of Paf1C family members in murine T-cell developmental subsets (ImmGen; GSE109125). B) Expression of PAF1C family members in human T-cell development (GSE22601).

We next wondered if Cdc73 might share similar functions as Notch1 and Ets1 in early T cells. To approach this question, we generated mice where we crossed *LckCre* mice with $Cdc73^{f/f}$ mice to generate *LckCre* $Cdc73^{f/f}$ mice ($Cdc73^{\Delta/\Delta}$ mice). *LckCre* induces Cre recombinase in pre-T cells while $Cdc73^{f/f}$ mice have loxP sites flanking exon 2 of *Cdc73*(Wang et al. 2008b). Upon Cre mediated recombination, exon 2 is deleted to produce $Cdc73^{\Delta/\Delta}$ mice. Like Notch-deficient and Ets1-deficient mice, $Cdc73^{\Delta/\Delta}$ mice had significantly smaller thymuses and exhibited severely impaired thymopoiesis as quantified by total thymocyte count (Fig. 3A-B). These mice also showed significant loss of early T cells by the DN4 stage as characterized by T-cell markers CD44 and CD25 and transmembrane markers CD27 and TCRß (Fig. 3C-H). Impaired DN-to-DP cell transition was also observed (Fig. 3I-O).

We next sought to understand at what point of T-cell development was the expression level of Cdc73 apparent, so we took $Cdc73^{\Delta/\Delta}$ mice and control mice and sorted their thymocytes into DN2b, DN3a, DN3b and DN4 populations. Expression analysis of these sorted DN subsets

showed that *Cdc73* deletion was first visible at the DN3a stage however had the strongest effect at the DN4 stage (Fig. 1.3P). This effect is consistent with the DN4 population showing the most significant loss of cell number (Fig. 3H) and loss of classic Notch target genes including *Hes1* and *Myc* (Fig. 3Q-R). Thus, like *Notch1* and *Ets1*, *Cdc73* play an important role in promoting transition from the DN-to-DP stages.

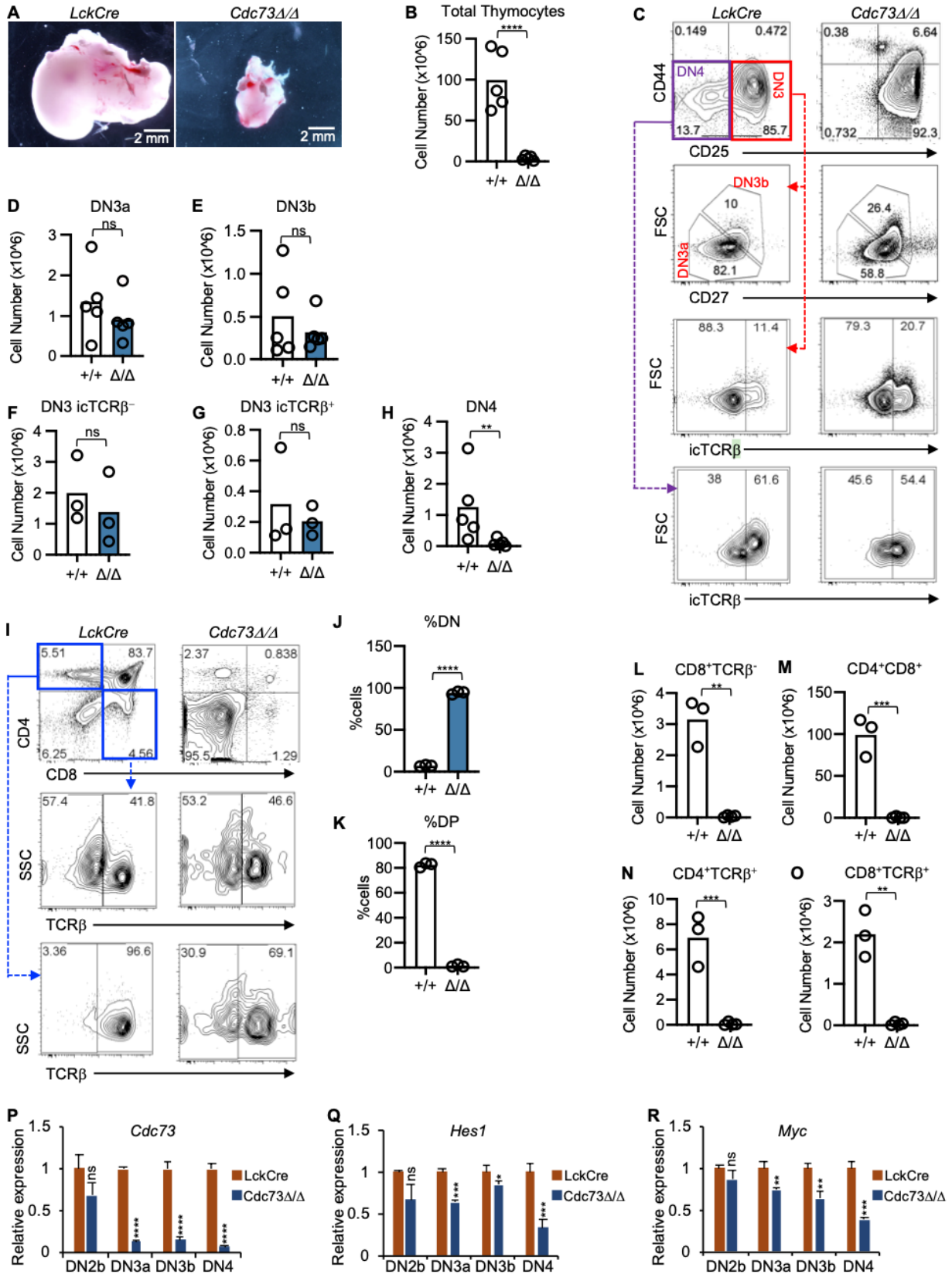
A
LckCre
Cdc73Δ/Δ
2 mm
2 mm
B
Total Thymocytes
Cell Number (x10^6)
+/+ Δ/Δ
C
LckCre
Cdc73Δ/Δ
CD44
CD25
DN4
DN3
DN3b
DN3a
FSC
CD27
icTCRβ
D
DN3a
E
DN3b
F
DN3 icTCRβ⁻
G
DN3 icTCRβ⁺
H
DN4
I
LckCre
Cdc73Δ/Δ
CD4
CD8
SSC
TCRβ
J
%DN
%cells
K
%DP
L
CD8⁺TCRβ⁻
M
CD4⁺CD8⁺
N
CD4⁺TCRβ⁺
O
CD8⁺TCRβ⁺
P
Cdc73
Q
Hes1
R
Myc
Relative expression
LckCre
Cdc73Δ/Δ
DN2b DN3a DN3b DN4

Figure 3 Cdc73 is important for Notch-dependent T-cell development

A-H) Representative images of thymuses (A); absolute thymocyte counts (B); representative flow cytometric profiles of DN subsets (C); and absolute numbers of DN3a (D), DN3b (E), DN3 icTCRβ- (F), DN3 icTCRβ+ (G), and DN4 (H) subsets in LckCre control and LckCre Cdc73f/f (Cdc73Δ/Δ) mice. I-O) Representative flow cytometric profiles of CD4/CD8 subsets (I); %DN (J); %DP (K); and absolute numbers of ISP (L), DP (M), CD4 SP (N), and CD8 SP (O) thymic subsets in LckCre control and Cdc73Δ/Δ mice. DN3a=Lineage-CD44-CD25+FSCloCD27-. DN3b=Lineage-CD44-CD25+FSChiCD27+. DN4=Lineage-CD44-CD25-. ISP=CD8+TCRb-. DP=CD4+CD8+. CD4 SP=CD4+TCRb+. CD8 SP=CD8+TCRb+. *P<0.05; **P<0.01; ***P<0.001; ****P<0.0001. P-R) Relative expression of Cdc73 (P), Hes1 (Q), and Myc (R) in sorted thymic subsets from LckCre mice (red) and Cdc73Δ/Δ mice (blue).

2.3 Cdc73 is important for murine Notch-induced T-ALL maintenance

Next, we wondered whether the dependence of T-cell precursors on Cdc73 would be conserved after they transform to leukemia. To test this possibility, we used a well-established murine model of Notch-induced T-ALL (Pear et al. 1996; Aster et al. 2000). The activated NOTCH1 allele, ΔE, models leukemia-associated human NOTCH1 alleles that trigger ligand-independent Notch activation38,39. We transduced bone marrow stem and progenitor cells from Rosa26CreERT2 or Rosa26CreERT2 Cdc73f/f mice with activated Notch1 (ΔE /Notch1) (Schroeter et al. 1998; Weng et al. 2003) and transplanted the cells into sub-lethally irradiated recipient mice to generate primary tumors (Fig. 4A, 5A).

When these mice developed primary tumors, we created a tumor bank by harvesting the spleen, thymus, or lymph nodes (LN) and transplanted the tumors into secondary recipients. These mice were later injected with tamoxifen to delete Cdc73 or oil as a vehicle control. In contrast to control T-ALL mice (Fig. 5B), Cdc73f/f T-ALL mice treated with tamoxifen showed reduced blast or white blood cell counts of 700-fold or 11-fold (Fig. 5C). Median survival was unchanged in control T-ALL mice (Fig. 5D) but prolonged by >200% or 84% in Cdc73f/f T-ALL mice (Fig. 5E). This data suggests that Cdc73 is important for the maintenance of Notch-induced T-ALL.

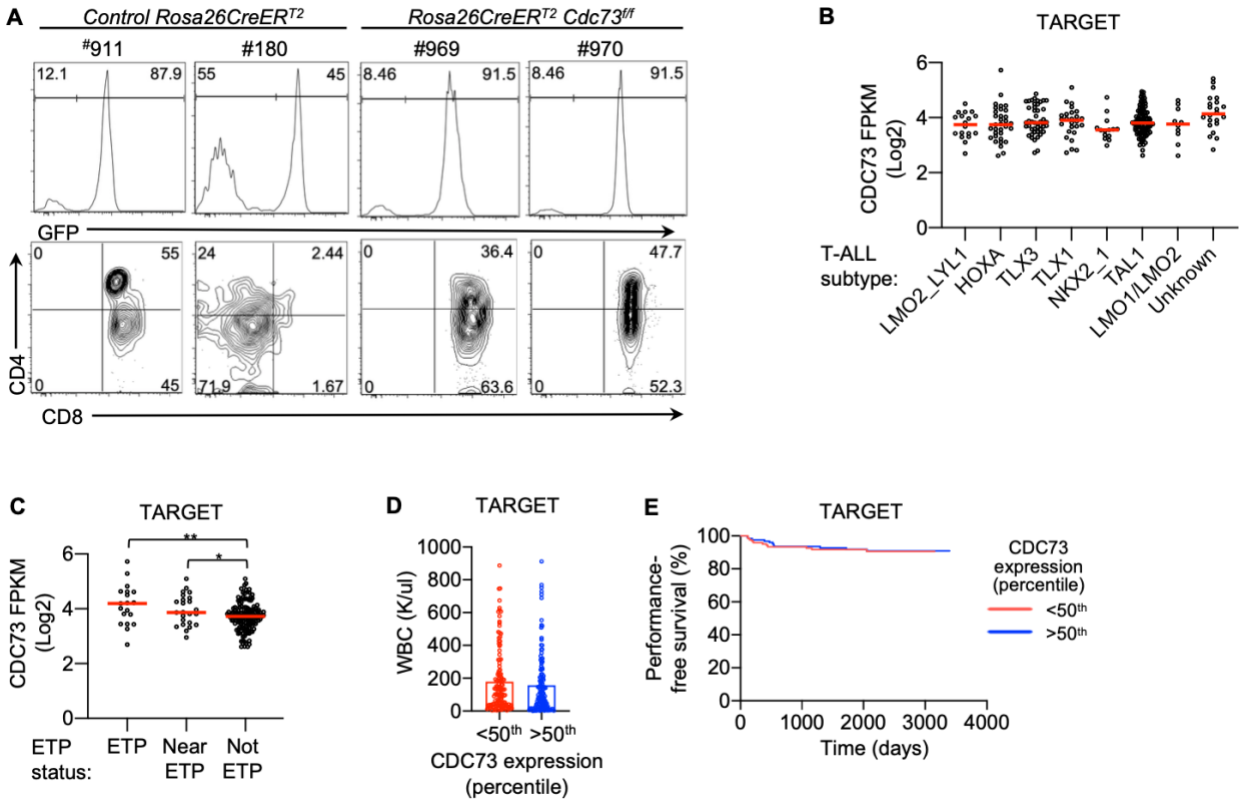

Figure 4 CDC73 is expressed in diverse T-ALL subsets

A) Representative CD4/CD8 flow cytometric profiles of GFP+ splenic tumors induced by activated Notch1 alleles (ΔE/Notch1) in Rosa26CreERT2 control and Rosa26CreERT2 Cdc73f/f mice. B-C) CDC73 expression according to T-ALL subtype (B) and ETP status (C) in the TARGET database. D) White blood cell (WBC) counts of T-ALL patients stratified by CDC73 expression. E) Survival curves of T-ALL patients stratified by CDC73 expression. (Liu et al. 2017). TARGET=Therapeutically Applicable Research to Generate Effective Treatments (TARGET) (https://ocg.cancer.gov/programs/target) initiative, phs000218. The ALL project team was headed by Stephen P. Hunger, M.D. at the University of Colorado Cancer Center, Denver, CO, USA. The dbGaP Sub- study ID was phs000463/phs000464. The data used for this analysis are available at https://portal.gdc.cancer.gov/projects.

2.4 Cdc73 is important for human *NOTCH1*-activated T-ALL propagation and maintenance

In a clinically annotated cohort of pediatric T-ALL, *CDC73* is expressed across all oncogenomic and developmental subgroups (Fig. 4B-C). *CDC73* expression is not associated with WBC (Fig. 4D) or survival (Fig. 4E).

To test the functional importance of *CDC73* for human T-ALL cell proliferation, we transduced *CDC73* shRNAs into *NOTCH1*-activated, ETS1-dependent T-ALL cells with

effective suppression of CDC73 protein (Fig. 5F). *CDC73* knockdown reduced proliferation of NOTCH1-activated T-ALL cell lines by 2-9-fold (Fig. 5G). To test the anti-tumor effects of *CDC73* inactivation in non-immortalized human T-ALL cells, we took advantage of the success of shRNA protocols in knocking down gene expression in Notch-activated patient-derived xenografts (PDXs) (Yost et al. 2013; McCarter et al. 2020b). We acquired several T-ALL PDX samples from the University of Michigan Heme Malignancies Tissue Bank and the Public Repository of Xenografts (ProXe, gift of Andrew Weng), that have been analyzed by RNA-Seq1,17 and all highly express activated NOTCH1, CDC73 and other PAF1C subunits. *CDC73* knockdown reduced viability of PDX cells by 5 or 6-fold (Fig. 5H-I). Transplantation of these cells into immunodeficient NSG mice showed that *CDC73* knockdown significantly prolonged survival (Fig. 5J). Taken together, these results demonstrate strong and highly prevalent *CDC73*-dependency in human NOTCH1-activated T-ALL.

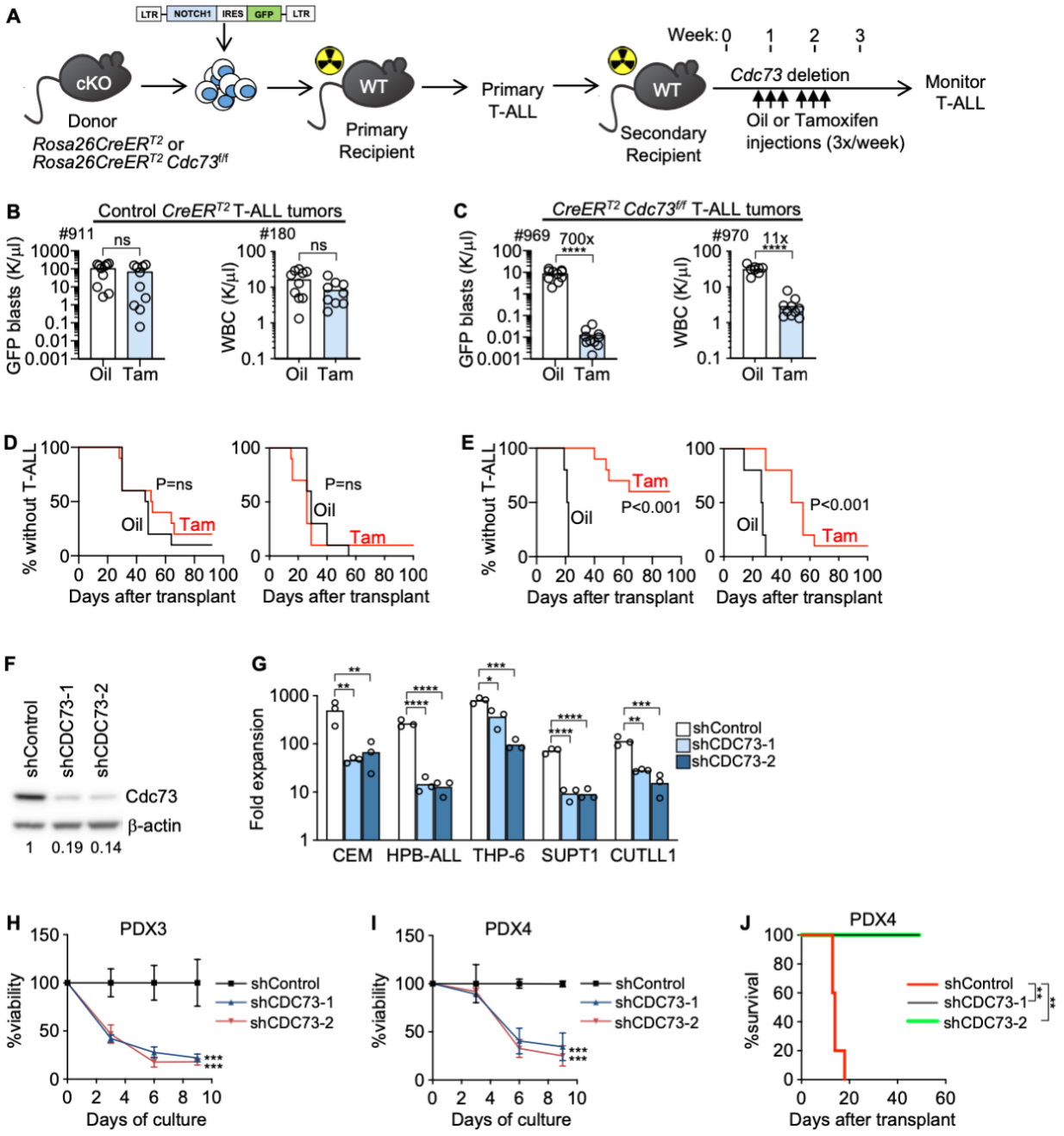

Figure 5 Cdc73 is important for Notch-induced T-ALL maintenance

A) Experimental strategy to study dependence of Notch-induced T-ALL maintenance on Cdc73. Tam=25mg/kg tamoxifen. B-E) Mice were injected with 2 independent DE/Notch1-induced Rosa26CreERT2 control T-ALL tumors (B, D) or 2 independent DE/Notch1-induced Rosa26CreERT2 Cdc73f/f murine T-ALL tumors (C, E). Numbers indicate tumor IDs. Peripheral blood GFP+ counts or WBC (B-C) at 2.5 weeks post-transplant and survival (D-E) were measured. F) Western blot showing CDC73 knockdown in shRNA-transduced CEM cells. Numbers indicate relative band intensity. G) Fold expansion (Day 9 cell count/Day 0 cell count) of Notch1-activated T- ALL cells transduced with two independent shCDC73. H-I) Viability of conventional T-ALL PDX cells transduced with shCDC73 in OP9-DL4 stromal cell culture. N=3. J) Leukemia-free survival of NSG mice injected with PDX4 cells transduced with shCDC73 that were passaged in NSG mice for 24 weeks. N=5. **P<0.01; ***P<0.001; ****P<0.0001.

2.5 Discussion

Notch signaling is an essential pathway that controls important developmental activities such as T-cell fate and specification in diverse tissues. Due to its essential role in the maintenance of normal tissue homeostasis, inhibiting the entire Notch pathway as an approach to treat T-ALL poses several barriers. The most prominent and commonly used therapy, gamma-secretase inhibitors (GSIs), has been shown to cause gastrointestinal toxicity, leading researchers to investigate safer options to target the oncogenic Notch pathway in T-ALL (Krop et al. 2012; Tolcher et al. 2012). Understanding how Notch functions in T-cell development and leukemogenesis is an important step in the quest to develop anti-Notch therapies that specifically target oncogenic Notch signaling. Our lab and others look at pathways that intersect with Notch as a potential therapeutic window to treat T-ALL.

The polymerase associated factor complex (Paf1c), a scaffold complex consisting of 5 subunits, was previously linked to the Notch pathway in the *Drosophila* model. When complex member *Rft1* was mutated in this model, the flies displayed "notches" in their wings and impaired transcription of Notch target genes (Tenney et al. 2006). This finding confirmed that the Paf1c must play an important role in wing development by regulation of Notch and its target genes. More recent studies have evaluated other Paf1c members and their link to the Notch pathway, such as Paf1c member Cdc73. A study in breast cancer cells confirmed the *NOTCH-CDC73* interaction by showing that *CDC73* can bind intracellular-Notch (ICN) and can direct the activation of Notch signals (Kikuchi et al. 2016). My project extends field by investigating the role of Cdc73 in T-cell development and Notch-activated T-ALL.

Starting with T-cell development, we first showed that conditional knockout of Cdc73, using the Cre-lox system, specifically the LckCre promoter, led to a significantly smaller thymus and reduced thymocyte cellularity in our mouse model (Fig. 3A-B). We used the LckCre-lox model because *Lck* is a T-cell lineage specific tyrosine kinase that is critical for T-cell development and activation (Chiang and Hodes 2016). Our results implied that Cdc73 played an important role in developing thymocytes, which made sense given the essential function of *NOTCH1* and other PAF1c members in wing development in the *Drosophila* model (Tenney et al. 2006). We used publicly available data from Immgen to check the expression levels of PAF1c members for both mouse and human T-cell subsets and confirmed that *CDC73* was expressed across all developmental stages of T-cell development (Fig. 2A-B). It was also interesting to see that out of all the other PAF1c members, *CDC73* was expressed the lowest across all T-cell stages.

We then questioned if Cdc73 was important at specific stages of T-cell development in our mouse model and saw that Cdc73 was important for the transition from the DN3 to DN4 stages (Fig. 3C-H). Given that the DN3 stage is where the Lck promoter is activated, this data made sense. Additionally, we saw a block in the transition from the DN to DP stage of T-cell development (Fig. 3I-O). Within the thymus, T-cells progress through the DN-DP stages within the cortex of the thymus. In order for T-cells to enter the final stages of maturation into the single positive stages in the medulla of the thymus, they must undergo positive selection which is a maturation process of immature CD4+ CD8+ thymocytes that are induced by T-cell receptor (TCR) signals (Chiang and Hodes 2016). My data suggests that Cdc73 plays an important role during this process, however, the mechanism by which this occurs is still unknown.

To further support this, our relative expression level data from sorted thymocyte subsets showed decreasing Cdc73 relative expression levels in our conditional knockout model starting at the DN3a, DN3b and DN4 stages (Fig. 3P). This was consistent with the relative expression levels of Notch target genes such as *Hes1* and *Myc*, with the strongest expression differences seen across the DN4 stage (Fig. 3Q-R). Together, this data suggests that Cdc73 plays an essential role in early T-cell development however the mechanism by which Cdc73 might be interacting with Notch target genes to orchestrate T-cell development was still in question.

To study the role of Cdc73 in Notch-activated T-ALL, we used mouse models where bone marrow from $CreER^{T2}Cdc73^{f/f}$ mice or control mice were transduced with activated-Notch1 before being transplanted into the mice. We showed that knockdown of Cdc73 in mice injected with Notch-activated T-ALL showed significantly reduced blast counts and extended survival compared to our controls (Fig. 5B-E). This suggested that Cdc73 plays an important role in T-ALL tumor survival in a Notch-activated mouse model. We followed up these experiments by confirming the importance of Cdc73 in human T-ALL cell lines and PDX models. We saw that knockout of *CDC73* in our human T-ALLs significantly reduced proliferation of these tumor lines, again, suggesting that Cdc73 is important for T-ALL tumor survival (Fig. 5G). Additionally, in our PDX models, which are a more translational model, we showed that PDX's transduced with *CDC73* significantly reduced cell viability, and when injected into immunocompromised NSG mice, the mice showed a significant increase in survival compared to controls (Fig. 5H-J). Together, this data confirms that like *NOTCH1, CDC73* is important for T-cell development and T-ALL maintenance.

Understanding the importance of Cdc73 in T-cell development and Notch-activated T-ALL was the first step in our goal of finding a therapeutic window to treat T-ALL. To do this we

sought to understand how we can target Cdc73 or Notch in T-ALL by looking at differentially expressed genes. In this way, we can spare inhibiting Notch function in normal T-cell developing which only targeting oncogenic Notch. There are still several things we do not know about how Cdc73 might be interacting with Notch, however, such as determining if Cdc73 is directly interacting with Notch or if it is interacting with Notch though other Notch cofactors. We also want to understand the mechanism by which Cdc73 and Notch are interacting to activate T-ALL. These questions and others make up the remaining aims of my project.

Chapter 3 Cdc73 Activates Gene Expression Important For Notch-Induced T-ALL[2]

3.1 Cdc73 promotes gene expression in pathways co-regulated by ETS1 and NOTCH1

We sought to understand the underlying mechanism by which Cdc73 is required for Notch1-activated T-ALL maintenance as I wrote about in my last chapter. Towards this goal, we started by generating two independent Notch-induced *CreER^{T2} Cdc73$^{f/f}$* T-ALL cell lines (969 and 970) and one control *CreER^{T2}* cell line. To do this, we transferred the tumors described in figure 5A to cell culture media and cultured them over a period of weeks. We confirmed that upon addition of 4-hydroxytamoxifen (OHT), *Cdc73* was able to be deleted in these cells but not in the control (Fig. 7A). Additionally, deletion of *Cdc73* impaired cell proliferation in our growth assay (Fig. 6A). In contrast, OHT treatment had no effect on control *CreER^{T2}* cells. This data suggested that our cell lines were sensitive to deletion of Cdc73.

Next, we were interested in identifying differentially expressed genes upon loss of Cdc73 in our cell lines. To do this, we performed Bromouridine-sequencing (Bru-seq) (Paulsen et al. 2013; Paulsen et al. 2014) in these cells. The purpose of Bru-seq is to measure nascent mRNA transcripts following *Cdc73* deletion using bromouridine (BrdU) labeling techniques. Bru-seq is an optimal way to measure nascent RNA over other RNA labeling methods due to BrdU being less toxic compared to other labeling methods. Additionally, there is a wide availability of ani-

[2] Adapted from Cdc73 protects Notch-induced T-cell leukemia cells from DNA damage and mitochondrial stress Ashley F. Melnick, Anna C. McCarter, Shannon Liang, Yiran Liu, Qing Wang, Nicole A. Dean, Elizabeth Choe, Nicholas Kunnath, Geethika Bodanapu, Carea Mullin, Fatema Akter, Karena Lin, Brian Magnuson, Surinder Kumar, David B. Lombard, Andrew G. Muntean, Mats Ljungman, JoAnn Sekiguchi, Russell J.H. Ryan, Mark Y. Chiang. bioRxiv 2023.01.22.525059; doi: https://doi.org/10.1101/2023.01.22.525059. The data from this chapter was completed with the help from those listed in the acknowledgements section of this manuscript.

BrdU antibodies to study transcriptional regulation (Paulsen et al. 2014). In this method, after RNA is BrdU labeled, the RNA is captured using anti-BrdU antibodies that are conjugated to magnetic beads. The isolated RNA can then be used to generate cDNA libraries that can be sent for deep sequencing. The sequencing data can be analyzed and mapped across the entire genome including both introns and exons (Paulsen et al. 2013). Bru-seq is also superior relative to other RNA labeling methods because of its ability to measure and estimate the rate of transcription across the genome. It can normalize the data to the length of the gene using "reads per thousand base pairs per 1 million reads" (RPKM) (Paulsen et al. 2013). Using Bru-seq, we identified 1062 differentially expressed genes ("Cdc73 target genes") that were shared between our *Cdc73*$^{f/f}$ T-ALL cells but not by control cells (Fig. 6B, Fig. 7B).

Consistent with previous studies, we did not observe large scale downregulation of all gene of expression, indicating that Cdc73 is regulating specific genes. This led to us ask the question, in what context is Cdc73 regulating these specific genes to drive T-ALL? Towards this question, we performed a gene set enrichment analysis (GSEA) using a list of high-confidence direct NOTCH1 target genes in T-ALL (Wang et al. 2014). Our analysis showed no significant enrichment for Cdc73-regulated target genes (Fig. 7C-D). However, *Cdc73* deletion significantly impaired the expression of 25% of Notch signature genes in both *Cdc73*$^{f/f}$ T-ALL cell lines at $q<0.05$ ($P=0.0216$, Fisher exact test). In contrast, GSEA using a list of high-confidence direct ETS1 target genes in T-ALL (McCarter et al. 2020b) showed strongly significant enrichment for Cdc73-regulated genes in both 969 cells (NES 3.26; FDR<0.001) and 970 cells (NES 2.75; FDR<0.001) (Fig. 6C-D). Additionally, *Cdc73* deletion impaired expression of 22% of ETS1 signature genes at $q<0.05$ ($P=0.0003$, Fisher exact test). These data are consistent with our

protein-protein interaction and ChIP-Seq data showing stronger interaction of CDC73 with ETS1 than with NOTCH1 (Fig. 1A-C, 1F-G).

Given Cdc73 only regulates a subset of Notch1 and ETS1 target genes, we next wondered what pathways Cdc73, ETS1, and Notch might be co-regulating. Towards this goal, we ran a Hallmark GSEA analysis and several different pathways that were regulated by Cdc73. To hone in on what pathways we wanted to investigate further, we ranked the top six pathways in both of our *Cdc73*$^{f/f}$ T-ALL cell lines and compared them to previously identified pathways that are regulated by ETS1 and NOTCH1 (McCarter et al. 2020a). Comparing these 4 data sets, we identified DNA repair and oxidative phosphorylation (OXPHOS) gene signatures as the top two shared pathways enriched for Cdc73-induced, ETS1-induced, and Notch-induced genes (highlighted in blue in Fig. 6E-H). Thus, Cdc73 shares essential roles for T-cell leukemogenesis with Notch1 and Ets1 but also has partially overlapping functions with these factors in regulating gene expression.

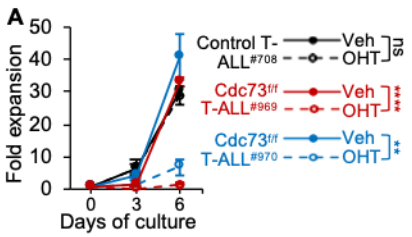

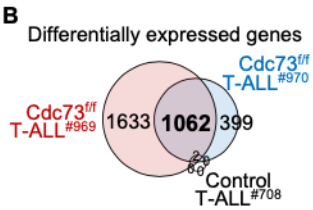

E Cdc73-induced genes (T-ALL$^{\#969}$)

Rank	Title of Hallmark set	NES	FDR
1	OXIDATIVE_PHOSPHORYLATION	3.83	<1E-5
2	MTORC1_SIGNALING	3.18	<1E-5
3	MITOTIC_SPINDLE	2.90	<1E-5
4	PROTEIN_SECRETION	2.85	<1E-5
5	DNA_REPAIR	2.11	0.0069
6	ADIPOGENESIS	2.11	0.0055

F Cdc73-induced genes (T-ALL$^{\#970}$)

Rank	Title of Hallmark set	NES	FDR
1	OXIDATIVE_PHOSPHORYLATION	3.52	<1E-5
2	MTORC1_SIGNALING	3.06	<1E-5
3	ADIPOGENESIS	2.98	<1E-5
4	DNA_REPAIR	2.12	0.0091
5	PROTEIN_SECRETION	1.95	0.0231
6	MITOTIC_SPINDLE	1.64	0.0816

G ETS1-induced genes (T-ALL^{THP6})

Rank	Title of Hallmark set	NES	FDR
1	MYC_TARGETS_V1	7.82	<1E-5
2	MYC_TARGETS_V2	6.31	<1E-5
3	OXIDATIVE_PHOSPHORYLATION	5.15	<1E-5
4	DNA_REPAIR	4.81	<1E-5
5	INTERFERON_ALPHA_RESPONSE	3.76	<1E-5
6	E2F_TARGETS	3.62	<1E-5

H Notch-induced genes (T-ALL^{THP6})

Rank	Title of Hallmark set	NES	FDR
1	MYC_TARGETS_V1	8.70	<1E-5
2	MYC_TARGETS_V2	6.95	<1E-5
3	OXIDATIVE_PHOSPHORYLATION	4.63	<1E-5
4	MTORC1_SIGNALING	4.41	<1E-5
5	UNFOLDED_PROTEIN_RESPONSE	4.35	<1E-5
6	DNA_REPAIR	3.16	<1E-5

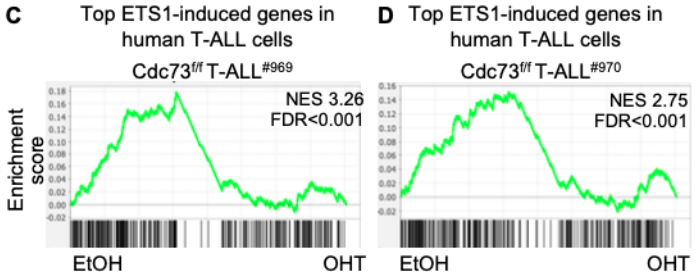

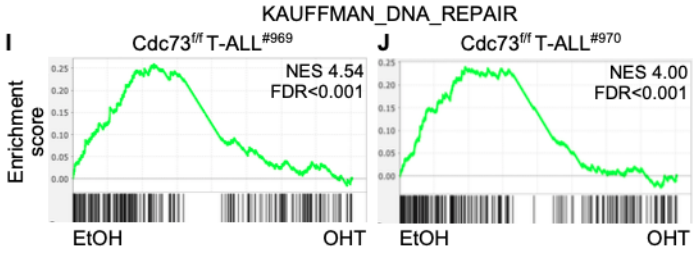

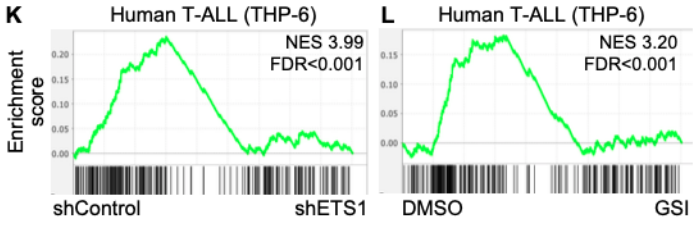

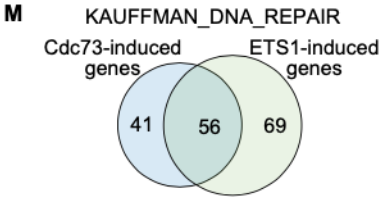

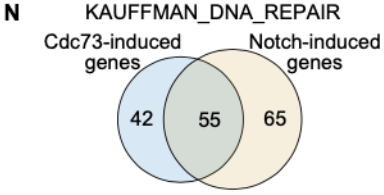

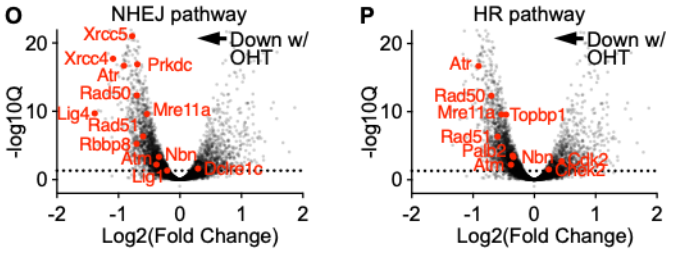

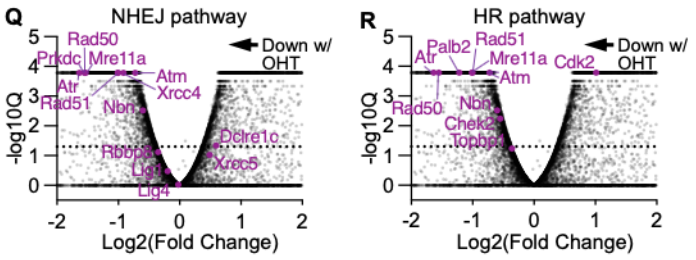

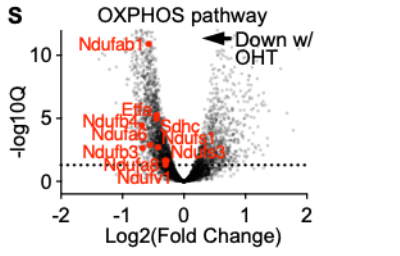

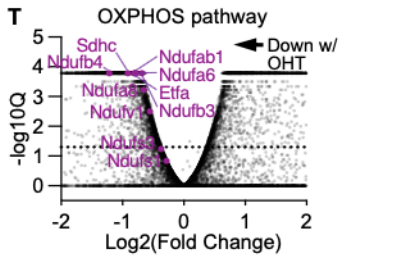

Figure 6 Cdc73 shares ETS1 and Notch-driven pathways

A) Rosa26CreERT2 Cdc73f/f T-ALL cells (969; 970) and control Rosa26CreERT2 T-ALL cells derived from tumors in Fig. 2C were treated with 3nM OHT (hydroxytamoxifen) to delete Cdc73 and measured for growth. Fold expansion=Day3 or Day6 cell count/Day 0 cell count. B) Venn diagram showing 1062 Cdc73 target genes shared by both Cdc73f/f T-ALL cell lines from (A). Target genes defined as FC>1.5; Padj<0.05 in Bru-Seq counts at 30h after OHT addition in both Cdc73f/f cell lines but not in controls. C-D) GSEA using the top 258 ETS1-induced gene list (McCarter et al., 2020) of Cdc73-induced genes in 969 (C) and 970 (D) cells. E-H) GSEA analyses showing the top 6 Hallmark pathways enriched for Cdc73- (E-F), ETS1- (G) and Notch- (H) induced target genes. ETS1 and Notch target genes were previously described in human THP-6 T-ALL cells (McCarter et al., 2020). Pathways shared across the 4 analyses are highlighted in blue. I-L) GSEA using the MSigDB C2 Kauffman_DNA_repair gene list of Cdc73-induced genes (I-J), ETS1-induced genes (K), and Notch-induced genes (L). M-N) Venn diagram showing overlap of Cdc73-induced and ETS1-induced (M) or Notch-induced (N) genes in the Kauffman_DNA_repair gene list. O-T) Volcano plots of significance vs. Bru-Seq (O-P, S) or RNA-Seq (Q-R, T) Log2FC data showing the control vs. OHT (Cdc73D/D) comparison and highlighting important genes in non-homologous end-joining (NHEJ; O, Q), homologous recombination (HR; P, R), and oxidative phosphorylation (OXPHOS; S-T) pathways in 969 T-ALL cells (O-P, S) and AML cells (Q-R, T) on background of all genes (grey) giving average RPKM>0.8. RNA-Seq analysis of Control and Cdc73-deleted AML cells were obtained from (Saha et al. 2019). **P<0.01; ****P<0.0001.

DNA repair is relatively understudied as a synthetic lethal vulnerability, but T-ALL oncogenes induce DNA damage through replicative stress (Kotsantis et al. 2018; Leon et al. 2020). DNA damage is a form of genetic instability first highlighted as a driving force of tumorigenesis in the famous “Hallmarks of Cancer” publication by Hanahan and Weinberg (Hanahan and Weinberg 2000). Many studies have shown that dysregulation of DNA replication, called replicative stress, is linked to genomic instability in early stages of cancer progression (Bartkova et al. ; Bartkova et al. ; Gorgoulis et al.). Replicative stress initiates a DNA damage response (DDR) in attempts to resolve the damage (Saldivar et al.). The DDR causes the recruitment of ATR kinase, leading to the phosphorylation of many downstream targets, such as CHK1 and histone H2AX (Kotsantis et al. 2018). In turn, CHK1 induces cell cycle arrest, allowing for enough time for the cell to repair any lesions and prevent early entry into mitosis with replicated DNA (Kotsantis et al. 2018). In cancers, ATR and CHK1 can induce replicative stress and has led to synthetic lethality in MYC-driven lymphomas (Murga et al.), an oncogene frequently mutated in T-ALL.

In our data sets, the most enriched DNA repair signature for Cdc73-induced genes in MSigDB was Kauffman_DNA_repair_genes, giving a FDR<0.001 for Cdc73-induced genes (NES 4-4.54, Fig. 6I-J), ETS1-induced genes (NES 3.94, Fig. 6K), and Notch-induced genes (NES 3.2, Fig. 6L). *Cdc73* deletion generally downregulated important DNA repair genes including *Atr* and *Lig4*, and other genes found in multiple pathways, such as non-homologous end joining (NHEJ; Fig. 6O, Fig. 7E) and homologous recombination (HR; Fig. 6P, Fig. 7F).

NHEJ is the primary pathway responsible for the repair of dsDNA breaks (Chang et al. 2017). dsDNA breaks can occur for multiple reasons, including but not limited to ionizing radiation, reactive oxygen species (ROS), or DNA replication errors (Chang et al. 2017). If NHEJ is compromised due to the inability of key proteins in the pathway, other pathways, such as HR, are activated. To test if Cdc73 functions were conserved in non-T cells, we interrogated our gene expression datasets of murine MLL-AF9 driven *Cdc73*$^{f/f}$ AML cells (Saha et al. 2019). Accordingly, *Cdc73* deletion in these cells led to general downregulation of the same DNA repair genes (Fig. 6Q-R).

OXPHOS is a synthetic lethal vulnerability in T-ALL since Notch promotes high anabolic demand (Kishton et al. 2016; Garcia-Bermudez et al. 2018; da Silva-Diz et al. 2021; Thandapani et al. 2021). In general, cancer cells often exhibit alterations in their metabolism to support their rapid and proliferative growth. This happens through various metabolic processes such as increased ATP production to help maintain high energy levels and cellular redox statuses (Kishton et al. 2016). Oncogenes such as MYC have been shown to induce ROS production and DNA damage (Maya-Mendoza et al. ; Vafa et al.). While it is unclear how ROS affects replicative stress, some data theorizes that increases in ROS production leads to

hyperproliferation of the cancer cells, leading to increased replicative stress (Di Micco et al. ; Ogrunc et al.).

In our data sets, of the OXPHOS gene lists in MSigDB, the Hallmark list gave the highest enrichment with FDR<0.001 for Cdc73-induced genes (NES 3.52-3.83, Fig. 7G-H), ETS1-induced genes (NES 5.15, Fig. 7I), and Notch-induced genes (NES 4.63, Fig. 7J). Analysis of core enrichment genes showed that ETS1 and Notch induce large fractions of Cdc73-induced OXPHOS genes (60% in Fig. 7K and 62% in Fig. 7L respectively). Conversely, Cdc73 induces large fractions of ETS1 and Notch-induced OXPHOS genes (56% and 41% respectively). *Cdc73* deletion generally downregulated important OXPHOS pathway genes including Ndufab1 and Ndufb4 (Fig. 6S, Fig. 7M). These same genes were also generally downregulated upon *Cdc73* deletion in AML cells (Fig. 6T) (Saha et al. 2019).

Expression analysis of sorted DN subsets showed loss of important DNA repair such as *Atr* and *Lig4* and OXPHOS genes including *Ndufab1* and *Ndufb4*, particularly at the DN4 cell stage when the strongest Cdc73 deletion was achieved (Fig. 7N). Taken together, this data suggests that like ETS1 and Notch, Cdc73 is important for promoting expression of genes that are important for DNA repair and OXPHOS. These roles appear to be conserved among early T cells, T-ALL cells, and Notch-independent/non-lymphoid AML cells.

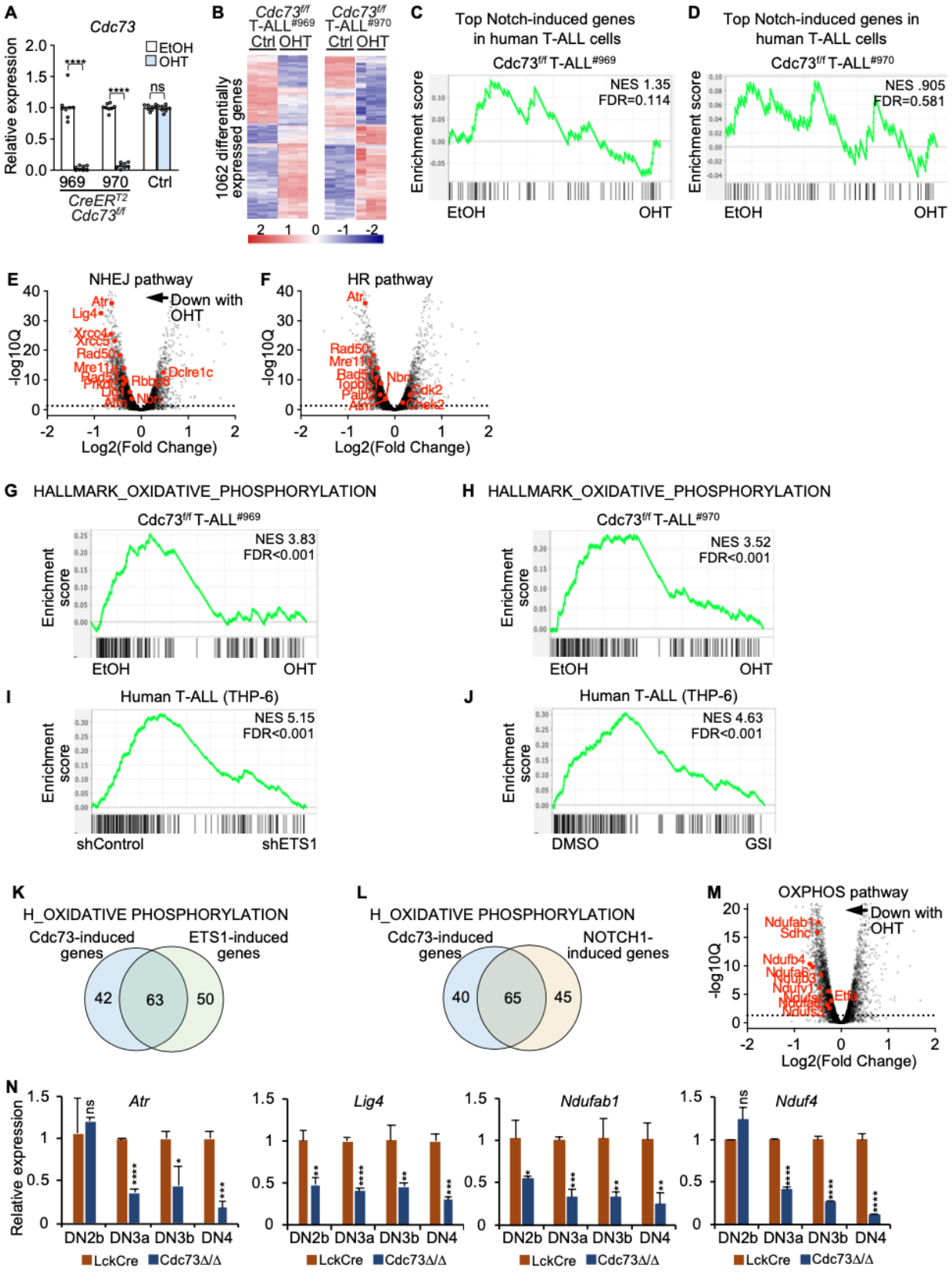

Figure 7 Cdc73 shares Notch- and ETS1 driven pathways

A) Relative expression of Cdc73 in the 969 and 970 Rosa26CreERT2 Cdc73f/f DE/Notch1-induced T-ALL cell lines and control Rosa26CreERT2 DE/Notch1-induced T-ALL cell line after treatment with OHT for 30 hours. B) Heatmap of 1062 differentially expressed genes upon Cdc73 deletion shared between the 969 and 970 cell lines. C-D) GSEA using the direct Notch target signature in T-ALL (Wang et al., 2014) of Cdc73-induced genes. E-F) Volcano plots of significance vs. Bru-Seq Log2FC data showing the control vs. OHT (Cdc73D/D) comparison and important genes in the non-homologous end-joining (NHEJ; E) and homologous recombination (HR; F) pathways in 970 T-ALL cells on background of all genes (grey) giving average RPKM>0.8. G-J) GSEA using the MSigDB Hallmark_Oxidative_Phosphorylation gene list of Cdc73-induced genes in 969 cells (G), Cdc73- induced genes in 970 cells (H), ETS1-induced genes in THP-6 cells (McCarter et al., 2020) (I), and Notch- induced genes in THP-6 cells (McCarter et al., 2020) (J). K-L) Venn diagram showing overlap of Cdc73- induced and ETS1-induced (K) or Notch-induced (L) genes in the Hallmark_Oxidative_Phosphorylation gene list. M) Volcano plot of significance vs. Bru-Seq Log2FC data showing the control vs. OHT (Cdc73D/D) comparison and important genes in the oxidative phosphorylation pathways in 970 T-ALL cells on background of all genes (grey) giving average RPKM>0.8. N) Relative expression of important DNA repair (Atr and Lig4) and oxidative phosphorylation (Ndufab1 and Nduf4) genes in sorted thymic subsets from LckCre mice (red) and Cdc73Δ/Δ mice (blue).

3.2 Cdc73 is important for genome integrity

Previous work by others showed that CDC73 is important for genome stability through maintenance of telomere length, homologous recombination repair, transcription-coupled repair, and R-loop clearance at H2BK120ub1-marked sites of transcriptional elongation (Gaillard et al. 2009; Tatum et al. 2011; Wahba et al. 2011; Herr et al. 2015; Nene et al. 2018; Shivji et al. 2018). In one paper, CDC73 was shown to interact with histone H2B to ensure efficient chromatin remodeling around double stranded breaks, promoting DNA accessibility for repair to occur downstream (Herr et al. 2015). We performed a DepMap analysis across many cancer types to evaluate how T-ALL compared to other cancers in its expression of DNA repair genes. Our data showed that T-ALL cells express the highest levels of DNA repair target genes that are shared between Cdc73, Notch and Ets1, suggesting that DNA damage repair must play an important role in the maintenance of T-ALL (Fig. 8A).

Given these data and our data suggesting Cdc73 promotes expression of genes important for DNA repair, we then wondered if Cdc73 helps preserve genome integrity in T-ALL. To test this, we treated *Cdc73*$^{f/f}$ T-ALL cell lines with OHT and measured gH2AX expression. gH2AX is a marker of DNA double-strand (ds) breaks, where histone H2AX gets phosphorylated by

ATR upon dsDNA damage (Kishton et al. 2016). Consistently, OHT treatment of both *Cdc73*$^{f/f}$ T-ALL cell lines, but not the control cell line, effectively suppressed Cdc73 expression and induced gH2AX expression (Fig. 9A). Further, CDC73 knockdown had similar effects in SUP-T1 and CUTLL1, two human T-ALL cell lines that, like the *Cdc73*$^{f/f}$ T-ALL cell lines, are Notch-induced (Fig. 9B).

Since γH2AX signals cluster at promoters of genes regardless of expression level in T-ALL cell lines (Seo et al. 2012), we examined localization of gH2AX at the promoters of a panel of genes. Based on our data showing global losses of DNA repair gene expression, we predicted that loss of Cdc73 would protect the genomic integrity of even non-expressed genes. Consistently, our qChIP data showed that *Cdc73* deletion induced gH2AX localization to chromatin at non-expressed genes (*Hbaa1*; *Col1a1*) to similar extent as expressed genes (*Myc*; *Lig4*) (Fig. 8B). In contrast, OHT had no effect in control cells (Fig. 8C).

To confirm that *Cdc73* deletion led to spontaneous DNA damage, we performed blinded metaphase spread assays to visually assess chromosomal damage. The slides were blinded by another lab mate before imaging and the data was not deidentified until after the analysis was complete by a second lab mate. The analysis consisted of counting the chromosomes and tracking any damage to them. This included quantifying breaks, gaps, fragments, and fusions of any of the chromosomes. Consistently, across multiple rounds of dropping, imaging, and analysis, we observed an increase chromosomal damage in *Cdc73*$^{f/f}$ T-ALL cells upon treatment with OHT (Fig. 9C-E).

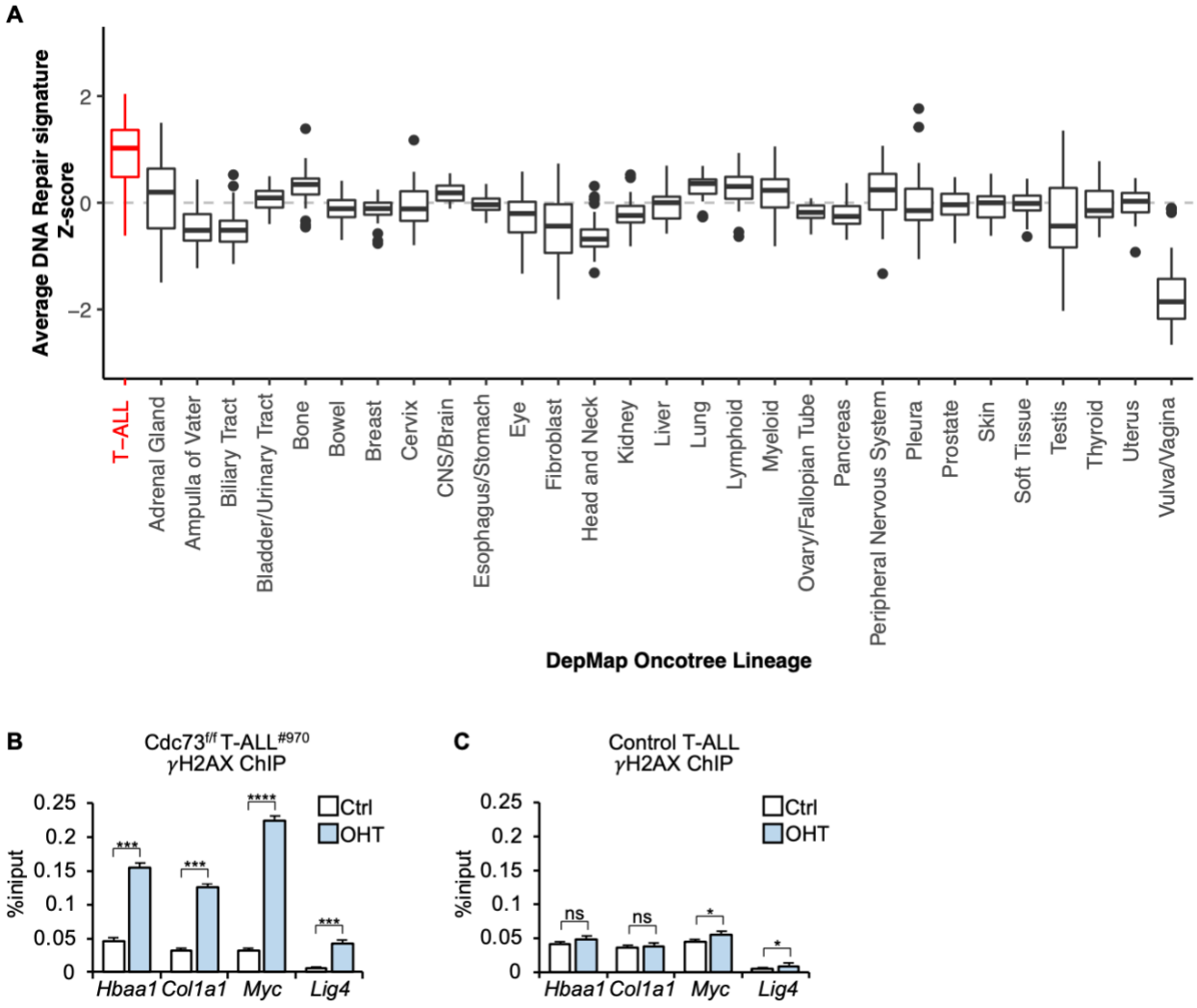

Figure 8 Cdc73 is important for genome integrity

A) Average z-scores of RNA-Seq expression of 34 DNA repair target genes induced by Cdc73, ETS1, and Notch based on GSEA core enrichment analysis using the Kauffman_DNA_repair gene list (Table S1) across all cell lines grouped by Oncotree lineage in DepMap 22Q4. B-C) γH2AX qChIP in Cdc73f/f T-ALL cells (970, B) and control Rosa26CreERT2 T-ALL cells (C) treated with OHT for 30 hours.

We next wondered if these cells were undergoing apoptotic events, a cellular method of programmed cell death to get rid of unwanted or damaged cells. As expected, DNA damage upon loss of *Cdc73* led to small but significant increases in apoptosis (Fig. 9F-G). Next, we sought to determine if T-ALL cells are sensitive to DNA repair inhibition. To test this possibility, we treated both *Cdc73*$^{f/f}$ and human T-ALL cell lines with berzosertib, an an inhibitor

of the apical DNA damage protein kinase, ATR, being tested in advanced clinical trials due to its excellent safety profile. Consistently, these cells were highly sensitive to this drug given low nanomolar GI50 (Fig. 9H). Together, this data suggests that Cdc73 promotes DNA repair globally through gene expression, which extends previous studies and might help protect T-ALL cells from chromosomal damage.

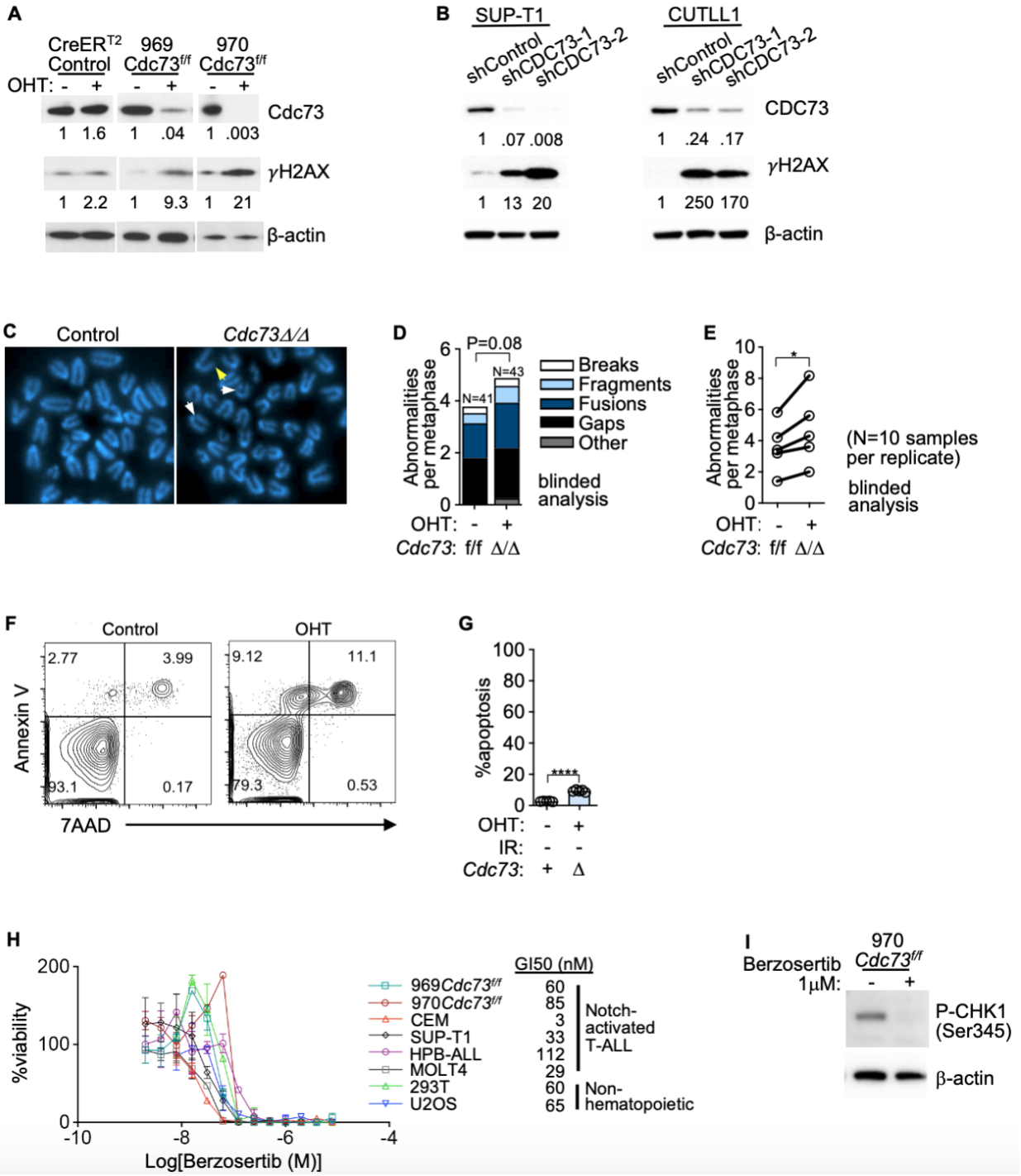

Figure 9 Cdc73 is important for DNA damage repair

A) Western blot for γH2AX in Rosa26CreERT2 Cdc73f/f T-ALL cells (969; 970) and control Rosa26CreERT2 T-ALL cells treated with OHT (hydroxytamoxifen) for 30 hours to delete Cdc73. Numbers represent band intensities normalized to b-actin loading control. B) Western blot for γH2AX in human NOTCH1-induced human T-ALL cell lines (SUP-T1; CUTLL1) transduced with shCDC73. C-E) Representative metaphase spreads (C) and quantification of metaphase abnormalities in aggregate (D) or per replicate (E) in blinded analyses of Cdc73f/f T-ALL cells treated with OHT for 30 hours. White arrows=gaps; yellow arrow=break. F-G) Representative Annexin V/7- AAD flow

cytometric plots (F) and Annexin V+/7-AAD- scatterplot (G) of Cdc73f/f T-ALL cells treated with vehicle (Control) or OHT for 30 hours (Cdc73D/D). H) Dose response curves of Notch-activated T-ALL cell lines and 2 non-hematopoietic tumor cell lines (U2OS and 293T) treated with berzosertib (ATR inhibitor in clinical trials). I) Western blot in UV-treated 970 cells showing effect of berzosertib on P-Chk1, a downstream target of Atr.

3.3 Cdc73 is important for oxidative phosphorylation

Supraphysiological Notch signals in T-ALL create high demand for mitochondrial ATP production (Kishton et al. 2016). Recently, a relationship between NOTCH1 and elevated OXPHOS gene expression has been established as a critical driver for leukemia cell survival, highlighting OXPHOS as a potential therapeutic target in T-ALL (Baran et al. 2022). We performed a DepMap analysis across many cancer types to evaluate how T-ALL compared to other cancers in its expression of OXPHOS genes. Our data showed that T-ALL cells express average levels of OXPHOS target genes that are shared between Cdc73, Notch and Ets1 (leftmost group in Fig. 10).

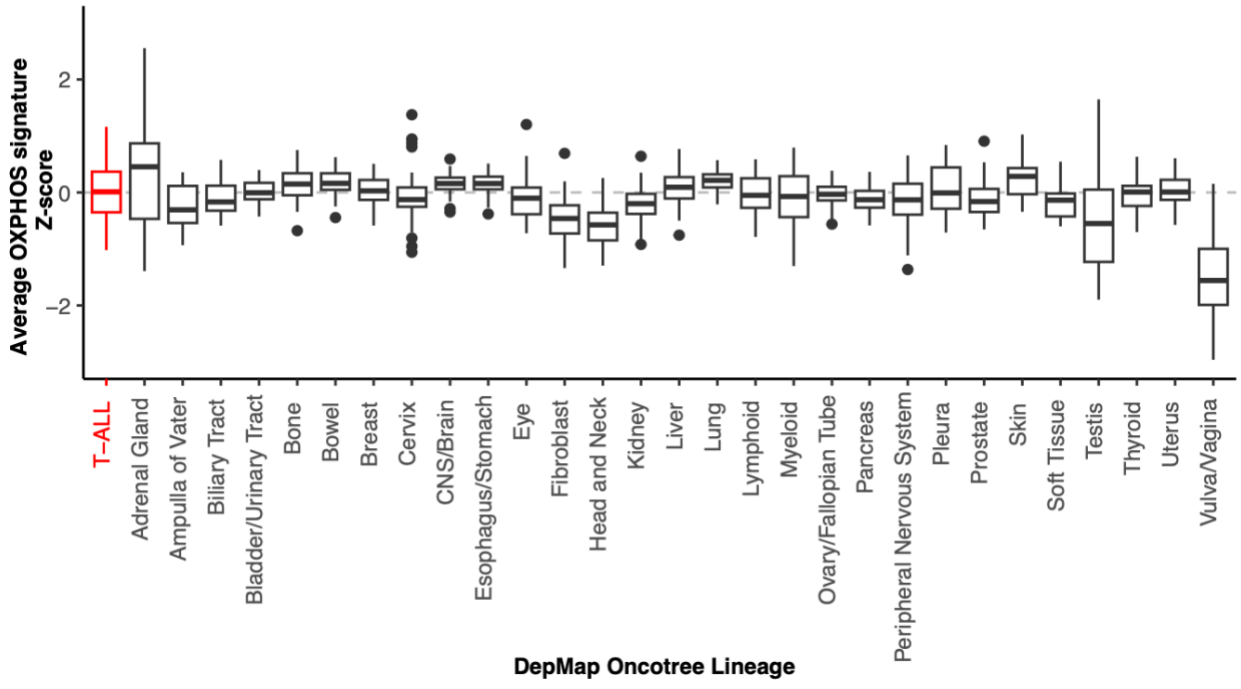

Figure 10 T-ALL express an average amount of OXPHOS genes compared to other cancers

Average z-scores of RNA-Seq expression of 38 OXPHOS genes induced by Cdc73, ETS1, and Notch based on GSEA core enrichment analysis using the Hallmark_oxidative_phosphorylation gene list across all cell lines grouped by lineage in DepMap 22Q4.

Since Cdc73 promotes expression of genes important for the electron transport chain (Fig. 6S; Fig. 7M) and has been shown to interact with NOTCH1, we considered the possibility that Cdc73 helps maintain membrane potential to protect T-ALL cells from metabolic stress. Membrane potential is a readout of energy storage during the oxidative phosphorylation process. The mitochondrial membrane potential is generated by proton pumps, generally regulated by genes in the electron transport chain (ETC) complexes I, III, and IV (Zorova et al.). To test if Cdc73 plays a role in maintaining mitochondrial membrane potential, we treated *Cdc73*$^{f/f}$ T-ALL cell lines with OHT and measured mitochondrial membrane potential of live cells using the tetramethylrhodamine methyl ester assay (TMRM). To assess changes in membrane potential, we incorporated the use of a mitochondrial uncoupler, FCCP. When added to cells, FCCP will collapse the membrane potential by disrupting ATP synthesis, causing protons to flood across the cell membrane. Addition of FCCP would causes a decrease in TMRM staining, or a shift to the left when looking at the mean fluorescent index (MFI). In our data, we saw that *Cdc73* deletion reduced membrane potential to nearly the same degree as FCCP (Fig. 11A-B), suggesting that Cdc73 plays an important role in the maintenance of mitochondrial potential.

Based on our gene expression analysis, we also predicted that *Cdc73* deletion would reduce reactive oxygen species (ROS). ROS are generated during mitochondrial oxidative metabolism. Oxidative stress will occur when there is an overproduction of ROS in a cell (Ray et al.). In turn, oxidative stress can lead to largescale damage of the cell, implicating problems in many different diseases including cancer (Ishikawa et al. 2008; Trachootham et al. 2009). We performed a CellROX assay to asses ROS production with deletion of Cdc73. We used TBHP

(tert-Butyl hydroperoxide) as a positive control, as it is a strong oxidant that will causes an increase in ROS production. Our CellROX assay showed that loss of *Cdc73* significantly reduced ROS production compared to controls (Fig. 11C-D). Additionally, our gene expression analyses also predicted impaired oxygen consumption with loss of *Cdc73*. This suggests that Cdc73 might be driving ROS production in T-ALL though mechanisms we do not quite understand yet.

The last measure we looked at in the context of mitochondrial metabolism was oxygen consumption rates. The oxygen consumption rate (OCR) is a measure of cellular respiration rate and mitochondrial function, as the mitochondria produce ATP. Several studies have shown how cells can reprogram their metabolic demand to meet energy needs in cancer phenotypes (Koppenol et al. 2011; Zheng 2012). We wanted to understand if *Cdc73* played a role in the oxidative demand in T-ALL. To answer this question, we performed a mitochondrial stress test using a Seahorse assay extracellular flux analyzer. This assay incorporates the use of three drugs, Oligomycin, FCCP, and a mixture of rotenone and antimycin A. Oligomycin is an inhibitor of ATP synthesis. It blocks the production of ATP from ADP by blocking its proton channel in the ETC complex V (Lee and O'Brien 2010). Addition of this drug causes a decrease in the OCR. FCCP in this assay is also used to uncouple the membrane by stimulating the ETC to operate at its maximum capacity, causing a strong and rapid increase in the OCR (Kumar et al. 2021). Rotenone and antimycin A are added last in this assay. Rotenone inhibits the ETC complex I, causing a decrease in ATP production, ROS production, and mitochondrial potential (Won et al.). Antimycin A causes a block in the passage of protons in ETC complexes III, thereby inhibiting respiration (Pham et al. 2000). The combination of these drugs causes the OCR to drop below the basal OCR. Our mitochondrial stress test showed that *Cdc73* deletion reduced basal

respiration and the mitochondrial ATP production rates of live cells (Fig. 11E-G). In contrast, treating control T-ALL cells with OHT had no significant effect (Fig. 11H-J). To confirm if this effect was consisted in human T-ALL, we performed the same test in human Notch-induced CUTLL1 cells. CDC73 knockdown in live human Notch-induced T-ALL cells also impaired oxygen consumption rates (Fig. 11K-M). Together, this data suggests that Cdc73 promotes OXPHOS, which might help protect T-ALL cells from the metabolic stresses of supraphysiological Notch signaling.

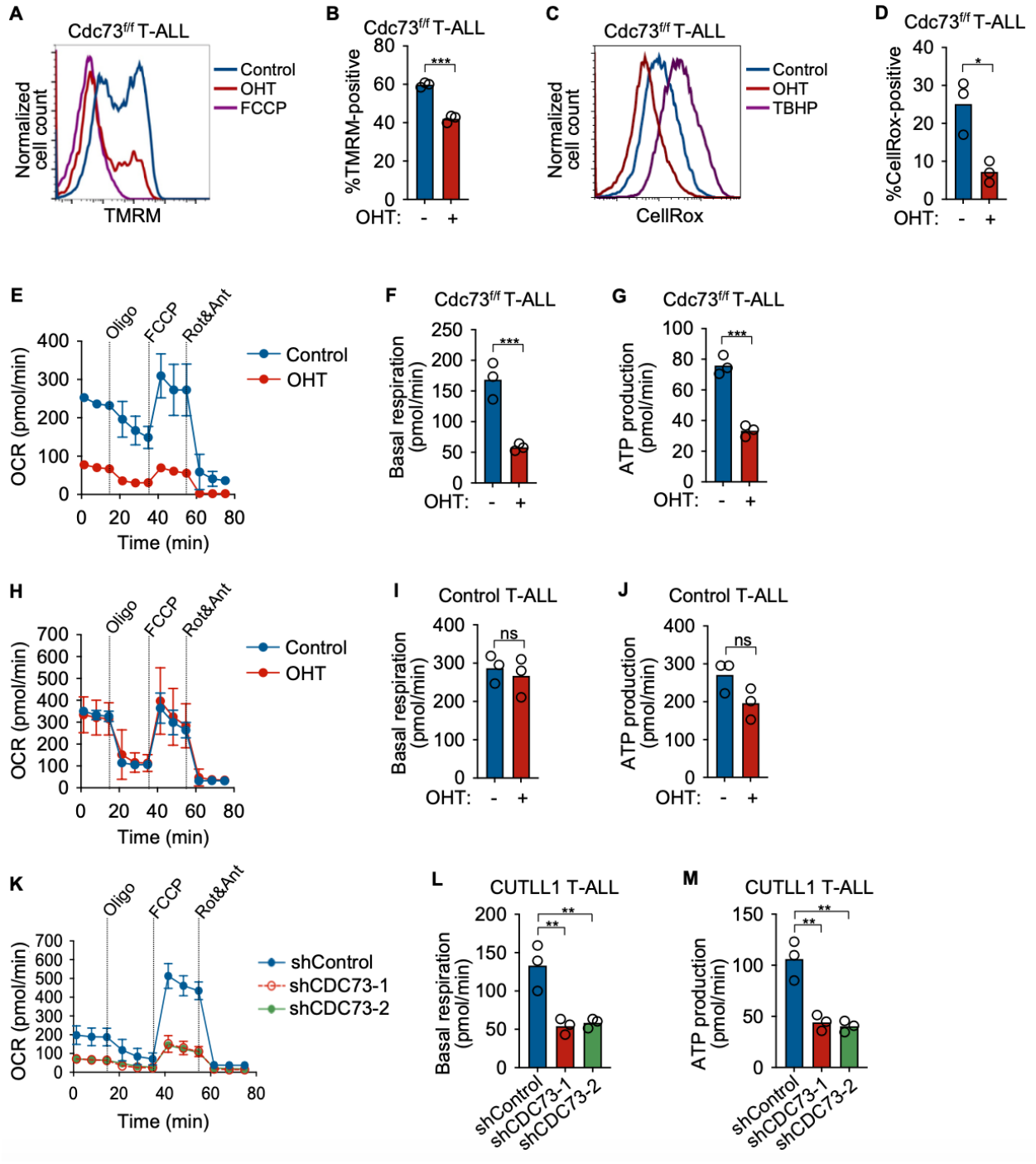

Figure 11 Cdc73 is important for oxidative phosphorylation

A-B) Representative flow cytometric histogram (A) and MFI scatterplot (N=3) (B) showing mitochondrial membrane potentials measured by tetramethylrhodamine methyl ester (TMRM) assay on live Dapi- Rosa26CreERT2 Cdc73f/f T-ALL cells (970) treated with OHT (hydroxytamoxifen) for 30 hours to delete Cdc73. FCCP was added as positive control. C- D) Representative flow cytometric histogram (C) and MFI scatterplot (N=3) (D) showing mitochondrial ROS production measured by the CellROX assay on live Dapi- 970 cells treated with OHT for 30 hours to delete Cdc73. TBHP was added as a positive control. E-M) Seahorse XFe96 instrument measurements of real time oxygen consumption rate (OCR) normalized to live cell number and protein concentration under basal conditions or in

response to the indicated mitochondrial inhibitors (E,H,K) and scatterplots of basal (F,I,L) and ATP production (G,J,M) respiration phases of 970 cells treated with OHT for 30 hours to delete Cdc73 (E-G), control Rosa26CreERT2 cells treated with OHT for 30 hours (H-J); and CUTLL1 cells at 4 days after transduction with two independent shCDC73 (K-M).

3.4 Discussion

Previous studies have identified potentially 'lethal' dsDNA breaks in T-ALL caused by genetic mutations such as RAG1/2 or by production of ROS (Callén et al. 2007; Silva et al. 2011). One paper even stated that T-ALL cells could be addicted to DNA repair machinery to survive spontaneous or induced double stranded breaks (DSBs) (Dasgupta et al.). Therefore, targeting these pathways might be an ideal solution to take advantage of T-ALL cells addiction to DNA repair machinery, by removing components they are addicted to.

My data suggests that *Cdc73* plays an important role in the DNA damage repair pathway and OXPHOS pathway, along with ETS1 and NOTCH1. I showed that deletion of *Cdc73* increased the expression of DNA repair marker γH2AX in murine and human Notch-induced T-ALL cell lines, implying that DNA repair mechanisms turn on when transcriptional machinery, such as members of the PAF1c like *Cdc73,* are mutated (Fig. 9A-B). The mechanism by which they get turned on and what repair pathway specifically gets turned on is yet to be determined. We confirmed that deleting *Cdc73* causes visible damage to the chromosomes (Fig. 9C) and that it sends some cells into apoptosis (Fig. 9F-G). This suggests that T-ALL cells might enter a programmed cell death because damage to the cell is too significant to repair. It also suggests that *Cdc73* has an essential function in DNA damage repair, which might support the cells addiction to DNA repair machinery.

ATM and ATR are PI3K -like serine/threonine kinases that are activated under genotoxic stress conditions that are important for cell death and survival, cell proliferation, and DNA

repair. Interestingly, ATR is also a gene that was down regulated with loss of Cdc73 in the DNA damage repair pathway in T-ALL (Fig. 7E-F). Using an ATR inhibitor, berzosertib, we confirmed that T-ALL cells were sensitive to ATR inhibition (Fig. 9H). Additionally, we confirmed that protein expression of P-Chk1, a target downstream of ATR in the HR pathway, was decreased when my murine cell lines were treated with berzosertib. This implies that DNA repair inhibitors like berzosertib can successfully down regulate DNA repair pathways that T-ALL cells might be addicted to.

Oxidative phosphorylation (OXPHOS) has been shown to be a critical pathway for leukemia cell survival. Recent studies have identified *NOTCH1* to directly regulate OXPHOS and OXPHOS gene expression (Baran et al. 2022). Other cancers, such as B-ALL, have also shown a reliance on OXPHOS as a major metabolic regulator of the cancer type (Chen et al.). Through my research, I have been able to show that *Cdc73* plays an important role in the mitochondrial metabolic regulation of T-ALL. I have shown that loss of *Cdc73* causes a decrease in mitochondrial potential, ROS production, basal OCR and ATP production (Fig. 11A-G, K-M). Together this data suggests that *Cdc73* might be driving a metabolic phenotype that is keeping the T-ALL cells alive and addicted to DNA repair machinery. In my next chapter, I investigate the mechanism by which Cdc73 is regulating these gene pathways and how it fits into the large picture of *Cdc73* and its role in T-ALL maintenance.

Chapter 4 Cdc73 Mechanistically Activates T-ALL Gene Expression Through Canonical and Non-Canonical Functions[3]

4.1 Cdc73 does not primarily promote DNA repair and OXPHOS gene expression though enhancers

Previous groups have shown that the Paf1C regulates enhancer activity by altering eRNA synthesis and H3K27ac deposition (Chen et al. 2017; Ding et al. 2021). To explore this in the context of T-ALL, we used human THP-6 T-ALL cells and performed CDC73 ChIP-seq. Consistent with the other groups data, we observed strong CDC73 ChIP-Seq signals at intergenic regulatory elements relative to promoters (Fig. 12A). This suggest that Cdc73 has important functions at both the promoter and enhancer regions. We next wanted to test whether Cdc73 is regulating enhancer activity in T-ALL, so we performed H3K27ac ChIP-Seq in our *CreER^{T2} Cdc73$^{f/f}$* T-ALL cell lines (969 and 970) and control *CreER^{T2}* T-ALL cell line after OHT treatment. In further support of enhancer functions for Cdc73, our H3K27ac ChIP-Seq showed differential H3K27ac signals upon *Cdc73* deletion at FDR<0.05 (Fig. 12B, 13A-B). In contrast, OHT had little effect on the control cells (Fig. 13C).

Next, we wanted to determine how many peaks were "dynamic H3K27ac peaks". We defined these peaks based on differential H3K27ac signals at FDR<0.05 in the same direction for

[3] Adapted from Cdc73 protects Notch-induced T-cell leukemia cells from DNA damage and mitochondrial stress Ashley F. Melnick, Anna C. McCarter, Shannon Liang, Yiran Liu, Qing Wang, Nicole A. Dean, Elizabeth Choe, Nicholas Kunnath, Geethika Bodanapu, Carea Mullin, Fatema Akter, Karena Lin, Brian Magnuson, Surinder Kumar, David B. Lombard, Andrew G. Muntean, Mats Ljungman, JoAnn Sekiguchi, Russell J.H. Ryan, Mark Y. Chiang. bioRxiv 2023.01.22.525059; doi: https://doi.org/10.1101/2023.01.22.525059. The data from this chapter was completed with the help from those listed in the acknowledgements section of this manuscript.

both *CreER^{T2} Cdc73$^{f/f}$* T-ALL cell lines but not the control *CreER^{T2}* T-ALL cell line. When we intersected our CDC73 ChIP-seq and H3K27Ac ChIP-seq datasets, we obtained 9,139 "dynamic H3K27ac peaks". In general, *Cdc73* deletion decreased H3K27ac signals at dynamic intergenic H3K27ac peaks (Fig.12C, 13D). Together, these data suggest that Cdc73 can promote enhancer activity more than it represses enhancer activity in the context of T-ALL.

Since Paf1C regulates enhancer activity through eRNA synthesis (Chen et al. 2017; Ding et al. 2021), we next wanted to identify any enhancers that are directly regulated by Cdc73. To do this, we integrated our dynamic H3K27ac dataset with a differential analysis of eRNA expression. To look at eRNA expression, we performed BruUV-seq on the *CreER^{T2} Cdc73$^{f/f}$* T-ALL cell lines (969 and 970) and control *CreER^{T2}* T-ALL cell line. BruUV-seq is a nascent RNA technique that detects and quantifies rapidly degraded RNAs, such as eRNAs, and is performed using living cells (Magnuson et al. 2015). This method utilizes UV light to introduce random transcription-blocking DNA lesions into the genome, prior to using bromouridine (BrU) labeling. The lesions cause elongating RNA Pol II to stall. By only blocking transcription elongation and not initiation, the UV light can redistribute transcriptional reads that enhance nascent RNA signals towards the 5' end around promoters and enhancers, which allows for better identification of transcription start sites (TSS) (Magnuson et al. 2015). Using this method, we identified 609 differential eRNAs at $q<0.05$ upon *Cdc73* deletion that were shared by both *Cdc73$^{f/f}$* T-ALL cell lines but not by the control cell line (Fig.12D-E, 13E-F).

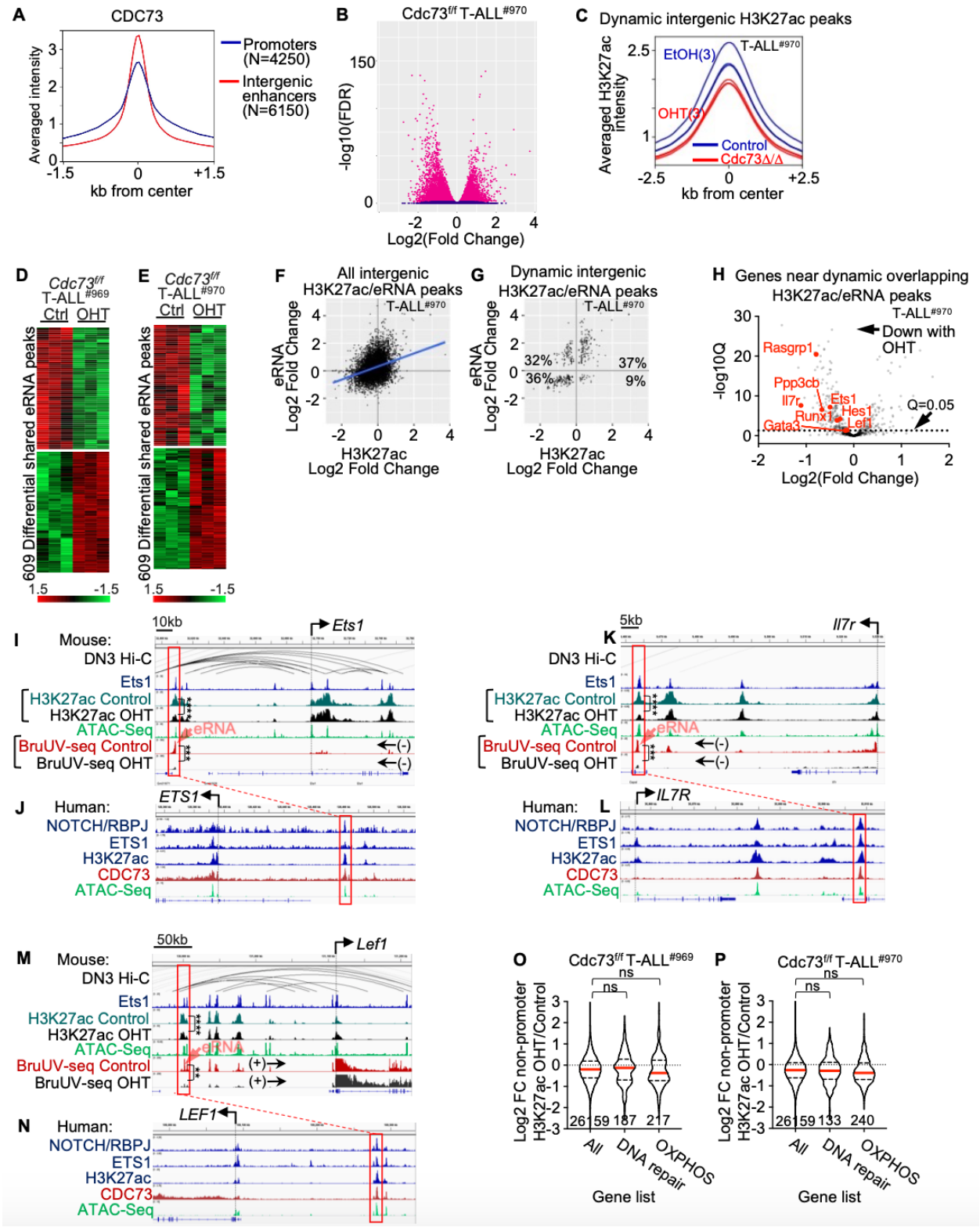

Figure 12 Cdc73 does not primarily promote DNA repair and OXPHOS gene expression through enhancers

A) Metagene plots of intergenic and promoter CDC73 ChIP-Seq signals in THP-6 cells. B) Volcano plots of significance vs. Log2(Fold Change OHT/Control) H3K27ac ChIP-Seq signals of Rosa26CreERT2 Cdc73f/f T-ALL

cells (970) upon treatment with 6nM OHT for 30 hours. C) Metagene plots of dynamic intergenic H3K27ac signals (FDR<0.05 in 969 and 970 cells but not in control cells) in 970 cells. D-E) Heatmaps of differential eRNA peaks shared between the 969 (E) and 970 (E) cell lines. eRNAs were defined as intergenic BruUV-Seq peaks or intragenic peaks that were antisense in direction relative to mRNAs. F-G) BruUV-Seq Log2(OHT/Control) versus H3K27ac Log2(OHT/Control) scatterplots of all overlapping intergenic peaks (F) or overlapping dynamic intergenic peaks (G) in Cdc73f/f 970 T-ALL cells. Overlapping "dynamic peaks" were defined as giving q<0.05 and FDR<0.05 in the same direction for the BruUV-Seq and H3K27ac comparisons respectively in both Cdc73f/f T-ALL cells but not in control T-ALL cells. H) Volcano plot of significance vs. Bru-Seq Log2(OHT/Control) of genes nearest OHT-downregulated dynamic intergenic BruUV-Seq and H3K27ac overlapping peaks in 970 Cdc73f/f T-ALL cells. I-N) Display tracks of indicated ChIP-Seq and ATAC-seq datasets at the Ets1 (I-J), Il7r (K-L), and Lef1 (M-N) loci in mouse 969 cells (I, K, M) or human THP-6 cells (J, L, N) showing nearest mouse-human homologous enhancers in red boxes that contain overlapping dynamic intergenic eRNA and H3K27ac peaks. Ets1 ChIP- seq (GSM461516); ATAC-seq (GSM2461649); DN3 Hi-C (GSE79422) analyzed in (Kashiwagi et al. 2022). O-P) Violin plots showing H2K27ac ChIP-Seq Log2FC in 969 cells (O) and 970 cells (P) at non-promoter H2K27ac peaks nearest all genes, DNA repair genes, and OXPHOS genes in the GSEA enrichment cores of 969 and 970 cells (Table S1). OHT was added for 30 hours to delete Cdc73. Numbers below violin plots represent number of genes. **FDR<0.01; ***FDR<0.001; ****FDR<0.0001.

Next, we integrated the H3K27ac and BruUV-seq datasets to identify intergenic H3K27ac and eRNA peaks that overlapped in both T-ALL cell lines. There was no correlation between changes in eRNA and H3K27ac signal in control cells (Fig. 13G). In contrast, there was modest correlation in *Cdc73*$^{f/f}$ T-ALL cells (Fig. 12F, 13H). To determine the genomic locations where Cdc73 might have a strong and direct effect on enhancers, we defined "dynamic eRNA peaks" as giving q<0.05 in the same direction for the BruUV-seq comparison in both *Cdc73*$^{f/f}$ T-ALL cells but not in control T-ALL cells. We saw that changes in dynamic intergenic H3K27ac signals showed no correlation in control cells (Fig. 13I), however there was strong correlation in both *Cdc73*$^{f/f}$ T-ALL cells with changes in dynamic intergenic eRNA signals (r>0.66; Fig. 12G, 13J-K). Together, this data suggests that CDC73 can coordinate and regulate eRNA synthesis and enhancer activity in the context of T-ALL, extending previous data in other cell types.

We were next interested in identifying direct target genes of Cdc73. To do this, we associated overlapping dynamic intergenic H3K27ac and eRNA peaks that diminish upon *Cdc73* deletion with the nearest expressed genes. We found that *Cdc73* deletion downregulated H3K27ac/eRNA peaks that were associated with *Cdc73* deletion downregulated expression of

several known genes that are important for maintaining T-ALL proliferation. These include genes such as *Il7r, Ets1, Rasgrp1,* and *Lef1* (Hartzell et al. 2013; Ksionda et al. 2016; Oliveira et al. 2019; Silva et al. 2021; Carr et al. 2022) (Fig. 12H-N, 13L-N). *Il7r* and *Lef1* are known direct Notch target genes (Spaulding et al. 2007; Gonzalez-Garcia et al. 2009; Wang et al. 2014). *Lef1* is Notch1 dependent in T-cell lymphomas but not T-cell progenitors. (Spaulding et al. 2007). Additionally, Notch1 can be found at the *Lef1* promoter (Spaulding et al. 2007). *IL7R* expression is impaired by defective Notch signaling. Additionally, Notch1 can bind to the *IL7R* promoter to regulate *IL7R* transcription. Importantly, in our data, we consistently observed CDC73 occupancy at homologous human enhancers (Fig. 12J, 12L, 12N, 13N). RBPJ/Notch and ETS1 occupancy was often observed, but not consistently.

In our analysis of publicly available Hi-C datasets of DN3 cells we confirmed interactions of these enhancers with respective promoters, except for the previously described Notch-dependent *Il7r* enhancer (Wang et al. 2014), presumably because DN3 cells express little *Il7r*. Interestingly, we did not observe association of overlapping dynamic intergenic H3K27ac/eRNA peaks with core enrichment genes from our GSEA pathway analyses in DNA repair (Fig. 6I-J, Appendix Table 1-3) or OXPHOS (Fig. 7G-H, Appendix Table 4-5). Furthermore, we did not observe any differences in H3K27ac signal changes upon *Cdc73* deletion at non-promoter peaks nearest DNA repair or OXPHOS genes relative to all genes in both cell lines (Fig. 12O-P, 13O-R). Together, this data suggests that Cdc73 can activate enhancers that induce important T-ALL driver genes. However, these non-canonical functions do not appear to induce expression of DNA repair and OXPHOS genes.

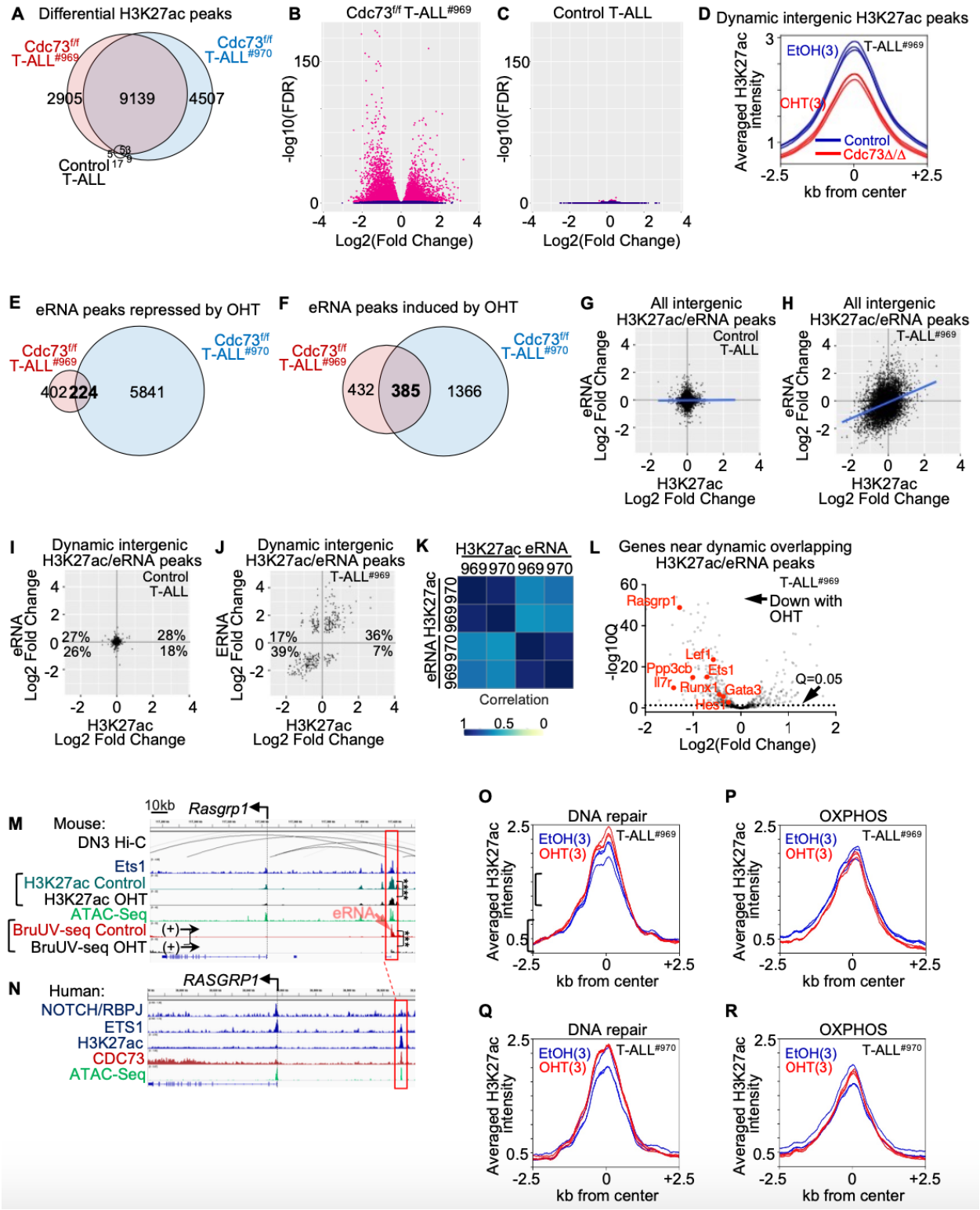

Figure 13 Cdc73 does not primarily promote DNA repair and oxidative phosphorylation pathways through enhancers

A) Venn diagram of differential H3K27ac (FDR<0.05) in Rosa26CreERT2 Cdc73f/f T-ALL cells (969; 970) and control Rosa26CreERT2 T-ALL cells upon treatment with 6nM OHT for 30 hours. B-C) Volcano plots of significance

vs. Log2(OHT/Control) H3K27ac ChIP-Seq signals of 969 (B) and control (C) cells in (A). D) Metagene plot of dynamic intergenic H3K27ac signals (defined as FDR<0.05 in 969 and 970 cells but not in control cells) in 969 cells. E-F) Venn diagram of differential eRNAs in Cdc73f/f T-ALL cells (969; 970) that were repressed (E) or induced (F) upon treatment with 6nM OHT for 30 hours. eRNAs were defined as intergenic BruUV-Seq peaks or intragenic peaks that were antisense in direction relative to mRNAs. No differential eRNAs were identified after OHT treatment of control T-ALL cells. G-J) BruUV-Seq Log2(OHT/Control) versus H3K27ac Log2(OHT/Control) scatterplots of all overlapping intergenic peaks (G-H) or overlapping dynamic intergenic peaks (I-J) in control T-ALL cells (G, I) and Cdc73f/f T-ALL cells (969; H, J). Overlapping "dynamic peaks" were defined as giving q<0.05 and FDR<0.05 in the same direction for the BruUV-Seq and H3K27ac comparisons respectively in both Cdc73f/f T-ALL cells but not in control T-ALL cells. K) Spearman's correlation coefficient analysis of eRNA and H3K27ac Log2(OHT/Control) from (J and Fig. S7G) in 969 and 970 Cdc73f/f T-ALL cells. L) Volcano plot of significance vs. Bru-Seq Log2(OHT/Control) of genes nearest overlapping OHT-downregulated dynamic intergenic BruUV-Seq and H3K27ac peaks in 969 Cdc73f/f T-ALL cells. M-N) Display tracks of indicated ChIP-Seq and ATAC-Seq datasets at the Rasgrp1 locus in mouse 969 cells (M) or human THP-6 cells (N) showing nearest mouse-human homologous enhancers in red boxes that contain overlapping dynamic intergenic eRNA and H3K27ac peaks. Ets1 ChIP-seq (GSM461516); ATAC-seq (GSM2461649); DN3 Hi-C (GSE79422) analyzed in (Kashiwagi et al. 2022). O-R) Metagene plots of H3K27ac signals at non-promoter H2K27ac peaks nearest DNA repair (O, Q) and OXPHOS genes (P, R) from Table S1 in 969 cells (O-P) and 970 cells (Q-R). **FDR<0.01; ***FDR<0.001; NS=not significant.

4.2 Cdc73 promotes DNA repair and OXPHOS genes through canonical functions at gene bodies

Since Cdc73 did not appear to induce expression of either DNA repair or OXPHOS genes through its role at enhancers, we considered the possibility that Cdc73 could be inducing these genes through its well-established canonical functions in promoting mRNA synthesis at gene bodies. To test this, we performed a CDC73 Chip-seq experiment in human THP-6 T-ALL cells and first counted the number of CDC73 tags between the transcriptional start site (TSS) and transcriptional termination site (TTS) of GSEA core enrichment genes in found DNA repair or OXPHOS gene sets (Appendix Tables 1-6, Fig. 14A). Consistent with our previous data, we found that CDC73 tags were generally more abundant at DNA repair and OXPHOS genes relative to all expressed genes. We compared this data using our ETS1 ChIP-seq data and RBPJ/Notch ChIP-seq data in the same human T-ALL cell line and saw that like CDC73, ETS1 and RBPJ/Notch tags were also more abundant at promoters of DNA repair and OXPHOS genes (Fig. 14B-C). This observation is consistent with our ChIP-Seq and gene expression analyses showing that CDC73 intersects with both the ETS1 and Notch pathways. Together, this data

suggests that CDC73, ETS1 and Notch might function at the promoters of DNA repair and OXPHOS genes to regulate T-ALL.

To further investigate the role of CDC73 at gene bodies, we wanted to look at a very-well established histone mark important in transcriptional elongation, H2BK120ub1. We chose H2BK120ub1 since one of the best-established mRNA functions of Paf1C is to promote transcriptional elongation by recruiting the Bre1-Rad6 E3 ubiquitin ligase complex to monoubiquitinate H2BK120 (Ng et al. 2003; Kim et al. 2009; Kim and Roeder 2009; Van Oss et al. 2016; Chen et al. 2021). Additionally, Bre1-mutated flies displayed a notched wing phonotype and paired transcription of Notch target genes, leading to defective expression (Bray et al. 2005).To look at H2BK120 monoubiquitination, we performed H2BK120ub1 ChIP-Seq on our *CreER*^{T2} *Cdc73*$^{f/f}$ T-ALL cell lines upon treatment with OHT to delete *Cdc73*. Consistent with its H2BK120 monoubiquitination functions, *Cdc73* deletion reduced the greatest H2BK120ub1 signal at mouse genes that were ranked in the top tercile of CDC73 signal at homologous human genes (Fig. 15A, 15D). This is relative to the middle tercile (Fig. 15B, 15E) and bottom tercile CDC73 signal (Fig. 15C, 15F) in both *Cdc73*$^{f/f}$ cell lines. *Cdc73* deletion also generally downregulated H2BK120ub1 signals at DNA repair and OXPHOS genes relative to all genes in both *Cdc73*$^{f/f}$ cell lines (Fig. 14D-H, Fig. 15G-I).

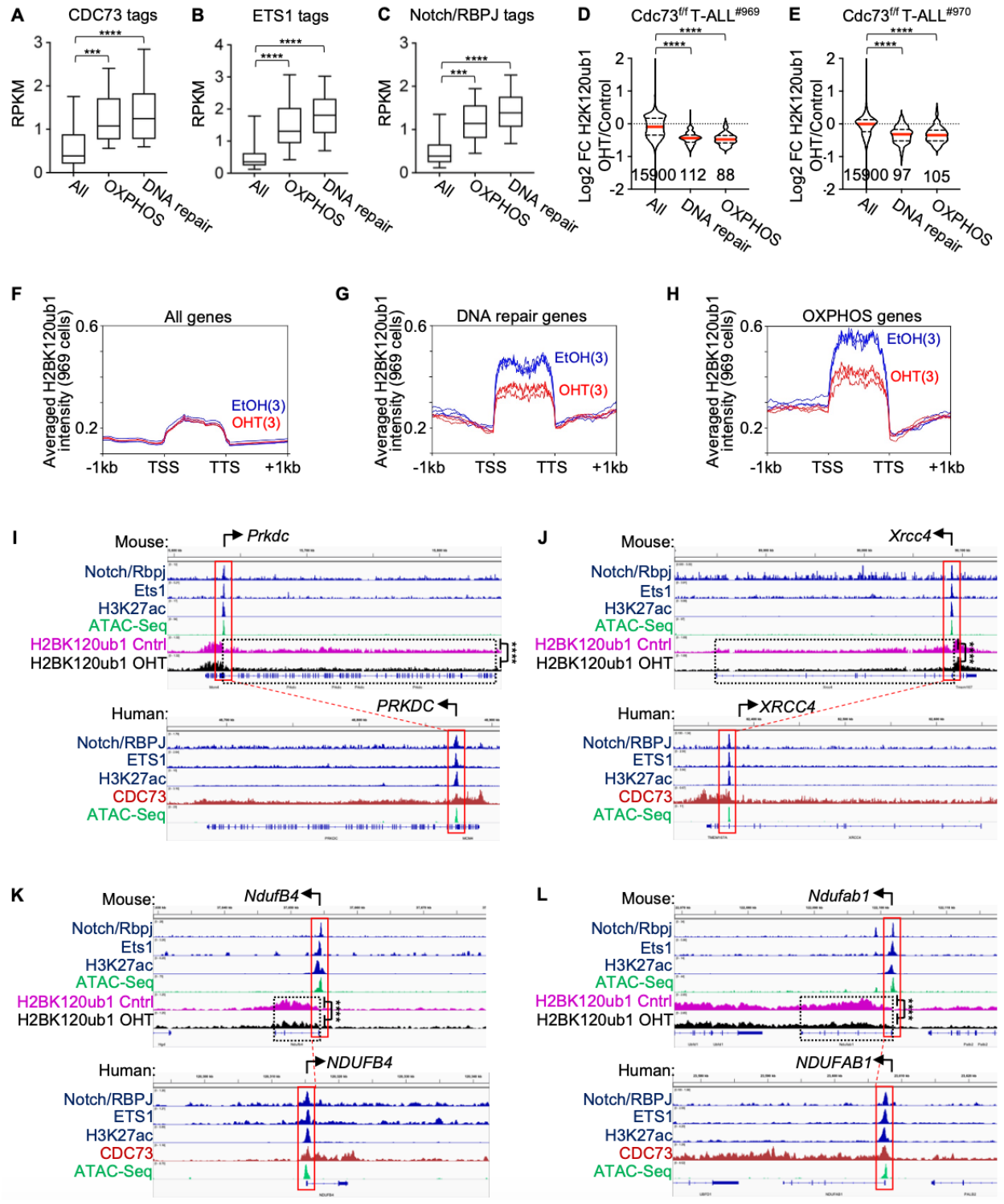

Figure 14 Cdc73 promotes DNA repair and OXPHOS gene expression through canonical mRNA functions at gene bodies

A-C) Box and whisker plots of CDC73 (A), ETS1 (B), and Notch/RBPJ (C) tag counts in human THP-6 cells at gene bodies (A) and promoters (B-C) of all genes, OXPHOS genes, and DNA repair genes shared by the GSEA enrichment cores in Cdc73f/f 969 and 970 T-ALL cells (Fig. 3I, Fig. S4G, Table S1). D-E). Violin plots showing H2BK120ub1

ChIP-Seq Log2FC in 969 cells (D) and 970 cells (E) for all genes, DNA repair genes, and OXPHOS genes in the GSEA enrichment cores of 969 and 970 cells (Table S1). OHT was added for 30 hours to delete Cdc73. F-H) Metagene plots of H2BK120ub1 signals in EtOH- (blue) and OHT- (red) treated 969 cells at all genes (F), DNA repair genes (G), and OXPHOS genes (H) in core enrichment genes of GSEA analyses (Table S1). I-L) Display tracks of indicated ChIP-Seq and ATAC- Seq datasets at important DNA repair genes (I-J) and OXPHOS genes (K-L) in mouse 969 cells (top) or human THP-6 cells (bottom) showing representative tracks and FDR values upon OHT addition (Cdc73 deletion) of H2BK120ub1 signals between TSS and TTS. ****FDR<0.0001. ATAC-seq (GSM2461649). Ets1 ChIP-Seq (GSM2461515).

We were interested to see if we could identify specific DNA repair and OXPHOS genes where we saw downregulation of H2BK120ub1 signal at their gene bodies. For example, we observed significant downregulation (FDR<0.01) of H2BK120ub1 counts at important DNA repair genes such as *Prkdc*, *Xrcc4, Rad50* and *Atr* (Fig. 14I-J; Fig. 15J-K). We also saw significant downregulation (FDR<0.01) of H2BK120ub1 counts at important OXPHOS genes such as *NdufB4*, *Ndufab1*, *Etfa*, and *Ndufa6* (Fig. 14K-L, 15L-M). Importantly, broad CDC73 signals were consistently observed across the gene bodies of the homologous human genes for both DNA repair and OXPHOS genes (bottom panels, Fig. 14I-L and Fig. 15J-M).

As expected, based on our genome-wide analyses of ETS1 and RBPJ/Notch binding in Fig. 14B-C, we also consistently observed occupancy of these factors at the promoters of the mouse genes and human homologs. DNA repair and OXPHOS genes generally showed higher H2BK120ub1 and CDC73 signals relative to all genes, which is consistent with its monoubiquitinating functions. Core enrichment analysis showed that Notch induces 5 out the 8 genes while ETS1 induces all 8 genes. Together, our data suggests that CDC73 might directly induce DNA repair and OXPHOS genes through promoting H2BK120 monoubiquitination and mRNA synthesis and to support ETS1 and NOTCH1 functions.in Notch-driven T-ALL.

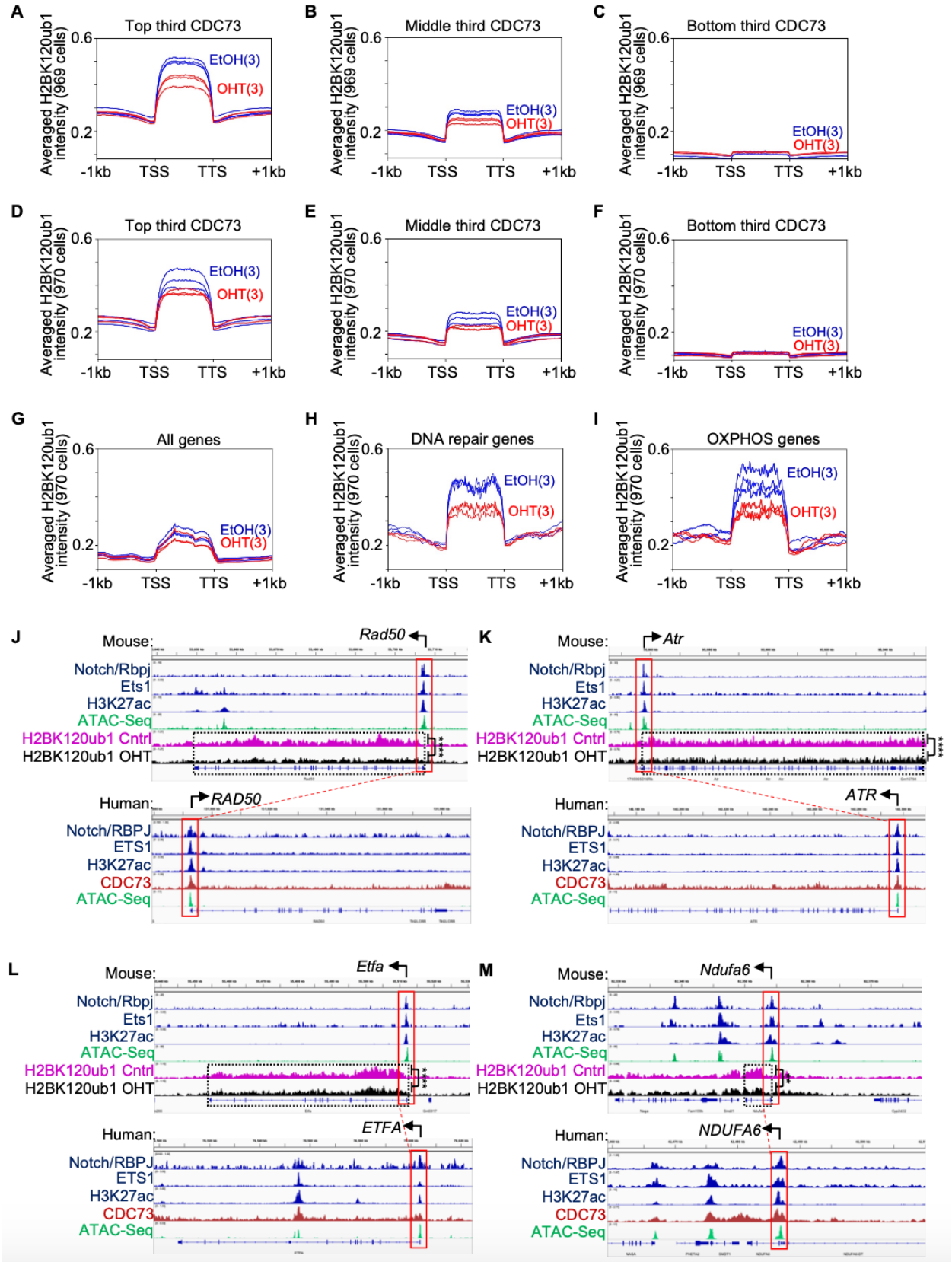
A
Top third CDC73
Averaged H2BK120ub1 intensity (969 cells)
EtOH(3)
OHT(3)
-1kb TSS TTS +1kb
B
Middle third CDC73
C
Bottom third CDC73
D
Top third CDC73
Averaged H2BK120ub1 intensity (970 cells)
E
Middle third CDC73
F
Bottom third CDC73
G
All genes
H
DNA repair genes
I
OXPHOS genes
J
Mouse:
Rad50
Notch/Rbpj
Ets1
H3K27ac
ATAC-Seq
H2BK120ub1 Cntrl
H2BK120ub1 OHT
Human:
RAD50
Notch/RBPJ
ETS1
CDC73
K
Atr
ATR
L
Etfa
ETFA
M
Ndufa6
NDUFA6

Figure 15 Cdc73 promotes DNA repair and OXPHOS gene at gene bodies

A-F) Metagene plots of H2BK120ub1 signals in EtOH (blue) and OHT (red) treated 969 cells (A-C) and 970 cells (D-F) at genes with CDC73 signals of human homologs in THP-6 cells ranked at the top tercile (A,D), middle tercile (B,E), and bottom tercile (C,F). G-I) Metagene plots of H2BK120ub1 signals in EtOH- (blue) and OHT- (red) treated 970 cells at all genes (G), DNA repair genes (H), and OXPHOS genes (I) in core enrichment genes of GSEA analyses (Fig. 3J, Fig. S4H, Table S1). J-M) Display tracks of indicated ChIP-Seq and ATAC-Seq datasets at DNA repair genes (J-K) and OXPHOS genes (L-M) in mouse 969 cells (top) or human THP-6 cells (bottom) showing representative tracks and FDR values upon OHT addition (Cdc73 deletion) of H2K120ub1 signals between TSS and TTS. **FDR<0.01. ****FDR<0.0001. ATAC-seq (GSM2461649). Ets1 ChIP-Seq (GSM2461515).

4.3 Discussion

With the importance of Notch signaling controlling developmentally important activities in many tissues, this raises multiple difficulties for developing anti-Notch therapies that directly target Notch. Emerging evidence originating in *Drosophila* highlights an alternative strategy of targeting transcriptional regulators that co-bind Notch-occupied regulatory elements (Bray 2016; Falo-Sanjuan and Bray 2019).

Previous work showed that NOTCH1 bound CDC73 in breast cancer cells and relied on Paf1C to induce Notch target gene expression for *Drosophila* wing development (Bray et al. 2005; Tenney et al. 2006; Kikuchi et al. 2016). In T-ALL, cells hijack transcriptional programing, like NOTCH1 and the PAF1c, from normal T-cell development to drive proliferation. In chapter 2, we confirmed the NOTCH1-CDC73 interaction in T-ALL cells. However, in chapters 3 and 4, we determined that this interaction is context dependent. This was shown in my previous chapters by RBPJ/Notch co-occupying only a subset of CDC73-bound elements, which were highly enriched for ETS motifs and ETS1 occupancy. We saw ETS1 interacted with CDC73 and ETS1 knockdown generally impaired CDC73 binding to chromatin where ETS1 was also bound. We extend previous studies by showing that chromatin context, here CDC73 interacting with ETS1 in T-ALL, might restrict the NOTCH1-CDC73 interaction.

From a functional standpoint, Cdc73 has been shown to act as a tumor suppressor in some cancers (Carpten et al. 2002b; Wang et al. 2005; Hanks et al. 2014) and as an oncogene in other cancers like Acute Myeloid Leukemia (AML) (Muntean et al. 2010; Zeng and Xu 2015; Zhi et al. 2015; Karmakar et al. 2017; Saha et al. 2019). In chapter 3, we showed that the role of Cdc73 in T-ALL is more consistent with functioning as an oncogene. We show this in chapter 2 where *Cdc73* deletion in mice impaired Notch-dependent T-cell development and leukemogenesis in mouse and human models. This was consistent with our chromatin profiling, gene expression analyses in chapter 3, showing that Cdc73, Notch and Ets1 converge at only on a subset of Cdc73-induced pathways, including DNA repair and OXPHOS. This was notable in this chapter, where we saw an enhancement in ~60% of Cdc73 target genes involved in DNA repair and OXPHOS through canonical functions. Alternatively, Cdc73 functioned at key oncogenes like *Il7r* and *Lef1* through non-canonical enhancer functions.

Conversely, CDC73 also intersects and supports a subset of Notch and ETS1 functions, however we show no evidence that Cdc73 performs these actions exclusively in a Notch-dependent or T-ALL-specific context. On the contrary, Cdc73 does appear to have similar functions in MLL-driven AML cells, which are Notch-independent and non-lymphoid.

Previous work by others showed that CDC73 is important for genome stability at telomeres and actively transcribed genes (Gaillard et al. 2009; Tatum et al. 2011; Wahba et al. 2011; Herr et al. 2015; Nene et al. 2018; Shivji et al. 2018). In this chapter, we extend this work further by showing that Cdc73 might have a more global effect. We show this though our data that suggests Cdc73 promotes the expression of DNA repair genes, particularly those required for double-stranded DNA break repair, and often intersecting with the Notch pathway at ~60% of these genes. Consistently, our data shows that *Cdc73* deletion increased chromosomal damage

and induced γH2AX expression. This data provides rationale for looking further into Cdc73 functions at the promoter regions in the context of T-ALL.

Previous groups have shown that T-ALL cells are particularly dependent on the electron transport chain. This is due to Notch-dependent and independent pathways that upregulate two important pathways in T-ALL, MYC and mTORC1. This, therefore, raises demand for ATP production, to generate and fuel anabolic cancer processes (Palomero et al. 2006; Kishton et al. 2016; Garcia-Bermudez et al. 2018; da Silva-Diz et al. 2021; Thandapani et al. 2021). In chapters 3 and 4, we showed that Cdc73 might help replenish cellular energy by enhancing OXPHOS target genes. We saw that these genes often intersect with the Notch pathway at ~60% of these genes. Together with previous studies, our data suggests that Cdc73 can promote a gene expression program important for DNA repair and mitochondrial function. This implies that at some point, Notch intersected with Cdc73 at these specific genes in attempts to mitigate the genotoxic and metabolic stresses of supraphysiological Notch signaling (Fig. 16).

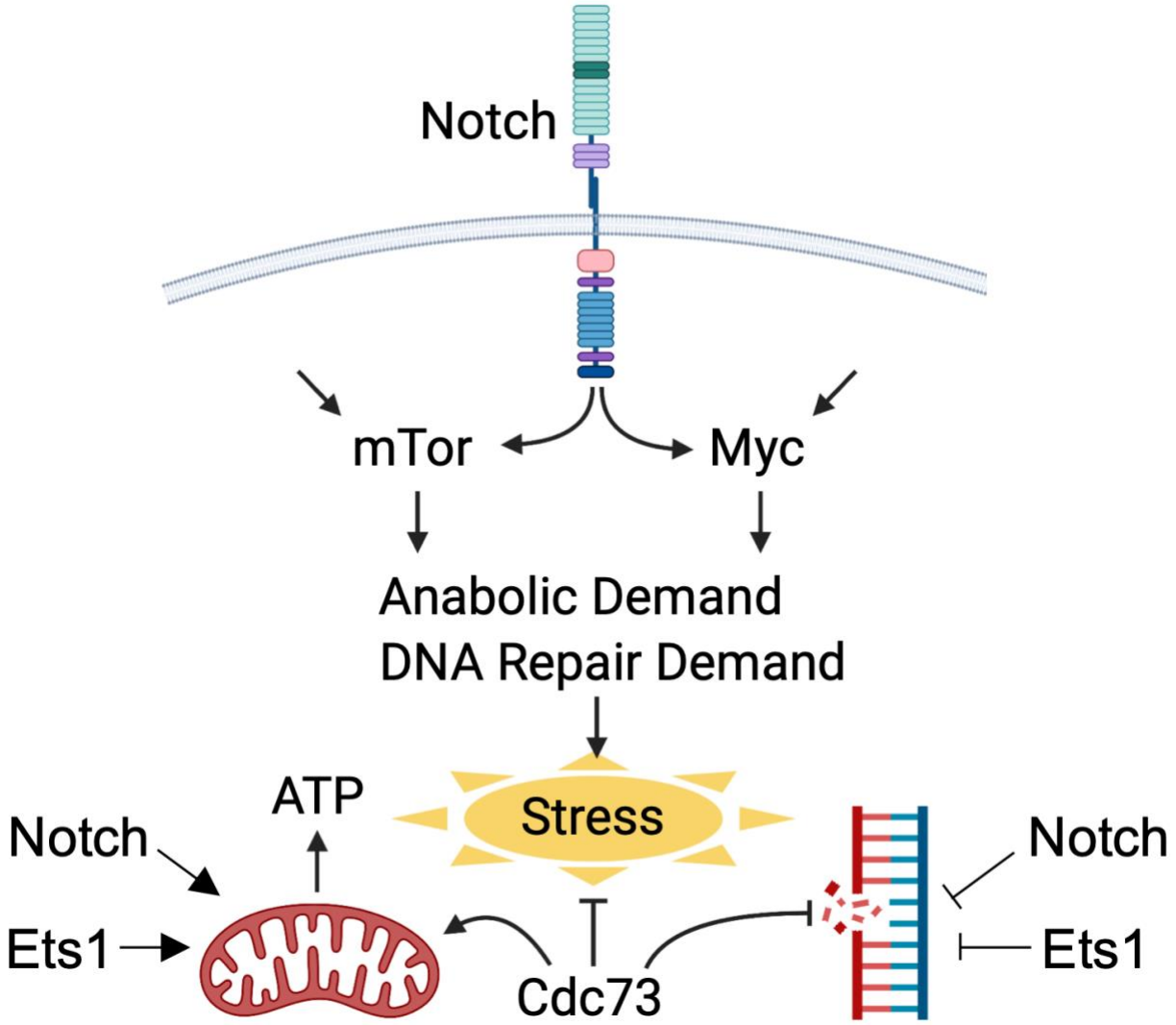

Figure 16 Cdc73, Notch, and Ets1 signals intersect at gene expression to mitigate metabolic and genotoxic stresses of elevated Notch signals

Elevated Notch signals induce major oncogenic pathways, mTorc1 and Myc, which increases demand for cellular energy and DNA repair. Notch, Ets1, and Cdc73 induce mRNA synthesis of a subset of highly expressed genes in DNA repair and oxidative phosphorylation pathways to support elevated and oncogenic Notch functions. Generated using Biorender.

Previous studies by others showed divergent roles of the Paf1C in regulating enhancer activity in colon cancer cells and embryonic stem (ES) cells (Chen et al. 2017; Ding et al. 2021). In the colon cancer study (Chen et al. 2017), they saw that PAF1 repressed eRNA transcription and enhancer activity by maintaining the paused state of Pol II (Chen et al. 2015). In contrast, in

the ES cell study (Ding et al. 2021), they found that Ctr9, a member of the PAF1c, stimulated eRNA transcription and enhancer activity, consistent with the consensus view of Paf1C as an activator of transcription (Jaehning 2010; Yu et al. 2015). This implies that these complexities might be explained by the context dependent nature of Cdc73, or by another positive function for Paf1C in promoting transcriptional elongation beyond the promoter (Hou et al. 2019).

Data from this chapter and chapter 3 is more consistent with the consensus view of Paf1C as an activator of transcription. Our integrated data analysis in chapter 3 showed that *Cdc73* deletion impaired both H3K27ac signals, an indicator of active enhancer activity, and eRNA synthesis at CDC73-bound enhancers associated with known T-ALL drivers. This data also suggested that differential enhancer activity was not linked to differential expression of Cdc73-induced DNA repair or OXPHOS genes. Instead, our mechanistic data from this chapter showed an integrated analysis of CDC73 and H2BK120ub1 signals, suggesting that Cdc73 primarily induces these genes by promoting mRNA synthesis, which is the consensus primary function of the Paf1C. This interpretation is in line with the consensus view that enhancers regulate lineage and developmental stage-specific gene expression while promoters regulate housekeeping gene expression.

From a therapeutic standpoint, my data suggests that DNA repair, oxidative phosphorylation, and CDC73 might be therapeutic targets in T-ALL. However, we are mindful that targeting CDC73 might be toxic based on studies of ubiquitous *Cdc73* deletion (Wang et al. 2008a). Therefore, it is important to focus on future studies, looking at the CDC73 interactome. This will help identify ways to safely and selectively target CDC73 functions which can be explored though mechanisms such as inhibitors of protein-protein interactions.

This study supports the notion that T-ALL cells are a cancer type that is sensitive to inhibition of general transcriptional machinery, as shown in chapter 3. This approach was once considered to be too toxic and dangerous to block, given its vital functions in normal cells (Ott 2014). Previous work showed that T-ALL cells are highly dependent on cofactors of RNA Pol II, such as CDK7, MYC, and BRD4 (Bisgrove et al. 2007; Rahl et al. 2010; Kwiatkowski et al. 2014; Roderick et al. 2014). In this project, we extend so-called "transcriptional addiction" in T-ALL to include CDC73. Previous data from our lab has shown that leukemia-associated NOTCH1 alleles are weak transactivators (Chiang et al. 2008). This current work extends that by suggesting that oncogenic Notch might overcome its inherent weakness by working through local intersection at chromatin by co-binding with transcription factors and powerful RNA synthesis machinery. This, thereby, would induce only the most highly active chromatin and expressed genes. The intersection of these pathways might highlight transcriptional vulnerabilities that could be exploited to target Notch signals without directly targeting the Notch complex, thereby mitigating toxicities.

Chapter 5 Conclusions and Future Directions

5.1 Conclusions

In T-ALL, overactivation of Notch1 leads to an overaccumulation of Notch1 in the membrane. With Notch possessing essential functions in both normal tissue homeostasis and T-ALL, global inhibition of Notch using pan-Notch inhibitors such as gamma-secretase inhibitors, leads to undesirable consequences in the patients receiving them. Thus, the challenge lies in only targeting oncogenic Notch signals. Work by our lab and others supports a model where we only target oncogenic Notch signals by understanding how Notch cofactors interact with Notch. In theory, we can utilize Notch co-factors to down regulate oncogenic Notch signaling. In this dissertation, we studied Cdc73, a member of the Paf1c, shown to interact with Notch in multiple models, including drosophila, yeast, and breast cancer cells. The Paf1c canonically functions at promoter regions and has also been shown to function non-canonically at enhancer regions.

Our studies have shown that Cdc73, Notch, and Notch-cofactor Ets1, co-regulate several pathways in the context of Notch-induced T-ALL, including DNA repair and oxidative phosphorylation. We showed that CDC73, NOTCH, and ETS1 co-bind at the promoter regions of important DNA repair and oxidative phosphorylation genes. In support of a role for Cdc73 at these promoter regions, we also showed that occupancy of H2BK120ub1, a well-established histone mark important in transcriptional elongation, was decreased with loss of Cdc73. Additionally, CDC73, ETS1, and NOTCH1 tags were more frequently associated with DNA repair and OSPHOS genes compared to all genes. This data was supported by functional studies, showing that Cdc73 was important for maintaining membrane potential and oxygen consumption

in murine T-ALL and human T-ALL cell lines, which might explain why we saw increased chromosomal damage and increased DNA damage repair through our metaphase spreads and western blots, respectively. Together, my data suggests that CDC73 might directly induce DNA repair and OXPHOS genes by promoting H2BK120 monoubiquitination and mRNA synthesis and to support ETS1 and NOTCH1 functions.in Notch-driven T-ALL.

We were also able to show that CDC73, NOTCH, and ETS1 all co-bind at the enhancer regions of important T-ALL driver genes including Rasgrp1, Lef1, and Runx1, in human T-ALL cell lines. Using the well-established histone marker H3K27ac used to identify active enhancer activity, and Bru-UV-seq, a method for identifying nascently transcribed eRNAs, we saw that loss of Cdc73 decreased enhancer activity and eRNA production at these T-ALL driver genes in our mouse model, further suggesting a non-canonical role for Cdc73 in regulating enhancer activity. Together, my data suggests that Cdc73 can activate enhancers that induce important T-ALL driver genes.

In conclusion, my data supports a model that suggests Cdc73 is playing an essential role in driving Notch-induced T-ALL. The phenotype I've shown is characterized by an increase in T-ALL proliferation, metabolic needs of the cell, and active DNA damage repair. I've shown that by deleting Cdc73, you can decrease T-ALL proliferation, decrease tumor formation, and significantly improve survival outcomes in our human T-ALL cell lines, PDXs, mouse models, respectively. I've also identified potential areas for further study, including the role of Cdc73, Notch, and Ets1 in driving DNA repair and oxidative phosphorylation.

5.2 Future Directions

Through our research, we now know that Cdc73, Notch, and Ets1 proteins are regulating several pathways that are contributing to T-ALL including DNA repair and oxidative

phosphorylation. Future projects should focus on how these genes are regulating these pathways at the promoter regions. It would be interesting to perform ChIP-seq with antibodies against some of these DNA repair and OXPHOS proteins, such as Prkdc, Xxcr4, Ndufab1, and Ndufb4, to see if occupancy of target gene promoters' changes when you knockout Cdc73.

Since we show that Cdc73 is also regulating T-ALL driver activity at enhancer regions, it would be interesting to understand if this activity at the promoter regions is related to the role of Cdc73 at DNA repair and OXPHOS genes at the enhancer regions. One way to do this is to perform Hi-C analysis and look at enhancer and promoter looping. This method can show which promoters and looping to which enhancers.

Another way to understand if these enhancer/promoter dynamics is to create CRISPRi constructs that silence specific enhancer and promoter regions. For example, if you silence the Ndufab1 promoter region, what happens to Cdc73, Ets1, and Notch occupancy at that promoter? Does anything happen to occupancy at the T-ALL enhancer regions? What would happen if you knocked down Cdc73 and silenced these regions?

In summary, this research suggests further investigation into why and how Cdc73 functions at these different enhancer and promoter regions to drive the T-ALL phenotype. Understanding the mechanism by which Cdc73 works could reveal a potential therapeutic area to investigate for the treatment of T-ALL.

Chapter 6 Methods

6.1 Mice

C57/BL6 mice between the ages of 4-8 weeks and *LckCre* mice were purchased from Taconic. *Rosa26CreER^{T2} Cdc73$^{f/f}$* mice were generated by crossing *Cdc73$^{f/f}$* mice (a gift from Andy Muntean) (Wang et al. 2008a) with *Rosa26CreER^{T2}* mice (Jackson Labs). *Cdc73$^{f/f}$* mice were backcrossed to C57/BL6 strain at least five times prior to use. All mouse experiments were performed according to NIH guidelines and approved protocols from the Institutional Animal Care and Use Committee at the University of Michigan (Ann Arbor).

6.2 Cell lines

CUTLL1 cells were obtained from Adolfo Ferrando and Andrew Weng. All other cell lines including SUP-T1, LOUCY, HPB-ALL, CEM, THP-6, and OP9-DL4 cells were obtained as previously published (McCarter et al. 2020b). All human cell lines were authenticated using STR analysis prior to use (Genetica Corporation). Primary mouse T-ALL cell lines were derived by harvesting splenic or thymic tumors from *Rosa26CreER^{T2} Cdc73$^{f/f}$* or *Rosa26CreER^{T2} Cdc73$^{+/+}$* mice and culturing in 20% RPMI until growing well and then in 15% RPMI thereafter. All cell lines were cultured less than 3 months after resuscitation and tested for contaminants using MycoAlert (Lonza) every 1-3 months to ensure they were free of *Mycoplasma* contamination.

6.3 Antiboies and primers

These reagents are listed in Table S2.

6.4 Cell culture conditions

T-ALL cell lines were grown in RPMI1640 (Invitrogen) supplemented with FBS (Gibco), 2 mM l-glutamine, 2-mercaptoethanol [0.0005% (v/v), Sigma], penicillin, and streptomycin. 293T cells were maintained in DMEM (Invitrogen) with the same supplements except 2-mercaptoethanol. All cells were grown at 37°C under 5% CO_2. 4-hydroxytamoxifen was obtained from Sigma, diluted in ethanol, and used at 0.1% final concentration of ethanol. Puromycin (Sigma) was added to transduced cell cultures 48 hours after transduction for knockdown experiments.

6.5 Constructs and viral production

Flag-ETS1 (McCarter et al. 2020b), Flag-NOTCH1 (Pinnell et al. 2015), and Flag-CDC73 (Ropa et al. 2018) constructs were previously described. ShRNA constructs were obtained from Sigma: shControl (SHC002), shCDC73-1 (TRCN0000329742), and shCDC73-2 (TRCN0000329681). Retroviral and lentiviral production and tittering was performed as previously described (McCarter et al. 2020b). Lentivirus was concentrated using 30 kDa MWCO Amicon Ultra filters (Sigma).

6.6 Human patient expression data

Human patient data was based upon data generated by Therapeutically Applicable Research to Generate Effective Treatments (TARGET; https://ocg.cancer.gov/programs/target) initiative, phs000218. The ALL project team was headed by Stephen P. Hunger, M.D. at the University of Colorado Cancer Center, Denver, CO, USA. The dbGaP Sub-study ID was

phs000463/phs000464. The data used for this analysis are available at https://portal.gdc.cancer.gov/projects.

6.7 PDX experiments

PDX3 (M71) and PDX4 (2583AB) were obtained from Andrew Weng and Moshe Talpaz respectively. PDXs were expanded by injection into nonirradiated NOD-*scid*-IL2g^{null} (NSG) mice. De-identified human samples were obtained and used with approval from the University of Michigan Institutional Review Board and informed consent under guidelines established by the Declaration of Helsinki. Generation of PDX samples, transduction of PDX cells, and leukemia initiation experiments were performed as previously described (Yost et al. 2013; McCarter et al. 2020b) with transplantation into nonirradiated NSG mice followed by injection into a second cohort of NSG mice for survival analysis after 24 weeks. Mice injected with PDX cells were sacrificed when moribund.

6.8 Bone marrow transplantation

Bone marrow stem and progenitor cells of *Rosa26CreER*^{T2} or *Rosa26CreER*^{T2}*Cdc73*$^{f/f}$ mice were transduced with an activated *Notch1* allele (ΔE/Notch1). Transduced cells were injected into irradiated C57BL/6 mice to generate primary T-ALL tumors as previously described (Pear et al. 1996; Aster et al. 2000; McCarter et al. 2020b).

6.9 Flow cytometry

Flow cytometry and cell sorting was performed as previously described (McCarter et al. 2020b). Mitochondrial potential staining was done using TMRM (ThermoFisher). FCCP was obtained from Sigma. Reactive oxygen species staining was done using CellRox DeepRed

(ThermoFisher) and TBHP (Sigma). Each experimental condition was run in triplicate. The values displayed are representative of three biological replicates.

6.10 Co-immunoprecipitation (co-IP) and western blot

Flag-tagged co-IP was performed as previously described (Pinnell et al. 2015). Endogenous co-IP and Western blot was performed as previously described (McCarter et al. 2020b).

6.11 Dose response curves

Human and murine T-ALL cells were treated at increasing doses of berzosertib (Chemietek) for 9-10 days. CEM and LOUCY cells were treated for 16 days. Cells were stained with AO/PI and then counted using a CellDrop cell counter (DeNovix).

6.12 Quantitative PCR

QRT-PCR samples were prepared by extracting total RNA using the RNeasy Plus Mini Kit (Qiagen) according to manufacturer's protocol. Random primed total RNA (0.5ug) was reverse transcribed with SuperScript IV (Invitrogen). TaqMan Universal PCR Master Mix or Power SYBR Green PCR Master Mix (Applied Biosciences) were used to amplify transcripts using QuantStudio3 Pro Real-Time PCR System (Applied Biosystems). Relative expression of target genes was measured comparing against housekeeping controls β-actin or Ef1a.

6.13 Seahorse assay

Mitochondrial stress tests were performed using a Seahorse assay as described in a previously published protocol (Kumar et al. 2021) utilizing an Agilent Seahorse XFe96 Extracellular Flux Analyzer (Agilent). All cells were optimized for oligomycin concentration

(Sigma #O4876), FCCP concentration (Sigma #C2920) and seeding density. Seeding density for the 970, 708 and CUTLL1 cells were 250K, 200K, and 150K cells/well respectively. Final oligomycin concentrations for 970, 708 and CUTLL1 cells were 1mM, 2mM, and 1mM respectively. The final FCCP concentration for 970 and 708 cells was 2mM and CUTTL1 cells were 1uM. Final Rotenone/Antimycin A (Sigma #R8875, #A8674) concentrations for all cell lines were 0.5mM. CellTak (Corning #354240) was used to adhere cells to the plate. Murine T-ALL cells were analyzed at 48 hours after 9nM 4-OHT treatment. Human T-ALL cells were analyzed at 4 days after transduction of shCDC73. Dead cells were excluded by trypan blue staining and protein concentration by Bradford assay (Biorad) was performed to normalize results further to live cell seeding density. Data was analyzed using Wave software (Agilent).

6.14 Metaphase spreads

Murine T-ALL cells were treated with 9nM 4-OHT for 30h. Colcemid (10ug/ml) was added to arrest cells in metaphase. Pre-warmed KCl (37°C) was added by slowly dropping from a Pasteur pipette while gently shaking tube. Cells were fixed in ice cold fixative (3:1 methanol to acetic acid) three times and dropped onto slanted slides from about 10 feet using a Pasteur pipette and humid box. Slides were dried on a slide warmer and visualized under a light microscope to ensure metaphases were visible, then mounted using ProLong Gold Antifade Reagent with DAPI (Life Technologies). Slides were randomized and assigned identification codes independently by a second lab worker and blinded to the first lab worker before imaging on an Olympus BX-61 microscope and viewed with SKYview software (ASI). Blinded images were analyzed by the first lab worker using ImageJ software for chromosomal abnormalities and then unblinded.

6.15 Bru-seq and Bru-UV-seq library prep

Cells were split into fresh media upon treatment of the vehicle (ethanol) or OHT. Bru-seq and BruUV-seq were performed as previously described (Paulsen et al. 2013; Paulsen et al. 2014; Magnuson et al. 2015). Briefly, for BruUV-seq, cells were irradiated with 200 J/m^2 UV-C light. Bromouridine was added at 2mM to label cells in conditioned media directly following UV-irradiation for 30 min. Cells were then lysed directly in TRIzol followed by isolation of total RNA. The isolated total RNA was further treated with DNAse (TURBO DNA-free Kit; Invitrogen) and a spike-in cocktail of Bru-labeled and unlabeled RNA was mixed in with total RNA. Bru-labeled RNA was immunocaptured using anti-BrdU antibodies (BD Biosciences). Anti-BrdU monoclonal antibody was conjugated to magnetic beads and incubated with the RNA. Beads were washed with 200ul 0.1% BSA in PBS and resuspended in 0.1% BSA in PBS and diluted RNaseOUT. Spiked total RNA was added to the conjugated beads and incubated at RT with gentle rotation. Beads were washed, heated at 96^{o}C for 10 min and spun. Beads were captured and supernatant was saved as Bru-RNA. Next, rRNA was removed using FastSelect (Qiagen). First strand cDNA was synthesized via Superscript II, and cleanup was done using AMPure beads. To synthesize second strand, DNA polymerase was added, and cleanup was done using AMPure beads. End Repair was performed with T4 DNA Polymerase, and cleanup was done using AMPure beads. Adenylated 3' ends were added with Klenow Exo(-)polymerase, and cleanup was done using AMPure beads. Ligation of adaptors was done using the NEB quick ligation kit, and cleanup was done using AMPure beads. Size selection was performed using an agarose gel (3% gel using NuSieve 3:1 agarose). Gel slices were excised at 500bp and purified using the Qiagen QIAEXII kit. Uridine digestion and DNA fragment enrichment was done with USER enzyme. Samples were placed on ice and a universal ligation adapter and dual-index,

barcoded primers were added. PCR was performed, and AMPure beads were used to clean up. Pellet was resuspended in 5mM Tris pH 8.0 and incubated at 28℃. Beads were captured, and supernatant was transferred into a low-binding tube.

6.16 Bru-seq and Bru-UV-seq sequencing and analysis

Paired-end sequencing of libraries was performed on the NovaSeq 6000 (Illumina) by the University of Michigan Advanced Genomics Core. The resulting fastq reads were trimmed using BBDuk (BB Tools 38.46). Trimmed reads were aligned to the mouse ribosomal RNA (rRNA) repeating unit (GenBank BK000964.3) and mitochondrial genome (from the mm10 reference sequence) using Bowtie2 (2.3.3). Reads that did not align to rRNA or the mitochondrial genome were then aligned to the mouse genome build mm10/GRCm38 using STAR (v 2.5.3a) and a STAR index created from GENCODE annotation version M15 (Frankish et al. 2018, PMID 30357393). Coverages were determined as (1/read length) for each base in the genome using BEDTools2 2.28.0 (Quinlan and Hall 2010). These base coverages were used to obtain pseudo-read counts in strand-specific genomic features, such as genes, using BEDtools intersect. Differential gene expression for Bru-seq was performed using DESeq2 1.18.1 (Love et al. 2014. PMID 25516281). Differentially expressed genes were defined as having fold changes>1.5 (up or down) and adjusted p-values < 0.05. The apeglm method was used for $\log_2$ fold change shrinkage (Zhu, et al. 2018).

To identify peaks in the BruUV-seq data, plus- and minus-strand read pairs were first separated using Sambamba 0.8.0 and then MACS 2.2.7.1 was used to call peaks and summits for each strand. The MACS2 p-value threshold was set to 0.01 and read duplicates were retained. Differential peak analysis was performed using DiffBind 3.6 (Ross-Innes et al. 2012) and the parameter summits=FALSE was set for the dba.count function to ensure consensus peaks were

built around whole peaks from MACS2. These consensus peaks were used for downstream analyses. DESeq2 was the underlying quantification and differential testing method used by DiffBind. DeepTools 3.5.1 was used to generate signal files in bigWig format from uniquely mapped reads. Signal was RPKM-normalized using the total number of uniquely mapped reads in a given library. BruUV-seq peaks were classified in terms of proximity and orientation with respect to TSS and bodies of annotated transcripts, using closestsBed from bedtools 2.30.0, querying TSS coordinates against the 5' coordinates of BruUV-seq peaks. Only protein-coding transcripts were used, and genes were required to be expressed (mean Bru-seq RPKM>0.25 across samples). Where TSS coordinates are identical, the longer transcript was used. Peaks were classified as "TSS" if within 2 kb of the closest TSS, "gene body" if overlapping gene (sense orientation only), or "intergenic" if not classified as TSS or gene body (this includes peaks antisense to expressed genes).

To create the eRNA heatmaps (Fig. S7D-E), normalized counts data and peak data were filtered for intergenic peaks and antisense gene body peaks. Data was further subset into downregulated genes using cutoff of FDR<0.05 and FC<0; upregulated genes had cutoff of FDR<0.05 and FC>0. These subsets of downregulated and upregulated genes were log transformed, then used to generate a heatmaps separated by cell line using R package pheatmap (1.0.12).

6.17 ChIP-PCR, library preparation and sequencing

ChIP-PCR and ChIP-Seq library preparation and sequencing was performed as previously described (McCarter et al. 2020b) with the following additions. All reactions were followed by a SPRI bead cleanup using AMPure or SPRISelect beads. Size selection for the library was performed by using AMPure or SPRISelect selection. Paired-end sequencing of

H3K27ac, H2BKUb1, CDC73, and ETS1 ChIP libraries and unenriched control input libraries were performed using Nova-seq or Next-seq with approximately 20M reads per sample.

6.18 ChIP-seq analysis

ChIP-seq alignment, filtering, track generation, peak calling, overlaps, and differential binding analyses were performed as previously published (McCarter et al. 2020b). The exception was that for mouse cells the reads were aligned to the mm10 genome assembly and post filtered for known ENCODE blacklist regions in mice. For differential H3K27ac peak analysis in OHT vs. vehicle treated 969, 970, and 708 cells, DiffBind 3.6 was used (parameter summits=FALSE). DESeq2 was chosen for the analysis method and adjusted p-value< 0.05 was used as the significance threshold. Consensus peaks from DiffBind were used in downstream analyses. Signal files in bigWig format were produced with bamCoverage (DeepTools 3.5.1). Intergenic peaks (>2 kb from expressed gene TSS) were centered and the average (unstranded) signal was plotted for given samples +/-2.5 kb from the center using computeMatrix and plotProfile (DeepTools; Fig 13E).

For differential H2BK120ub1 peak analysis comparing control versus OHT, HOMER analyzeRepeats.pl was first run on mm10 genes to count tags on the full gene body (TSS to TTS) in a strand-insensitive manner, with parameters: -raw -gid -count genes -strand both. Results were then passed to HOMER getDiffExpression.pl which used DESeq2 to quantify and test differential histone ubiquitination across OHT vs EtOH comparisons in each cell line. Metagene plots were created using DeepTools for all genes or OXPHOS and DNA repair genes (Table S1). The bigwig display files were used as the input file scores to be plotted. The computeMatrix (“scale-regions”) tool was used to generate a score per genome matrix -1kb from the TSS and +1kb from the TTS. This matrix was then input into plotProfile to create the metagene plot of

scores over genes. H3K27Ac and BruUV-seq consensus peaks were integrated using closestBed (bedtools), querying H3K27Ac peaks against BruUV-seq 5' coordinates and requiring peaks to overlap (distance = 0). Dynamic intergenic H3K27ac/eRNA peak pairs were defined as having adjusted p-values<0.05 (OHT/control) in both assays and in both 969 and 970 cells. As per BruUV-seq peak classification described above, the "intergenic" definition included peaks that were >2 kb from expressed gene TSS and those antisense to gene bodies. CDC73 signal was quantified over gene bodies using multiBamCov (bedtools), where genes were defined by the human GENCODE version 27 basic annotation and uniquely mapped reads (mapping quality>30). RPKM was computed using the total number of uniquely mapped reads in the original alignments (mapping quality>30). ETS1 and RBPJ promoter regions were quantified in the same manner as CDC73, except limited to the first 2kb of each gene.

6.19 Differential analysis of CDC73 signals comparing control and ETS1 knockdown conditions

Active nucleosome free regions (NFRs) in THP-6 cells were defined as ATAC-Seq peaks associated with the top one-third of H3K27ac signal within a +/-4kb window (15,000 intervals) based on previously published datasets (McCarter et al. 2020b). Intersect function from BEDtools 2.30.0 (Quinlan and Hall 2010) (https://github.com/arq5x/bedtools2/blob/master/README.md) was used to intersect active NFR intervals with control CDC73 ChIP-seq peaks from two experiments. Intersected bed files were concatenated to find all intervals where control CDC73 peaks overlap with active NFR intervals. We performed differential binding analysis using Diffbind 3.6 (Ross-Innes et al. 2012) (https://bioconductor.org/packages/release/bioc/html/DiffBind.html) and EdgeR algorithm (Robinson et al. 2010; McCarthy et al. 2012)

(https://bioconductor.org/packages/release/bioc/html/edgeR.html) to compare CDC73 binding in control (N=2) vs. shETS1-2 (N=2), and shETS1-3 (N=2) samples. We designated the previously identified intervals where control CDC73 peaks overlap with active NFRs as "all CDC73 peaks". We defined "dynamic ETS1 peaks" as intervals where ETS1 binding decreases (FC<0) with FDR<0.1 for both shETS1-2 and shETS1-3 (McCarter et al. 2020b). We intersected these intervals with "all CDC73 peaks" and designated resulting intervals as "CDC73 peaks X dynamic Ets1 peaks".

Violin plots were generated to compare CDC73 binding fold change at "all CDC73 intervals" and "CDC73 peaks X dynamic Ets1" for shETS1-2 and shETS1-3 treated samples. Plots also display median, 1st and 3rd quartiles. Using deepTools Galaxy computeMatrix and plotHeatmap (Ramirez et al. 2016), we generated metagene plots at "CDC73 x dynamic Ets1 peaks" intervals using ChIP-Seq reads from CDC73 shControl, CDC73 shETS1-2, and CDC73 shETS1-3 bigwig files (McCarter et al. 2020b).

6.20 Additional statistical information

Unless otherwise indicated, P-values were derived from two-sided two-sample t-tests of Log2-transformed data for comparisons in experiments involving two groups and 1-way ANOVA of Log2-transformed data for pairwise contrasts in experiments with more than two groups. Unless otherwise stated, horizontal lines are means and values are shown as mean $\pm$ standard deviation. Survival curves (or time to event data) was tested with log-rank tests comparing pairs of groups. Gene set enrichment analysis (GSEA) was performed using GSEAv4.1.0 (Broad Institute) and gene lists from MSigDBv7.4 and custom lists of high confidence human direct NOTCH1 and ETS1 target gene signatures in T-ALL (Wang et al. 2014; McCarter et al. 2020b).

Appendices

Kaufmann_DNA_repair (112 genes)
LIG4, RAD51B, XRCC4, FANCD2, FANCL, NEIL3, CETN3, ATR, WRN, RAD18, XRCC5, RBBP8, SMC2, PRKDC, RAD54B, POLE, PMS1, RPA3, MBD4, RAD51AP1, TOP3A, PARP2, RAD51, BRIP1, MSH2, CCNH, RFC4, FANCB, MRE11, DCLRE1B, MLH1, EME1, TDP1, POLA1, N4BP2, POLK, TOPBP1, FANCC, DDB2, RAD54L, SMC1A, NUDT1, TOP2B, TDG, BLM, ATM, MLH3, ALKBH3, TEP1, RFC1, RAD1, XPC, POLQ, CHEK1, POLD1, GTF2H4, MTOR, MBD5, NBN, TERF1, RAD51C, UBE2V2, ERCC6, RAD51D, XPA, RAD52, FANCE, UBE2I, DUT, RAD17, HMGB2, ATRX, CRY1, ENDOV, APEX2, MSH3, TOP3B, RECQL5, CDK7, MPG, RFC2, FEN1, MBD2, RFC3, FANCA, LIG1, WDR33, CRY2, EXO1, APTX, MSH6, RAD23A, SMC3, TP53, UBE2D3, BRCA2, ERCC4, RFC5, SMC4, RAD21, POLE4, SSRP1, XRCC3, RRM1, MBD1, ALKBH2, GTF2H3, REV3L, MGMT, SUPT16H, PARP4, CETN2

Appendix Table 1 Core enrichment genes in Kaufmann_DNA_repair for Cdc73-induced target genes in 969 cells

Kaufmann_DNA_repair (97 genes)
LIG4, FANCL, CETN3, FANCD2, XRCC4, RAD51B, ATR, WRN, XRCC3, POLD1, XRCC5, RAD18, NEIL3, NUDT1, TOP3A, EME1, RAD54L, POLE, RPA3, FANCB, DCLRE1B, RFC4, MBD4, FANCE, MLH1, PARP2, MSH2, ENDOV, PMS1, RAD54B, CCNH, RAD51AP1, RAD23A, RUVBL2, PRKDC, RAD51, RFC2, MRE11, UBE2I, DUT, MTOR, RFC5, DDB2, TOP3B, ALKBH3, RAD52, XPC, TDP1, FANCC, SMC2, RAD1, RBBP8, TOPBP1, FANCA, GTF2H4, MUS81, TDG, ALKBH2, NEIL1, ERCC4, GTF2H3, CRY2, POLD2, MMS19, LIG1, XPA, MBD3, ERCC6, APTX, BLM, UBA1, BRIP1, LIG3, NBN, CETN2, TOP2B, ATM, FEN1, TERT, POLK, RECQL5, FANCG, POLA1, N4BP2, SMC1A, CDK7, POLM, RAD9A, TP53, RAD51C, MLH3, MPG, EXO1, RAD17, CHAF1A, NEIL2, RAD51D

Appendix Table 2 Core enrichment genes in Kaufmann_DNA_repair for Cdc73-induced target genes in 970 cells

Kaufmann_DNA_repair (34 genes)
RAD51B, ATR, WRN, RAD18, XRCC5, PRKDC, PMS1, TOP3A, CCNH, DCLRE1B, TDP1, POLA1, RAD54L, MLH3, ALKBH3, RAD1, XPC, POLD1, GTF2H4, NBN, RAD51C, RAD52, DUT, TOP3B, CDK7, RFC2, CRY2, EXO1, APTX, RAD23A, ERCC4, RFC5, XRCC3, ALKBH2

Appendix Table 3 Core enrichment genes in Kaufmann_DNA_repair list that are shared between Cdc73-induced, Notch-induced, and Ets1-induced target genes

Hallmark_Oxidative_Phosphorylation (88 genes)
MTRF1, NDUFB3, COX7A2L, NDUFB4, TOMM70, ECHS1, FH, MDH1, NDUFAB1, ACADSB, VDAC3, DECR1, OPA1, NDUFB1, ATP5F1C, OAT, ABCB7, HSPA9, AIFM1, SUPV3L1, MRPS22, ATP6V1G1, NDUFV2, PRDX3, ACADM, NDUFA6, IDH1, IMMT, ETFA, SLC25A12, HADHA, NDUFS1, FXN, SDHC, MDH2, NDUFB2, ATP5PB, NDUFS4, ATP5PF, UQCRC2, ACAA2, COX10, MRPL15, SDHB, RETSAT, TIMM9, MRPL11, DLD, UQCRB, ETFDH, CYB5R3, ALDH6A1, ATP6V1D, HADHB, NDUFA8, CYB5A, IDH3B, FDX1, UQCRFS1, NDUFS3, NDUFA2, SUCLG1, NDUFS2, NQO2, NDUFV1, CPT1A, ATP5PD, RHOT1, AFG3L2, NDUFS7, ACAT1, PDP1, UQCR10, MTX2, ATP5MF, ATP6V1C1, COX5A, NDUFS6, MRPL35, UQCRQ, PDHX, MTRR, TIMM17A, VDAC1, COX6B1, COX7C, NDUFA9, OXA1L

Appendix Table 4 Core enrichment genes in Hallmark_Oxidative_Phosphorylation for Cdc73-induced target genes in 969 cells

Hallmark_Oxidative_Phosphorylation (105 genes)
IDH1, ECHS1, NDUFB4, PRDX3, MTRF1, MDH1, ACADM, NDUFA6, ACADSB, SDHC, IDH3B, FH, NDUFAB1, NDUFS7, CYB5R3, CPT1A, TOMM70, OAT, NDUFB3, MDH2, SUPV3L1, ATP5F1C, SDHB, NDUFS2, COX7A2L, RETSAT, NDUFV1, HADHA, ACAA2, AIFM1, IMMT, ATP6V1G1, CYB5A, NDUFV2, FXN, NDUFB1, NDUFB2, NDUFA3, OPA1, ALDH6A1, SUCLG1, ETFDH, MRPL11, FDX1, VDAC3, TIMM50, MRPS22, ATP5PF, NDUFA8, DECR1, NDUFS1, NQO2, COX10, TIMM9, SLC25A12, NDUFS3, AFG3L2, UQCR10, UQCRC2, ETFA, MRPL15, HSPA9, NDUFB7, HADHB, MTRR, ABCB7, GOT2, ATP5PB, IDH2, UQCRFS1, UQCRQ, NDUFS4, TIMM13, UQCRC1, ATP6V0E1, VDAC1, PDHX, OXA1L, MRPL35, RHOT1, NDUFS6, PHYH, ATP6V1D, IDH3A, COX6B1, ATP5F1D, SLC25A5, MFN2, LDHA, GPX4, PDP1, ATP6V1C1, ALAS1, DLD, NDUFA9, NDUFA5, MRPL34, ATP5MF, HSD17B10, ATP6AP1, CYC1, ACO2, OGDH, TIMM17A, GRPEL1

Appendix Table 5 Core enrichment genes in Hallmark_Oxidative_Phosphorylation for Cdc73-induced target genes in 970 cells

Hallmark_Oxidative_Phosphorylation (39 genes)
IDH3B, UQCRQ, HSPA9, NDUFS3, TIMM17A, OXA1L, NDUFS6, UQCR10, AFG3L2, UQCRFS1, MDH2, VDAC3, SUPV3L1, CPT1A, NDUFAB1, DLD, VDAC1, MTRR, TIMM9, NDUFA9, MTRF1, OPA1, NDUFV1, NDUFV2, NDUFS2, FDX1, SDHB, NDUFS1, FH, PDHX, ETFA, SUCLG1, FXN, ECHS1, NDUFA8, COX10, ATP6V1C1, ABCB7, AIFM1

Appendix Table 6 Core enrichment genes in Hallmark_Oxidative_Phosphorylation list that are shared between Cdc73-induced, Notch-induced, and Ets1-induced target genes

Flow cytometry reagent	Color	Manufacturer	Cat Number	Clone
Mouse				
B220	FITC	Biolegend	103205	RA3-6B2
7-AAD	7-AAD	Biolegend	420403	N/A
annexin-V	APC	Biolegend	640920	N/A
c-Kit	APC-Cy7	Biolegend	105825	2B8
c-Kit	PE	Biolegend	105807	2B8
CD11b	APC	Biolegend	101211	M1/70
CD11b	FITC	Biolegend	101205	M1/70
CD11b	APCcy7	Biolegend	101225	M1/70
CD11c	FITC	Biolegend	117306	N418
CD19	FITC	BD Biosciences	553785	ID3
CD19	PEcy7	Biolegend	115519	6D5
CD25	PE	Biolegend	102007	PC61
CD25	BV605	Biolegend	102035	PC61
CD27	PE-Cy7	Biolegend	124215	LG.3A10
CD28	FITC	Biolegend	122010	E18
CD3	FITC	Biolegend	100305	145-2C11
CD4	FITC	Biolegend	100539	RM4-5
CD4	FITC	Biolegend	100515	RM4-5
CD44	FITC	Biologend	103011	IM7
CD45	FITC	Biolegend	304011	H130
CD8a	FITC	Biolegend	100705	53-6.7
CD8b	FITC	Biolegend	140403	53-5.8
CellRox Deep Red	FITC	Invitrogen	C10422	N/A
Flt3	FITC	Biolegend	135309	A2F10
Gr1	FITC	Biolegend	108407	RB6-8C5
Gr1	FITC	Biolegend	108405	RB6-8C5
Gr1	FITC	Biolegend	108415	RB6-8C5
IgM	FITC	eBioscience	12-5790-82	II/41
IL7Ra	FITC	Biolegend	135013	A7R34
Ly6d	FITC	Biolegend	138605	49-H4
CD45	FITC	Biolegend	103131	30-F11
NK1.1	FITC	Biolegend	108706	PK136
Sca-1	FITC	Biolegend	122523	E13-161.7
TCRb	FITC	Biolegend	109206	H57-597
TCRd	FITC	eBioscience	11-5711-82	eBioGL3
Ter119	FITC	eBioscience	11-5921-82	TER-119
Tetramethylrhodamine, Methyl Ester, Perchlorate (TMRM)	FITC	Invitrogen	T668	N/A
Human				
CD7	APC	Biolegend	343107	4H9
CD45	APC	Biolegend	304011	H130
LNGFR (CD271)	APC	Miltenyl Biotech	130-091-884	ME20.4-1.4H

Appendix Table 7 Flow cytometry reagents

Antibody	Use	Manufacturer	Cat Number	Clone
Ets1	Western Blot/Co-IP	Cell Signaling Technologies	14069S	D8O8A
Rabbit IgG	Co-Immunoprecipitation	Cell Signaling Technologies	2729S	N/A
ECL Rabbit IgG, HRP-linked whole Ab (from donkey)	Westen Blot Secondary Ab	GE Healthcare Life Sciences	NA934	N/A
ECL Mouse IgG, HRP-linked whole Ab (from sheep)	Westen Blot Secondary Ab	GE Healthcare Life Sciences	NA931	N/A
Peroxidase-conjugated AffiniPure Rabbit Anti-Sheep IgG	Western Blot Secondary Ab	Jackson ImmunoResearch	313-035-003	N/A
CDC73	Western Blot	R&D Systems	AF5508	N/A
anti-Parafibromin (Cdc73)	ChIP-Seq/Co-IP/Western Blot	Bethyl	A300-171A (discontinued)	N/A
anti-Rabbit IgG, peroxidase-linked species-specific whole antibody (from donkey)	Western Blot Secondary Ab	GE Healthcare Life Sciences	NA934	N/A
b-actin	Western Blot	Sigma	A5316	N/A
Ets1	ChIP-Seq	Santa Cruz	sc-350x (discontinued)	N/A
GAPDH	Western Blot	Cell Signaling Technologies	5174	D16H11
Goat anti-Mouse IgG (H+L), HRP	Western Blot Secondary Ab	Invitrogen	31430	N/A
H3K27Ac	ChIP-Seq	Active Motif	39133	N/A
Histone H2A.XS139ph	ChIP	Active Motif	39117/8	N/A
Phospho-Chk1 (Ser296)	Western Blot	Cell Signaling Technologies	90178	D3O9F
Phospho-Histone H2A.X (Ser139)	Western Blot	Cell Signaling Technologies	9718	20E3
Rabbit Anti-Goat IgG, HRP conjugate	Western Blot Secondary Ab	Millipore Sigma	AP106P	N/A
Ubiquityl-Histone H2B (Lys120)	ChIP-Seq	Cell Signaling Technologies	5546	D11

Appendix Table 8 Other antibodies

Mouse qRT-PCR primers	Forward (5' to 3')	Reverse (5' to 3')
m18S	GCGCCGCTAGAGGTGAAAT	GGCGGGTCATGGGAATAAC
mEf1a	CACTTGGTCGCTTTGCTGTT	GGTGGCAGGTGTTAGGGGTA
mEts1	CAAGCCGACTCTCACCATCA	ATTCCCAGTCGCTGCTGTTC
mAtr	GCTGGCCACCATCAGACAGC	ACGTCACCCTTGGACCACAGC
mB-actin	GCCCTGAGGCTCTTTTCCAG	TGCCACGGATTCCATACC
mCdc73	CCGGAAAGGAAGGCCAACCCA	AGCTGCACGCCGGACATAAACA
mHes1	GGAAATGACAGTGAAGCACCT	CAGCACACTTGGGTCTGTG
mLig4	GGGTGACTTGGAGCAGCTGAGG	TGGAGATGGGCTTCCGCCTT
mMyc	Taqman Mm00487803_m1	
mNdufab1	GTGAAACCCACACTGCTGTT	AGGTACCGTCTCTCTGGTCT
mNdufb4	ACCCTCGACCCTGCCGAGTA	CCCGTTTAAGCCGGGCCCTT
Mouse ChIP primers	Forward (5' to 3')	Reverse (5' to 3')
Fgg	GGTGGCAGATGGGAGGGAAC	CCAGGGGTGGGAGAAGGGAA
mCol1a1	TGCAGACAAGCCCCTCAGTG	ACGAAGGTGGCATGAAGGAAC
mHbaa1	TTCCTCATGCAAAGCGAACA	CCTGGTAGGCTGAGGCAAGA
mLig4	GGGTGACTTGGAGCAGCTGAG	TGGAGATGGGCTTCCGCCTT
mMyc	GCATAGACCTCATCTGCGGTTG	AAGGGGGAAGGACGAACGAATG
Genotyping primers	Forward (5' to 3')	Reverse (5' to 3')
LckCre	CCTCCTGTGAACTTGGTGCTTGAG	TGCATCGACCGGTAATGCAG
Cdc73	TCCTTTCCATTGTGCAGCTGGTTG	TGCCAGTGCAAGAACCTCATCCTA
Rosa26-CreERT2	AAAGTCGCTCTGAGTTGTTAT	CCTGATCCTGGCAATTTCG

Appendix Table 9 Primer's list

Bibliography

Adelman K, Wei W Fau - Ardehali MB, Ardehali Mb Fau - Werner J, Werner J Fau - Zhu B, Zhu B Fau - Reinberg D, Reinberg D Fau - Lis JT, Lis JT. Drosophila Paf1 modulates chromatin structure at actively transcribed genes.

Albert TK, Rigault C, Eickhoff J, Baumgart K, Antrecht C, Klebl B, Mittler G, Meisterernst M. 2014. Characterization of molecular and cellular functions of the cyclin-dependent kinase CDK9 using a novel specific inhibitor. *British journal of pharmacology* **171**: 55-68.

Artavanis-Tsakonas S, Rand Md Fau - Lake RJ, Lake RJ. Notch signaling: cell fate control and signal integration in development.

Asnafi V, Buzyn A, Le Noir S, Baleydier F, Simon A, Beldjord K, Reman O, Witz F, Fagot T, Tavernier E et al. 2009. NOTCH1/FBXW7 mutation identifies a large subgroup with favorable outcome in adult T-cell acute lymphoblastic leukemia (T-ALL): a Group for Research on Adult Acute Lymphoblastic Leukemia (GRAALL) study. *Blood* **113**: 3918-3924.

Aster JC. 2020. Notch Signaling in Context: Basic and Translational Implications. *Trans Am Clin Climatol Assoc* **131**: 147-156.

Aster JC, Xu L, Karnell FG, Patriub V, Pui JC, Pear WS. 2000. Essential roles for ankyrin repeat and transactivation domains in induction of T-cell leukemia by Notch1. *Mol Cell Biol* **20**: 7505-7515.

Balgobind BV, Van Vlierberghe P Fau - van den Ouweland AMW, van den Ouweland Am Fau - Beverloo HB, Beverloo Hb Fau - Terlouw-Kromosoeto JNR, Terlouw-Kromosoeto Jn Fau - van Wering ER, van Wering Er Fau - Reinhardt D, Reinhardt D Fau - Horstmann M, Horstmann M Fau - Kaspers GJL, Kaspers Gj Fau - Pieters R, Pieters R Fau - Zwaan CM et al. Leukemia-associated NF1 inactivation in patients with pediatric T-ALL and AML lacking evidence for neurofibromatosis.

Baran N, Lodi A, Dhungana Y, Herbrich S, Collins M, Sweeney S, Pandey R, Skwarska A, Patel S, Tremblay M et al. 2022. Inhibition of mitochondrial complex I reverses NOTCH1-driven metabolic reprogramming in T-cell acute lymphoblastic leukemia. *Nature Communications* **13**: 2801.

Bardelli V, Arniani S, Pierini V, Di Giacomo DA-O, Pierini TA-OX, Gorello P, Mecucci C, La Starza RA-O. T-Cell Acute Lymphoblastic Leukemia: Biomarkers and Their Clinical Usefulness. LID - 10.3390/genes12081118 [doi] LID - 1118.

Bartkova J, Horejsí Z Fau - Koed K, Koed K Fau - Krämer A, Krämer A Fau - Tort F, Tort F Fau - Zieger K, Zieger K Fau - Guldberg P, Guldberg P Fau - Sehested M, Sehested M Fau - Nesland JM, Nesland Jm Fau - Lukas C, Lukas C Fau - Ørntoft T et al. DNA damage response as a candidate anti-cancer barrier in early human tumorigenesis.

Bartkova J, Rezaei N Fau - Liontos M, Liontos M Fau - Karakaidos P, Karakaidos P Fau - Kletsas D, Kletsas D Fau - Issaeva N, Issaeva N Fau - Vassiliou L-VF, Vassiliou Lv Fau - Kolettas E, Kolettas E Fau - Niforou K, Niforou K Fau - Zoumpourlis VC, Zoumpourlis

Vc Fau - Takaoka M et al. Oncogene-induced senescence is part of the tumorigenesis barrier imposed by DNA damage checkpoints.
Bassan R, Bourquin JP, DeAngelo DJ, Chiaretti S. New Approaches to the Management of Adult Acute Lymphoblastic Leukemia.
Belver L, Ferrando A. 2016. The genetics and mechanisms of T cell acute lymphoblastic leukaemia. *Nature Reviews Cancer* **16**: 494.
Berquam-Vrieze KE, Nannapaneni K, Brett BT, Holmfeldt L, Ma J, Zagorodna O, Jenkins NA, Copeland NG, Meyerholz DK, Knudson CM et al. 2011. Cell of origin strongly influences genetic selection in a mouse model of T-ALL. *Blood* **118**: 4646-4656.
Bisgrove DA, Mahmoudi T, Henklein P, Verdin E. 2007. Conserved P-TEFb-interacting domain of BRD4 inhibits HIV transcription. *Proc Natl Acad Sci U S A* **104**: 13690-13695.
Borggrefe T, Liefke R. 2012. Fine-tuning of the intracellular canonical Notch signaling pathway. *Cell Cycle* **11**: 264-276.
Bradner JE, Hnisz D, Young RA. 2017. Transcriptional Addiction in Cancer. *Cell* **168**: 629-643.
Bray S, Musisi H, Bienz M. 2005. Bre1 is required for Notch signaling and histone modification. *Dev Cell* **8**: 279-286.
Bray SJ. 2016. Notch signalling in context. *Nat Rev Mol Cell Biol*.
Bray SJ, Gomez-Lamarca M. 2018. Notch after cleavage. *Curr Opin Cell Biol* **51**: 103-109.
Bride KL, Vincent TL, Im S-Y, Aplenc R, Barrett DM, Carroll WL, Carson R, Dai Y, Devidas M, Dunsmore KP. 2018. Preclinical efficacy of daratumumab in T-cell acute lymphoblastic leukemia. *Blood, The Journal of the American Society of Hematology* **131**: 995-999.
Callén E, Jankovic M, Difilippantonio S, Daniel JA, Chen H-T, Celeste A, Pellegrini M, McBride K, Wangsa D, Bredemeyer AL. 2007. ATM prevents the persistence and propagation of chromosome breaks in lymphocytes. *Cell* **130**: 63-75.
Carpten JD, Robbins CM, Villablanca A, Forsberg L, Presciuttini S, Bailey-Wilson J, Simonds WF, Gillanders EM, Kennedy AM, Chen JD. 2002a. HRPT2, encoding parafibromin, is mutated in hyperparathyroidism–jaw tumor syndrome. *Nature genetics* **32**: 676-680.
Carpten JD, Robbins CM, Villablanca A, Forsberg L, Presciuttini S, Bailey-Wilson J, Simonds WF, Gillanders EM, Kennedy AM, Chen JD et al. 2002b. HRPT2, encoding parafibromin, is mutated in hyperparathyroidism-jaw tumor syndrome. *Nat Genet* **32**: 676-680.
Carr T, McGregor S, Dias S, Verykokakis M, Le Beau MM, Xue HH, Sigvardsson M, Bartom ET, Kee BL. 2022. Oncogenic and Tumor Suppressor Functions for Lymphoid Enhancer Factor 1 in E2a(-/-) T Acute Lymphoblastic Leukemia. *Front Immunol* **13**: 845488.
Chang HHY, Pannunzio NR, Adachi N, Lieber MR. 2017. Non-homologous DNA end joining and alternative pathways to double-strand break repair. *Nature Reviews Molecular Cell Biology* **18**: 495-506.
Chaudhary K, Deb S, Moniaux N, Ponnusamy MP, Batra SK. 2007. Human RNA polymerase II-associated factor complex: dysregulation in cancer. *Oncogene* **26**: 7499-7507.
Chen CA-O, Hao XA-O, Lai XA-O, Liu LA-OX, Zhu J, Shao H, Huang D, Gu HA-O, Zhang TA-OX, Yu Z et al. Oxidative phosphorylation enhances the leukemogenic capacity and resistance to chemotherapy of B cell acute lymphoblastic leukemia. LID - 10.1126/sciadv.abd6280 [doi] LID - eabd6280.

Chen F, Liu B, Guo L, Ge X, Feng W, Li DF, Zhou H, Long J. 2021. Biochemical insights into Paf1 complex-induced stimulation of Rad6/Bre1-mediated H2B monoubiquitination. *Proc Natl Acad Sci U S A* **118**.

Chen FX, Woodfin AR, Gardini A, Rickels RA, Marshall SA, Smith ER, Shiekhattar R, Shilatifard A. 2015. PAF1, a Molecular Regulator of Promoter-Proximal Pausing by RNA Polymerase II. *Cell* **162**: 1003-1015.

Chen FX, Xie P, Collings CK, Cao K, Aoi Y, Marshall SA, Rendleman EJ, Ugarenko M, Ozark PA, Zhang A et al. 2017. PAF1 regulation of promoter-proximal pause release via enhancer activation. *Science* **357**: 1294-1298.

Cheok MH, Pottier N, Kager L, Evans WE. Pharmacogenetics in acute lymphoblastic leukemia. pp. 39-51. Elsevier.

Chiang MY, Xu L, Shestova O, Histen G, L'Heureux S, Romany C, Childs ME, Gimotty PA, Aster JC, Pear WS. 2008. Leukemia-associated NOTCH1 alleles are weak tumor initiators but accelerate K-ras-initiated leukemia. *Journal of Clinical Investigation* **118**: 14.

Chiang MY, Xu Ml Fau - Histen G, Histen G Fau - Shestova O, Shestova O Fau - Roy M, Roy M Fau - Nam Y, Nam Y Fau - Blacklow SC, Blacklow Sc Fau - Sacks DB, Sacks Db Fau - Pear WS, Pear Ws Fau - Aster JC, Aster JC. Identification of a conserved negative regulatory sequence that influences the leukemogenic activity of NOTCH1.

Chiang YJ, Hodes RJ. 2016. T-cell development is regulated by the coordinated function of proximal and distal Lck promoters active at different developmental stages. *European Journal of Immunology* **46**: 2401-2408.

Christensen S, Kodoyianni V Fau - Bosenberg M, Bosenberg M Fau - Friedman L, Friedman L Fau - Kimble J, Kimble J. lag-1, a gene required for lin-12 and glp-1 signaling in Caenorhabditis elegans, is homologous to human CBF1 and Drosophila Su(H).

Clappier E, Collette S, Grardel N, Girard S, Suarez L, Brunie G, Kaltenbach S, Yakouben K, Mazingue F, Robert A et al. 2010. NOTCH1 and FBXW7 mutations have a favorable impact on early response to treatment, but not on outcome, in children with T-cell acute lymphoblastic leukemia (T-ALL) treated on EORTC trials 58881 and 58951. *Leukemia* **24**: 2023-2031.

Coustan-Smith E, Mullighan Cg Fau - Onciu M, Onciu M Fau - Behm FG, Behm Fg Fau - Raimondi SC, Raimondi Sc Fau - Pei D, Pei D Fau - Cheng C, Cheng C Fau - Su X, Su X Fau - Rubnitz JE, Rubnitz Je Fau - Basso G, Basso G Fau - Biondi A et al. Early T-cell precursor leukaemia: a subtype of very high-risk acute lymphoblastic leukaemia.

da Silva-Diz V, Cao B, Lancho O, Chiles E, Alasadi A, Aleksandrova M, Luo S, Singh A, Tao H, Augeri D et al. 2021. A novel and highly effective mitochondrial uncoupling drug in T-cell leukemia. *Blood* **138**: 1317-1330.

Dasgupta Y, Golovine K, Nieborowska-Skorska M, Luo L, Matlawska-Wasowska K, Mullighan CG, Skorski T. Drugging DNA repair to target T-ALL cells.

De Keersmaecker K, Atak ZK, Li N, Vicente C, Patchett S, Girardi T, Gianfelici V, Geerdens E, Clappier E, Porcu M. 2013. Exome sequencing identifies mutation in CNOT3 and ribosomal genes RPL5 and RPL10 in T-cell acute lymphoblastic leukemia. *Nature genetics* **45**: 186-190.

De Keersmaecker K, Porcu M Fau - Cox L, Cox L Fau - Girardi T, Girardi T Fau - Vandepoel R, Vandepoel R Fau - de Beeck JO, de Beeck Jo Fau - Gielen O, Gielen O Fau - Mentens N, Mentens N Fau - Bennett KL, Bennett Kl Fau - Hantschel O, Hantschel O. NUP214-

ABL1-mediated cell proliferation in T-cell acute lymphoblastic leukemia is dependent on the LCK kinase and various interacting proteins.
De Smedt R, Morscio J, Goossens S, Van Vlierberghe P. Targeting steroid resistance in T-cell acute lymphoblastic leukemia.
De Smedt R, Morscio J, Reunes L, Roels J, Bardelli V, Lintermans B, Van Loocke W, Almeida A, Cheung LC, Kotecha RS et al. Targeting cytokine- and therapy-induced PIM1 activation in preclinical models of T-cell acute lymphoblastic leukemia and lymphoma.
Delgado-Martin C, Meyer LK, Huang BJ, Shimano KA, Zinter MS, Nguyen JV, Smith GA, Taunton J, Winter SS, Roderick JR et al. JAK/STAT pathway inhibition overcomes IL7-induced glucocorticoid resistance in a subset of human T-cell acute lymphoblastic leukemias.
Di Micco R, Fumagalli M Fau - Cicalese A, Cicalese A Fau - Piccinin S, Piccinin S Fau - Gasparini P, Gasparini P Fau - Luise C, Luise C Fau - Schurra C, Schurra C Fau - Garre M, Garre' M Fau - Nuciforo PG, Nuciforo Pg Fau - Bensimon A, Bensimon A Fau - Maestro R et al. Oncogene-induced senescence is a DNA damage response triggered by DNA hyper-replication.
Ding L, Paszkowski-Rogacz M, Mircetic J, Chakraborty D, Buchholz F. 2021. The Paf1 complex positively regulates enhancer activity in mouse embryonic stem cells. *Life Sci Alliance* **4**.
Dose M, Khan I, Guo Z, Kovalovsky D, Krueger A, von Boehmer H, Khazaie K, Gounari F. 2006. c-Myc mediates pre-TCR-induced proliferation but not developmental progression. *Blood* **108**: 2669-2677.
Eguchi-Ishimae M, Eguchi M Fau - Kempski H, Kempski H Fau - Greaves M, Greaves M. NOTCH1 mutation can be an early, prenatal genetic event in T-ALL.
Ellisen LW, Bird J Fau - West DC, West Dc Fau - Soreng AL, Soreng Al Fau - Reynolds TC, Reynolds Tc Fau - Smith SD, Smith Sd Fau - Sklar J, Sklar J. TAN-1, the human homolog of the Drosophila notch gene, is broken by chromosomal translocations in T lymphoblastic neoplasms.
Evangelisti C, Chiarini F, McCubrey JA, Martelli AM. 2018. Therapeutic targeting of mTOR in T-cell acute lymphoblastic leukemia: an update. *International journal of molecular sciences* **19**: 1878.
Eyquem S, Chemin K, Fasseu M, Bories JC. 2004. The Ets-1 transcription factor is required for complete pre-T cell receptor function and allelic exclusion at the T cell receptor beta locus. *Proc Natl Acad Sci U S A* **101**: 15712-15717.
Falo-Sanjuan J, Bray SJ. 2019. Decoding the Notch signal. *Dev Growth Differ*.
Ferrando AA, Neuberg DS, Staunton J, Loh ML, Huard C, Raimondi SC, Behm FG, Pui C-H, Downing JR, Gilliland DG et al. 2002. Gene expression signatures define novel oncogenic pathways in T cell acute lymphoblastic leukemia. *Cancer Cell* **1**: 75-87.
Filippakopoulos P, Knapp S. 2014. Targeting bromodomains: epigenetic readers of lysine acetylation. *Nature reviews Drug discovery* **13**: 337-356.
Follini E, Marchesini MA-O, Roti G. Strategies to Overcome Resistance Mechanisms in T-Cell Acute Lymphoblastic Leukemia. LID - 10.3390/ijms20123021 [doi] LID - 3021.
Fortini ME, Artavanis-Tsakonas S. The suppressor of hairless protein participates in notch receptor signaling.

Francette AM, Tripplehorn SA, Arndt KM. 2021. The Paf1 Complex: A Keystone of Nuclear Regulation Operating at the Interface of Transcription and Chromatin. *J Mol Biol* **433**: 166979.

Fryer CJ, White Jb Fau - Jones KA, Jones KA. Mastermind recruits CycC:CDK8 to phosphorylate the Notch ICD and coordinate activation with turnover.

Gaillard H, Tous C, Botet J, Gonzalez-Aguilera C, Quintero MJ, Viladevall L, Garcia-Rubio ML, Rodriguez-Gil A, Marin A, Arino J et al. 2009. Genome-wide analysis of factors affecting transcription elongation and DNA repair: a new role for PAF and Ccr4-not in transcription-coupled repair. *PLoS Genet* **5**: e1000364.

Gao J, Liu WJ. 2018. Prognostic value of the response to prednisone for children with acute lymphoblastic leukemia: a meta-analysis. *Eur Rev Med Pharmacol Sci* **22**: 7858-7866.

Garcia-Bermudez J, Baudrier L, La K, Zhu XG, Fidelin J, Sviderskiy VO, Papagiannakopoulos T, Molina H, Snuderl M, Lewis CA et al. 2018. Aspartate is a limiting metabolite for cancer cell proliferation under hypoxia and in tumours. *Nat Cell Biol* **20**: 775-781.

Godfrey L, Crump NT, Thorne R, Lau IJ, Repapi E, Dimou D, Smith AL, Harman JR, Telenius JM, Oudelaar AM et al. 2019. DOT1L inhibition reveals a distinct subset of enhancers dependent on H3K79 methylation. *Nat Commun* **10**: 2803.

Gonzalez-Garcia S, Garcia-Peydro M, Martin-Gayo E, Ballestar E, Esteller M, Bornstein R, de la Pompa JL, Ferrando AA, Toribio ML. 2009. CSL-MAML-dependent Notch1 signaling controls T lineage-specific IL-7R{alpha} gene expression in early human thymopoiesis and leukemia. *Journal of Experimental Medicine* **206**: 779-791.

Gordon WR, Roy M Fau - Vardar-Ulu D, Vardar-Ulu D Fau - Garfinkel M, Garfinkel M Fau - Mansour MR, Mansour Mr Fau - Aster JC, Aster Jc Fau - Blacklow SC, Blacklow SC. Structure of the Notch1-negative regulatory region: implications for normal activation and pathogenic signaling in T-ALL.

Gordon WR, Vardar-Ulu D Fau - Histen G, Histen G Fau - Sanchez-Irizarry C, Sanchez-Irizarry C Fau - Aster JC, Aster Jc Fau - Blacklow SC, Blacklow SC. Structural basis for autoinhibition of Notch.

Gorgoulis VG, Vassiliou Lv Fau - Karakaidos P, Karakaidos P Fau - Zacharatos P, Zacharatos P Fau - Kotsinas A, Kotsinas A Fau - Liloglou T, Liloglou T Fau - Venere M, Venere M Fau - Ditullio RA, Jr., Ditullio Ra Jr Fau - Kastrinakis NG, Kastrinakis Ng Fau - Levy B, Levy B Fau - Kletsas D et al. Activation of the DNA damage checkpoint and genomic instability in human precancerous lesions.

Hanahan D, Weinberg RA. 2000. The Hallmarks of Cancer. *Cell* **100**: 57-70.

Hanks S, Perdeaux ER, Seal S, Ruark E, Mahamdallie SS, Murray A, Ramsay E, Del Vecchio Duarte S, Zachariou A, de Souza B et al. 2014. Germline mutations in the PAF1 complex gene CTR9 predispose to Wilms tumour. *Nat Commun* **5**: 4398.

Hartzell C, Ksionda O, Lemmens E, Coakley K, Yang M, Dail M, Harvey RC, Govern C, Bakker J, Lenstra TL et al. 2013. Dysregulated RasGRP1 Responds to Cytokine Receptor Input in T Cell Leukemogenesis. *Sci Signal* **6**: ra21.

Herr P, Lundin C, Evers B, Ebner D, Bauerschmidt C, Kingham G, Palmai-Pallag T, Mortusewicz O, Frings O, Sonnhammer E et al. 2015. A genome-wide IR-induced RAD51 foci RNAi screen identifies CDC73 involved in chromatin remodeling for DNA repair. *Cell Discov* **1**: 15034.

Herranz D, Ambesi-Impiombato A, Palomero T, Schnell SA, Belver L, Wendorff AA, Xu L, Castillo-Martin M, Llobet-Navas D, Cordon-Cardo C et al. 2014. A NOTCH1-driven

MYC enhancer promotes T cell development, transformation and acute lymphoblastic leukemia. *Nat Med* **20**: 1130-1137.

Homminga I, Pieters R Fau - Langerak AW, Langerak Aw Fau - de Rooi JJ, de Rooi Jj Fau - Stubbs A, Stubbs A Fau - Verstegen M, Verstegen M Fau - Vuerhard M, Vuerhard M Fau - Buijs-Gladdines J, Buijs-Gladdines J Fau - Kooi C, Kooi C Fau - Klous P, Klous P Fau - van Vlierberghe P et al. Integrated transcript and genome analyses reveal NKX2-1 and MEF2C as potential oncogenes in T cell acute lymphoblastic leukemia.

Hosokawa H, Rothenberg EV. 2021. How transcription factors drive choice of the T cell fate. *Nat Rev Immunol* **21**: 162-176.

Hou L, Wang Y, Liu Y, Zhang N, Shamovsky I, Nudler E, Tian B, Dynlacht BD. 2019. Paf1C regulates RNA polymerase II progression by modulating elongation rate. *Proc Natl Acad Sci U S A* **116**: 14583-14592.

Howell VM, Haven CJ, Kahnoski K, Khoo SK, Petillo D, Chen J, Fleuren GJ, Robinson BG, Delbridge LW, Philips J. 2003. HRPT2 mutations are associated with malignancy in sporadic parathyroid tumours. *Journal of medical genetics* **40**: 657-663.

Hsieh JJ, Henkel T Fau - Salmon P, Salmon P Fau - Robey E, Robey E Fau - Peterson MG, Peterson Mg Fau - Hayward SD, Hayward SD. Truncated mammalian Notch1 activates CBF1/RBPJk-repressed genes by a mechanism resembling that of Epstein-Barr virus EBNA2.

Huether R, Dong L, Chen X, Wu G, Parker M, Wei L, Ma J, Edmonson MN, Hedlund EK, Rusch MC. 2014. The landscape of somatic mutations in epigenetic regulators across 1,000 paediatric cancer genomes. *Nature communications* **5**: 3630.

Irving J, Matheson E, Minto L, Blair H, Case M, Halsey C, Swidenbank I, Ponthan F, Kirschner-Schwabe R, Groeneveld-Krentz S et al. Ras pathway mutations are prevalent in relapsed childhood acute lymphoblastic leukemia and confer sensitivity to MEK inhibition.

Ishikawa K, Takenaga K, Akimoto M, Koshikawa N, Yamaguchi A, Imanishi H, Nakada K, Honma Y, Hayashi J-I. 2008. ROS-generating mitochondrial DNA mutations can regulate tumor cell metastasis. *Science* **320**: 661-664.

Jaehning JA. 2010. The Paf1 complex: platform or player in RNA polymerase II transcription? *Biochim Biophys Acta* **1799**: 379-388.

Jarriault S, Brou C Fau - Logeat F, Logeat F Fau - Schroeter EH, Schroeter Eh Fau - Kopan R, Kopan R Fau - Israel A, Israel A. Signalling downstream of activated mammalian Notch.

Jenkinson S, Koo K, Mansour MR, Goulden N, Vora A, Mitchell C, Wade R, Richards S, Hancock J, Moorman AV et al. 2013. Impact of NOTCH1/FBXW7 mutations on outcome in pediatric T-cell acute lymphoblastic leukemia patients treated on the MRC UKALL 2003 trial. *Leukemia* **27**: 41-47.

Justice NJ, Jan YN. Variations on the Notch pathway in neural development.

Karmakar S, Seshacharyulu P, Lakshmanan I, Vaz AP, Chugh S, Sheinin YM, Mahapatra S, Batra SK, Ponnusamy MP. 2017. hPaf1/PD2 interacts with OCT3/4 to promote self-renewal of ovarian cancer stem cells. *Oncotarget* **8**: 14806-14820.

Khanna A, Bhushan B, Chauhan PS, Saxena S, Gupta DK, Siraj F. 2018. High mTOR expression independently prognosticates poor clinical outcome to induction chemotherapy in acute lymphoblastic leukemia. *Clinical and experimental medicine* **18**: 221-227.

Kikuchi I, Takahashi-Kanemitsu A, Sakiyama N, Tang C, Tang PJ, Noda S, Nakao K, Kassai H, Sato T, Aiba A et al. 2016. Dephosphorylated parafibromin is a transcriptional coactivator of the Wnt/Hedgehog/Notch pathways. *Nat Commun* **7**: 12887.

Kim J, Guermah M, McGinty RK, Lee JS, Tang Z, Milne TA, Shilatifard A, Muir TW, Roeder RG. 2009. RAD6-Mediated transcription-coupled H2B ubiquitylation directly stimulates H3K4 methylation in human cells. *Cell* **137**: 459-471.

Kim J, Roeder RG. 2009. Direct Bre1-Paf1 complex interactions and RING finger-independent Bre1-Rad6 interactions mediate histone H2B ubiquitylation in yeast. *J Biol Chem* **284**: 20582-20592.

Kishton RJ, Barnes CE, Nichols AG, Cohen S, Gerriets VA, Siska PJ, Macintyre AN, Goraksha-Hicks P, de Cubas AA, Liu T et al. 2016. AMPK Is Essential to Balance Glycolysis and Mitochondrial Metabolism to Control T-ALL Cell Stress and Survival. *Cell Metab* **23**: 649-662.

Kopan R. 2012. Notch signaling. *Cold Spring Harb Perspect Biol* **4**.

Koppenol WH, Bounds PL, Dang CV. 2011. Otto Warburg's contributions to current concepts of cancer metabolism. *Nature Reviews Cancer* **11**: 325-337.

Kotsantis P, Petermann E, Boulton SJ. 2018. Mechanisms of Oncogene-Induced Replication Stress: Jigsaw Falling into Place. *Cancer Discov* **8**: 537-555.

Kox C, Zimmermann M, Stanulla M, Leible S, Schrappe M, Ludwig WD, Koehler R, Tolle G, Bandapalli OR, Breit S et al. 2010. The favorable effect of activating NOTCH1 receptor mutations on long-term outcome in T-ALL patients treated on the ALL-BFM 2000 protocol can be separated from FBXW7 loss of function. *Leukemia* **24**: 2005-2013.

Krogan NJ, Dover J Fau - Wood A, Wood A Fau - Schneider J, Schneider J Fau - Heidt J, Heidt J Fau - Boateng MA, Boateng Ma Fau - Dean K, Dean K Fau - Ryan OW, Ryan Ow Fau - Golshani A, Golshani A Fau - Johnston M, Johnston M Fau - Greenblatt JF et al. The Paf1 complex is required for histone H3 methylation by COMPASS and Dot1p: linking transcriptional elongation to histone methylation.

Krop I, Demuth T, Guthrie T, Wen PY, Mason WP, Chinnaiyan P, Butowski N, Groves MD, Kesari S, Freedman SJ et al. 2012. Phase I pharmacologic and pharmacodynamic study of the gamma secretase (Notch) inhibitor MK-0752 in adult patients with advanced solid tumors. *J Clin Oncol* **30**: 2307-2313.

Ksionda O, Melton AA, Bache J, Tenhagen M, Bakker J, Harvey R, Winter SS, Rubio I, Roose JP. 2016. RasGRP1 overexpression in T-ALL increases basal nucleotide exchange on Ras rendering the Ras/PI3K/Akt pathway responsive to protumorigenic cytokines. *Oncogene* **35**: 3658-3668.

Kumar S, Jones M, Li Q, Lombard DB. 2021. Assessment of Cellular Bioenergetics in Mouse Hematopoietic Stem and Primitive Progenitor Cells using the Extracellular Flux Analyzer. *J Vis Exp*.

Kwiatkowski N, Zhang T, Rahl PB, Abraham BJ, Reddy J, Ficarro SB, Dastur A, Amzallag A, Ramaswamy S, Tesar B et al. 2014. Targeting transcription regulation in cancer with a covalent CDK7 inhibitor. *Nature* **511**: 616-620.

La Starza R, Borga C, Barba G, Pierini V, Schwab C, Matteucci C, Lema Fernandez AG, Leszl A, Cazzaniga G, Chiaretti S et al. Genetic profile of T-cell acute lymphoblastic leukemias with MYC translocations.

La Starza R, Pierini V, Pierini T, Nofrini V, Matteucci C, Arniani S, Moretti M, Lema Fernandez AG, Pellanera F, Di Giacomo D et al. Design of a Comprehensive Fluorescence in Situ Hybridization Assay for Genetic Classification of T-Cell Acute Lymphoblastic Leukemia.

Lee O, O'Brien PJ. 2010. 1.19 - Modifications of Mitochondrial Function by Toxicants. in *Comprehensive Toxicology (Second Edition)* (ed. CA McQueen), pp. 411-445. Elsevier, Oxford.

Leon TE, Rapoz-D'Silva T, Bertoli C, Rahman S, Magnussen M, Philip B, Farah N, Richardson SE, Ahrabi S, Afonso Guerra-Assuncao J et al. 2020. EZH2 deficient T-cell acute lymphoblastic leukemia is sensitized to CHK1 inhibition through enhanced replication stress. *Cancer Discov*.

Li N, Fassl A, Chick J, Inuzuka H, Li X, Mansour MR, Liu L, Wang H, King B, Shaik S et al. Cyclin C is a haploinsufficient tumour suppressor.

Lieu YK, Kumar A, Pajerowski AG, Rogers TJ, Reddy EP. 2004. Requirement of c-myb in T cell development and in mature T cell function. *Proc Natl Acad Sci U S A* **101**: 14853-14858.

Lin S, Tian L, Shen H, Gu Y, Li JL, Chen Z, Sun X, You MJ, Wu L. 2013. DDX5 is a positive regulator of oncogenic NOTCH1 signaling in T cell acute lymphoblastic leukemia. *Oncogene* **32**: 4845-4853.

Liu YA-O, Easton J, Shao Y, Maciaszek J, Wang Z, Wilkinson MR, McCastlain KA-O, Edmonson M, Pounds SA-O, Shi L et al. The genomic landscape of pediatric and young adult T-lineage acute lymphoblastic leukemia.

Lonetti A, Cappellini A, Bertaina A, Locatelli F, Pession A, Buontempo F, Evangelisti C, Orsini E, Zambonin L, Neri LM et al. Improving nelarabine efficacy in T cell acute lymphoblastic leukemia by targeting aberrant PI3K/AKT/mTOR signaling pathway.

Lovén J, Hoke HA, Lin CY, Lau A, Orlando DA, Vakoc CR, Bradner JE, Lee TI, Young RA. 2013. Selective inhibition of tumor oncogenes by disruption of super-enhancers. *Cell* **153**: 320-334.

Magnuson B, Veloso A, Kirkconnell KS, de Andrade Lima LC, Paulsen MT, Ljungman EA, Bedi K, Prasad J, Wilson TE, Ljungman M. 2015. Identifying transcription start sites and active enhancer elements using BruUV-seq. *Sci Rep* **5**: 17978.

Maillard I, Schwarz BA, Sambandam A, Fang T, Shestova O, Xu L, Bhandoola A, Pear WS. 2006a. Notch-dependent T-lineage commitment occurs at extrathymic sites following bone marrow transplantation. *Blood* **107**: 3511-3519.

Maillard I, Tu L, Sambandam A, Yashiro-Ohtani Y, Millholland J, Keeshan K, Shestova O, Xu L, Bhandoola A, Pear WS. 2006b. The requirement for Notch signaling at the beta-selection checkpoint in vivo is absolute and independent of the pre-T cell receptor. *J Exp Med* **203**: 2239-2245.

Mansour MR, Abraham BJ, Anders L, Berezovskaya A, Gutierrez A, Durbin AD, Etchin J, Lawton L, Sallan SE, Silverman LB et al. Oncogene regulation. An oncogenic super-enhancer formed through somatic mutation of a noncoding intergenic element.

Mansour MR, Sulis ML, Duke V, Foroni L, Jenkinson S, Koo K, Allen CG, Gale RE, Buck G, Richards S et al. 2009. Prognostic implications of NOTCH1 and FBXW7 mutations in adults with T-cell acute lymphoblastic leukemia treated on the MRC UKALLXII/ECOG E2993 protocol. *J Clin Oncol* **27**: 4352-4356.

Marchesini M, Gherli A, Montanaro A, Patrizi L, Sorrentino C, Pagliaro L, Rompietti C, Kitara S, Heit S, Olesen CE et al. Blockade of Oncogenic NOTCH1 with the SERCA Inhibitor CAD204520 in T Cell Acute Lymphoblastic Leukemia.

Maude SL, Dolai S, Delgado-Martin C, Vincent T, Robbins A, Selvanathan A, Ryan T, Hall J, Wood AC, Tasian SK et al. Efficacy of JAK/STAT pathway inhibition in murine xenograft models of early T-cell precursor (ETP) acute lymphoblastic leukemia.

-. 2015. Efficacy of JAK/STAT pathway inhibition in murine xenograft models of early T-cell precursor (ETP) acute lymphoblastic leukemia.

Maya-Mendoza A, Ostrakova J, Kosar M, Hall A, Duskova P, Mistrik M, Merchut-Maya JM, Hodny Z, Bartkova J, Christensen C et al. Myc and Ras oncogenes engage different energy metabolism programs and evoke distinct patterns of oxidative and DNA replication stress.

Mazzucchelli R, Durum SK. Interleukin-7 receptor expression: intelligent design.

McCarter AC, Gatta GD, Melnick A, Kim E, Sha C, Wang Q, Nalamolu JK, Liu Y, Keeley TM, Yan R et al. 2020a. Combinatorial ETS1-Dependent Control of Oncogenic NOTCH1 Enhancers in T-cell Leukemia. *Blood Cancer Discovery*.

McCarter AC, Wang Q, Chiang M. 2018. Notch in Leukemia. *Adv Exp Med Biol* **1066**: 355-394.

McCarter AM, Della Gatta G, Melnick A, Kim E, Sha C, Wang Q, Nalamolu JK, Liu Y, Keeley TM, Yan R et al. 2020b. Combinatorial ETS1-dependent control of oncogenic NOTCH1 enhancers in T-cell leukemia. *Blood Cancer Discovery* **1**: 178-197.

McCarthy DJ, Chen Y, Smyth GK. 2012. Differential expression analysis of multifactor RNA-Seq experiments with respect to biological variation. *Nucleic Acids Res* **40**: 4288-4297.

Meyer LK, Huang BJ, Delgado-Martin C, Roy RP, Hechmer A, Wandler AM, Vincent TL, Fortina P, Olshen AB, Wood BL et al. 2020. Glucocorticoids paradoxically facilitate steroid resistance in T cell acute lymphoblastic leukemias and thymocytes. *The Journal of Clinical Investigation* **130**: 863-876.

Milani G, Matthijssens F, Van Loocke W, Durinck K, Roels J, Peirs S, Thénoz M, Pieters T, Reunes L, Lintermans B et al. Genetic characterization and therapeutic targeting of MYC-rearranged T cell acute lymphoblastic leukaemia.

Moorman AA-O, Schwab C, Winterman E, Hancock J, Castleton A, Cummins M, Gibson B, Goulden N, Kearns PA-O, James B et al. Adjuvant tyrosine kinase inhibitor therapy improves outcome for children and adolescents with acute lymphoblastic leukaemia who have an ABL-class fusion.

Muntean AG, Tan J, Sitwala K, Huang Y, Bronstein J, Connelly JA, Basrur V, Elenitoba-Johnson KS, Hess JL. 2010. The PAF complex synergizes with MLL fusion proteins at HOX loci to promote leukemogenesis. *Cancer Cell* **17**: 609-621.

Murga M, Campaner S, Lopez-Contreras AJ, Toledo LI, Soria R, Montaña MF, Artista L, Schleker T, Guerra C, Garcia E et al. Exploiting oncogene-induced replicative stress for the selective killing of Myc-driven tumors.

Mühlbacher V, Zenger M, Schnittger S, Weissmann S, Kunze F, Kohlmann A, Bellos F, Kern W, Haferlach T, Haferlach C. 2014. Acute lymphoblastic leukemia with low hypodiploid/near triploid karyotype is a specific clinical entity and exhibits a very high TP53 mutation frequency of 93%. *Genes, Chromosomes and Cancer* **53**: 524-536.

Nakagawa M, Shaffer AL, Ceribelli M, Zhang M, Wright G, Xiao W, Powell J, Petrus MN, Yang Y, Phelan JD. 2018. Targeting the HTLV-I-regulated BATF3/IRF4 transcriptional network in adult T cell leukemia/lymphoma. *Cancer Cell* **34**: 286-297.

Narita T, Ishida T, Ito A, Masaki A, Kinoshita S, Suzuki S, Takino H, Yoshida T, Ri M, Kusumoto S. 2017. Cyclin-dependent kinase 9 is a novel specific molecular target in

adult T-cell leukemia/lymphoma. *Blood, The Journal of the American Society of Hematology* **130**: 1114-1124.

Nene RV, Putnam CD, Li BZ, Nguyen KG, Srivatsan A, Campbell CS, Desai A, Kolodner RD. 2018. Cdc73 suppresses genome instability by mediating telomere homeostasis. *PLoS Genet* **14**: e1007170.

Ng HH, Dole S, Struhl K. 2003. The Rtf1 component of the Paf1 transcriptional elongation complex is required for ubiquitination of histone H2B. *J Biol Chem* **278**: 33625-33628.

O'Neil J, Grim J Fau - Strack P, Strack P Fau - Rao S, Rao S Fau - Tibbitts D, Tibbitts D Fau - Winter C, Winter C Fau - Hardwick J, Hardwick J Fau - Welcker M, Welcker M Fau - Meijerink JP, Meijerink Jp Fau - Pieters R, Pieters R Fau - Draetta G et al. FBW7 mutations in leukemic cells mediate NOTCH pathway activation and resistance to gamma-secretase inhibitors.

Ogrunc M, Di Micco R, Liontos M, Bombardelli LA-O, Mione M, Fumagalli M, Gorgoulis VG, d'Adda di Fagagna F. Oncogene-induced reactive oxygen species fuel hyperproliferation and DNA damage response activation.

Oliveira ML, Akkapeddi P, Ribeiro D, Melao A, Barata JT. 2019. IL-7R-mediated signaling in T-cell acute lymphoblastic leukemia: An update. *Adv Biol Regul* **71**: 88-96.

Olson CM, Jiang B, Erb MA, Liang Y, Doctor ZM, Zhang Z, Zhang T, Kwiatkowski N, Boukhali M, Green JL. 2018. Pharmacological perturbation of CDK9 using selective CDK9 inhibition or degradation. *Nature chemical biology* **14**: 163-170.

Oshima K, Khiabanian H, da Silva-Almeida AC, Tzoneva G, Abate F, Ambesi-Impiombato A, Sanchez-Martin M, Carpenter Z, Penson A, Perez-Garcia A et al. Mutational landscape, clonal evolution patterns, and role of RAS mutations in relapsed acute lymphoblastic leukemia.

Oswald F, Täuber B, Dobner T, Bourteele S, Kostezka U, Adler G, Liptay S, Schmid RM. 2001. p300 acts as a transcriptional coactivator for mammalian Notch-1. *Molecular and cellular biology* **21**: 7761-7774.

Ott CJ. 2014. Promising new strategies to target gene regulatory factors in T-cell acute lymphoblastic leukemia. *Int J Hematol Oncol* **3**: 379-381.

Ott CJ, Kopp N, Bird L, Paranal RM, Qi J, Bowman T, Rodig SJ, Kung AL, Bradner JE, Weinstock DM. 2012. BET bromodomain inhibition targets both c-Myc and IL7R in high-risk acute lymphoblastic leukemia. *Blood, The Journal of the American Society of Hematology* **120**: 2843-2852.

Padi SKR, Luevano LA, An N, Pandey R, Singh N, Song JH, Aster JC, Yu XZ, Mehrotra S, Kraft AS. Targeting the PIM protein kinases for the treatment of a T-cell acute lymphoblastic leukemia subset.

Paganin M, Ferrando A. Molecular pathogenesis and targeted therapies for NOTCH1-induced T-cell acute lymphoblastic leukemia.

Palomero T, Lim WK, Odom DT, Sulis ML, Real PJ, Margolin A, Barnes KC, O'Neil J, Neuberg D, Weng AP et al. 2006. NOTCH1 directly regulates c-MYC and activates a feed-forward-loop transcriptional network promoting leukemic cell growth. *Proc Natl Acad Sci U S A* **103**: 18261-18266.

Palomero T, Sulis Ml Fau - Cortina M, Cortina M Fau - Real PJ, Real Pj Fau - Barnes K, Barnes K Fau - Ciofani M, Ciofani M Fau - Caparros E, Caparros E Fau - Buteau J, Buteau J Fau - Brown K, Brown K Fau - Perkins SL, Perkins Sl Fau - Bhagat G et al. Mutational loss of PTEN induces resistance to NOTCH1 inhibition in T-cell leukemia.

Panin VM, Irvine KD. Modulators of Notch signaling.
Paulsen MT, Veloso A, Prasad J, Bedi K, Ljungman EA, Magnuson B, Wilson TE, Ljungman M. 2014. Use of Bru-Seq and BruChase-Seq for genome-wide assessment of the synthesis and stability of RNA. *Methods* **67**: 45-54.
Paulsen MT, Veloso A, Prasad J, Bedi K, Ljungman EA, Tsan YC, Chang CW, Tarrier B, Washburn JG, Lyons R et al. 2013. Coordinated regulation of synthesis and stability of RNA during the acute TNF-induced proinflammatory response. *Proc Natl Acad Sci U S A* **110**: 2240-2245.
Pear WS, Aster JC, Scott ML, Hasserjian RP, Soffer B, Sklar J, Baltimore D. 1996. Exclusive development of T cell neoplasms in mice transplanted with bone marrow expressing activated Notch alleles. *J Exp Med* **183**: 2283-2291.
Peirs S, Matthijssens F, Goossens S, Van de Walle I, Ruggero K, de Bock CE, Degryse S, Canté-Barrett K, Briot D, Clappier E et al. ABT-199 mediated inhibition of BCL-2 as a novel therapeutic strategy in T-cell acute lymphoblastic leukemia.
Penheiter KL, Washburn TM, Porter SE, Hoffman MG, Jaehning JA. 2005. A posttranscriptional role for the yeast Paf1-RNA polymerase II complex is revealed by identification of primary targets. *Mol Cell* **20**: 213-223.
Pham NA, Robinson BH, Hedley DW. 2000. Simultaneous detection of mitochondrial respiratory chain activity and reactive oxygen in digitonin-permeabilized cells using flow cytometry. *Cytometry: The Journal of the International Society for Analytical Cytology* **41**: 245-251.
Pinnell N, Yan R, Cho HJ, Keeley T, Murai MJ, Liu Y, Alarcon AS, Qin J, Wang Q, Kuick R et al. 2015. The PIAS-like Coactivator Zmiz1 Is a Direct and Selective Cofactor of Notch1 in T Cell Development and Leukemia. *Immunity* **43**: 870-883.
Piya S, Yang Y, Bhattacharya S, Sharma P, Ma H, Mu H, He H, Ruvolo V, Baran N, Davis RE et al. 2022. Targeting the NOTCH1-MYC-CD44 axis in leukemia-initiating cells in T-ALL. *Leukemia* **36**: 1261-1273.
Pui CH, Robison LL, Look AT. 2008. Acute lymphoblastic leukaemia. *Lancet* **371**: 1030-1043.
Quinlan AR, Hall IM. 2010. BEDTools: a flexible suite of utilities for comparing genomic features. *Bioinformatics* **26**: 841-842.
Rahl PB, Lin CY, Seila AC, Flynn RA, McCuine S, Burge CB, Sharp PA, Young RA. 2010. c-Myc regulates transcriptional pause release. *Cell* **141**: 432-445.
Rahman S, Magnussen M, León TE, Farah N, Li Z, Abraham BJ, Alapi KZ, Mitchell RJ, Naughton T, Fielding AK et al. Activation of the LMO2 oncogene through a somatically acquired neomorphic promoter in T-cell acute lymphoblastic leukemia.
Ramirez F, Ryan DP, Gruning B, Bhardwaj V, Kilpert F, Richter AS, Heyne S, Dundar F, Manke T. 2016. deepTools2: a next generation web server for deep-sequencing data analysis. *Nucleic Acids Res* **44**: W160-165.
Rauch DA, Olson SL, Harding JC, Sundaramoorthi H, Kim Y, Zhou T, MacLeod AR, Challen G, Ratner L. 2020. Interferon regulatory factor 4 as a therapeutic target in adult T-cell leukemia lymphoma. *Retrovirology* **17**: 1-10.
Ray PD, Huang Bw Fau - Tsuji Y, Tsuji Y. Reactive oxygen species (ROS) homeostasis and redox regulation in cellular signaling.
Relling MV, Ramsey LB. 2013. Pharmacogenomics of acute lymphoid leukemia: new insights into treatment toxicity and efficacy. *Hematology 2013, the American Society of Hematology Education Program Book* **2013**: 126-130.

Ribeiro D, Melão A, van Boxtel R, Santos CI, Silva A, Silva MC, Cardoso BA, Coffer PJ, Barata JT. 2018. STAT5 is essential for IL-7–mediated viability, growth, and proliferation of T-cell acute lymphoblastic leukemia cells. *Blood Advances* **2**: 2199-2213.

Robinson MD, McCarthy DJ, Smyth GK. 2010. edgeR: a Bioconductor package for differential expression analysis of digital gene expression data. *Bioinformatics* **26**: 139-140.

Rocha JC, Cheng C Fau - Liu W, Liu W Fau - Kishi S, Kishi S Fau - Das S, Das S Fau - Cook EH, Cook Eh Fau - Sandlund JT, Sandlund Jt Fau - Rubnitz J, Rubnitz J Fau - Ribeiro R, Ribeiro R Fau - Campana D, Campana D Fau - Pui C-H et al. 2005. Pharmacogenetics of outcome in children with acute lymphoblastic leukemia.

Roderick JE, Tesell J, Shultz LD, Brehm MA, Greiner DL, Harris MH, Silverman LB, Sallan SE, Gutierrez A, Look AT et al. 2014. c-Myc inhibition prevents leukemia initiation in mice and impairs the growth of relapsed and induction failure pediatric T-ALL cells. *Blood* **123**: 1040-1050.

Rodriguez S, Abundis C, Boccalatte F, Mehrotra P, Chiang MY, Yui MA, Wang L, Zhang H, Zollman A, Bonfim-Silva R et al. Therapeutic targeting of the E3 ubiquitin ligase SKP2 in T-ALL.

Ropa J, Saha N, Chen Z, Serio J, Chen W, Mellacheruvu D, Zhao L, Basrur V, Nesvizhskii AI, Muntean AG. 2018. PAF1 complex interactions with SETDB1 mediate promoter H3K9 methylation and transcriptional repression of Hoxa9 and Meis1 in acute myeloid leukemia. *Oncotarget* **9**: 22123-22136.

Ross-Innes CS, Stark R, Teschendorff AE, Holmes KA, Ali HR, Dunning MJ, Brown GD, Gojis O, Ellis IO, Green AR et al. 2012. Differential oestrogen receptor binding is associated with clinical outcome in breast cancer. *Nature* **481**: 389-393.

Saha N, Ropa J, Chen L, Hu H, Mysliwski M, Friedman A, Maillard I, Muntean AG. 2019. The PAF1c Subunit CDC73 Is Required for Mouse Hematopoietic Stem Cell Maintenance but Displays Leukemia-Specific Gene Regulation. *Stem Cell Reports* **12**: 1069-1083.

Sakamoto H, Ando K, Imaizumi Y, Mishima H, Kinoshita A, Kobayashi Y, Kitanosono H, Kato T, Sawayama Y, Sato S et al. 2022. Alvocidib inhibits IRF4 expression via super-enhancer suppression and adult T-cell leukemia/lymphoma cell growth. *Cancer Science* **113**: 4092-4103.

Saldivar JC, Cortez D, Cimprich KA. The essential kinase ATR: ensuring faithful duplication of a challenging genome.

Samon JB, Castillo-Martin M Fau - Hadler M, Hadler M Fau - Ambesi-Impiobato A, Ambesi-Impiobato A Fau - Paietta E, Paietta E Fau - Racevskis J, Racevskis J Fau - Wiernik PH, Wiernik Ph Fau - Rowe JM, Rowe Jm Fau - Jakubczak J, Jakubczak J Fau - Randolph S, Randolph S Fau - Cordon-Cardo C et al. Preclinical analysis of the γ-secretase inhibitor PF-03084014 in combination with glucocorticoids in T-cell acute lymphoblastic leukemia.

Sanchez-Irizarry C, Carpenter Ac Fau - Weng AP, Weng Ap Fau - Pear WS, Pear Ws Fau - Aster JC, Aster Jc Fau - Blacklow SC, Blacklow SC. Notch subunit heterodimerization and prevention of ligand-independent proteolytic activation depend, respectively, on a novel domain and the LNR repeats.

Sanchez-Martin M, Ambesi-Impiombato A, Qin Y, Herranz D, Bansal M, Girardi T, Paietta E, Tallman MS, Rowe JM, De Keersmaecker KA-O et al. Synergistic antileukemic therapies in NOTCH1-induced T-ALL.

Sanda T, Lawton Ln Fau - Barrasa MI, Barrasa Mi Fau - Fan ZP, Fan Zp Fau - Kohlhammer H, Kohlhammer H Fau - Gutierrez A, Gutierrez A Fau - Ma W, Ma W Fau - Tatarek J, Tatarek J Fau - Ahn Y, Ahn Y Fau - Kelliher MA, Kelliher Ma Fau - Jamieson CHM et al. Core transcriptional regulatory circuit controlled by the TAL1 complex in human T cell acute lymphoblastic leukemia.

Sava GP, Fan H, Coombes RC, Buluwela L, Ali S. 2020. CDK7 inhibitors as anticancer drugs.

Seo J, Kim SC, Lee HS, Kim JK, Shon HJ, Salleh NL, Desai KV, Lee JH, Kang ES, Kim JS et al. 2012. Genome-wide profiles of H2AX and gamma-H2AX differentiate endogenous and exogenous DNA damage hotspots in human cells. *Nucleic Acids Res* **40**: 5965-5974.

Serafin V, Lissandron V, Buldini B, Bresolin S, Paganin M, Grillo F, Andriano N, Palmi C, Cazzaniga G, Marmiroli S et al. Phosphoproteomic analysis reveals hyperactivation of mTOR/STAT3 and LCK/Calcineurin axes in pediatric early T-cell precursor ALL.

Shattuck TM, Välimäki S, Obara T, Gaz RD, Clark OH, Shoback D, Wierman ME, Tojo K, Robbins CM, Carpten JD. 2003. Somatic and germ-line mutations of the HRPT2 gene in sporadic parathyroid carcinoma. *New England Journal of Medicine* **349**: 1722-1729.

Shilatifard A. Chromatin modifications by methylation and ubiquitination: implications in the regulation of gene expression.

Shivji MKK, Renaudin X, Williams CH, Venkitaraman AR. 2018. BRCA2 Regulates Transcription Elongation by RNA Polymerase II to Prevent R-Loop Accumulation. *Cell Rep* **22**: 1031-1039.

Siebel C, Lendahl U. 2017. Notch Signaling in Development, Tissue Homeostasis, and Disease. *Physiol Rev* **97**: 1235-1294.

Silic-Benussi M, Cannizzaro E, Venerando A, Cavallari I, Petronilli V, La Rocca N, Marin O, Chieco-Bianchi L, Di Lisa F, D'Agostino DM. 2009. Modulation of mitochondrial K+ permeability and reactive oxygen species production by the p13 protein of human T-cell leukemia virus type 1. *Biochimica et Biophysica Acta (BBA)-Bioenergetics* **1787**: 947-954.

Silic-Benussi M, Cavallari I, Vajente N, Vidali S, Chieco-Bianchi L, Di Lisa F, Saggioro D, D'Agostino DM, Ciminale V. 2010. Redox regulation of T-cell turnover by the p13 protein of human T-cell leukemia virus type 1: distinct effects in primary versus transformed cells. *Blood, The Journal of the American Society of Hematology* **116**: 54-62.

Silic-Benussi M, Sharova E, Ciccarese F, Cavallari I, Raimondi V, Urso L, Corradin A, Kotler H, Scattolin G, Buldini B et al. 2022. mTOR inhibition downregulates glucose-6-phosphate dehydrogenase and induces ROS-dependent death in T-cell acute lymphoblastic leukemia cells. *Redox Biology* **51**: 102268.

Silva A, Almeida ARM, Cachucho A, Neto JL, Demeyer S, de Matos M, Hogan T, Li Y, Meijerink J, Cools J et al. 2021. Overexpression of wild-type IL-7Ralpha promotes T-cell acute lymphoblastic leukemia/lymphoma. *Blood* **138**: 1040-1052.

Silva A, Girio A, Cebola I, Santos CI, Antunes F, Barata JT. 2011. Intracellular reactive oxygen species are essential for PI3K/Akt/mTOR-dependent IL-7-mediated viability of T-cell acute lymphoblastic leukemia cells. *Leukemia* **25**: 960-967.

Silveira AB, Laranjeira AB, Rodrigues GO, Leal PC, Cardoso BA, Barata JT, Yunes RA, Zanchin NI, Brandalise SR, Yunes JA. PI3K inhibition synergizes with glucocorticoids but antagonizes with methotrexate in T-cell acute lymphoblastic leukemia.

Soulier J, Clappier E Fau - Cayuela J-M, Cayuela Jm Fau - Regnault A, Regnault A Fau - García-Peydró M, García-Peydró M Fau - Dombret H, Dombret H Fau - Baruchel A,

Baruchel A Fau - Toribio M-L, Toribio Ml Fau - Sigaux F, Sigaux F. HOXA genes are included in genetic and biologic networks defining human acute T-cell leukemia (T-ALL).

Spaulding C, Reschly EJ, Zagort DE, Yashiro-Ohtani Y, Beverly LJ, Capobianco A, Pear WS, Kee BL. 2007. Notch1 co-opts lymphoid enhancer factor 1 for survival of murine T-cell lymphomas. *Blood* **110**: 2650-2658.

Spits H. Development of alphabeta T cells in the human thymus.

Subramaniam Prem S, Whye Dosh W, Efimenko E, Chen J, Tosello V, De Keersmaecker K, Kashishian A, Thompson Mary A, Castillo M, Cordon-Cardo C et al. 2012. Targeting Nonclassical Oncogenes for Therapy in T-ALL. *Cancer Cell* **21**: 459-472.

Suzuki S Fau - Nagel S, Nagel S Fau - Schneider B, Schneider B Fau - Chen S, Chen S Fau - Kaufmann M, Kaufmann M Fau - Uozumi K, Uozumi K Fau - Arima N, Arima N Fau - Drexler HG, Drexler Hg Fau - MacLeod RAF, MacLeod RA. A second NOTCH1 chromosome rearrangement: t(9;14)(q34.3;q11.2) in T-cell neoplasia.

Szwed A, Kim E, Jacinto E. 2021. Regulation and metabolic functions of mTORC1 and mTORC2. *Physiological Reviews* **101**: 1371-1426.

Tanigaki K, Tsuji M, Yamamoto N, Han H, Tsukada J, Inoue H, Kubo M, Honjo T. 2004. Regulation of alphabeta/gammadelta T cell lineage commitment and peripheral T cell responses by Notch/RBP-J signaling. *Immunity* **20**: 611-622.

Tatarek J, Cullion K, Ashworth T, Gerstein R, Aster JC, Kelliher MA. 2011. Notch1 inhibition targets the leukemia-initiating cells in a Tal1/Lmo2 mouse model of T-ALL. *Blood* **118**: 1579-1590.

Tatum D, Li W, Placer M, Li S. 2011. Diverse roles of RNA polymerase II-associated factor 1 complex in different subpathways of nucleotide excision repair. *J Biol Chem* **286**: 30304-30313.

Tenney K, Gerber M, Ilvarsonn A, Schneider J, Gause M, Dorsett D, Eissenberg JC, Shilatifard A. 2006. Drosophila Rtf1 functions in histone methylation, gene expression, and Notch signaling. *Proc Natl Acad Sci U S A* **103**: 11970-11974.

Thandapani P, Kloetgen A, Witkowski MT, Glytsou C, Lee AK, Wang E, Wang J, LeBoeuf SE, Avrampou K, Papagiannakopoulos T et al. 2021. Valine tRNA levels and availability regulate complex I assembly in leukaemia. *Nature*.

Thompson BJ, Buonamici S Fau - Sulis ML, Sulis Ml Fau - Palomero T, Palomero T Fau - Vilimas T, Vilimas T Fau - Basso G, Basso G Fau - Ferrando A, Ferrando A Fau - Aifantis I, Aifantis I. The SCFFBW7 ubiquitin ligase complex as a tumor suppressor in T cell leukemia.

Tolcher AW, Messersmith WA, Mikulski SM, Papadopoulos KP, Kwak EL, Gibbon DG, Patnaik A, Falchook GS, Dasari A, Shapiro GI et al. 2012. Phase I study of RO4929097, a gamma secretase inhibitor of Notch signaling, in patients with refractory metastatic or locally advanced solid tumors. *J Clin Oncol* **30**: 2348-2353.

Tottone L, Zhdanovskaya N, Carmona Pestaña Á, Zampieri M, Simeoni F, Lazzari S, Ruocco V, Pelullo M, Caiafa P, Felli MP et al. 2019. Histone Modifications Drive Aberrant Notch3 Expression/Activity and Growth in T-ALL. *Frontiers in Oncology* **9**.

Trachootham D, Alexandre J, Huang P. 2009. Targeting cancer cells by ROS-mediated mechanisms: a radical therapeutic approach? *Nature reviews Drug discovery* **8**: 579-591.

Trimarchi T, Bilal E, Ntziachristos P, Fabbri G, Dalla-Favera R, Tsirigos A, Aifantis I. 2014. Genome-wide mapping and characterization of Notch-regulated long noncoding RNAs in acute leukemia. *Cell* **158**: 593-606.

Trinquand A, Tanguy-Schmidt A, Ben Abdelali R, Lambert J, Beldjord K, Lengline E, De Gunzburg N, Payet-Bornet D, Lhermitte L, Mossafa H et al. 2013. Toward a NOTCH1/FBXW7/RAS/PTEN-based oncogenetic risk classification of adult T-cell acute lymphoblastic leukemia: a Group for Research in Adult Acute Lymphoblastic Leukemia study. *J Clin Oncol* **31**: 4333-4342.

Vafa O, Wade M Fau - Kern S, Kern S Fau - Beeche M, Beeche M Fau - Pandita TK, Pandita Tk Fau - Hampton GM, Hampton Gm Fau - Wahl GM, Wahl GM. c-Myc can induce DNA damage, increase reactive oxygen species, and mitigate p53 function: a mechanism for oncogene-induced genetic instability.

Van Oss SB, Cucinotta CE, Arndt KM. 2017. Emerging Insights into the Roles of the Paf1 Complex in Gene Regulation. *Trends Biochem Sci* **42**: 788-798.

Van Oss SB, Shirra MK, Bataille AR, Wier AD, Yen K, Vinayachandran V, Byeon IL, Cucinotta CE, Heroux A, Jeon J et al. 2016. The Histone Modification Domain of Paf1 Complex Subunit Rtf1 Directly Stimulates H2B Ubiquitylation through an Interaction with Rad6. *Mol Cell* **64**: 815-825.

Van Vlierberghe P, Pieters R Fau - Beverloo HB, Beverloo Hb Fau - Meijerink JPP, Meijerink JP. Molecular-genetic insights in paediatric T-cell acute lymphoblastic leukaemia.

Verstovsek S, Kantarjian H, Mesa RA, Pardanani AD, Cortes-Franco J, Thomas DA, Estrov Z, Fridman JS, Bradley EC, Erickson-Viitanen S. 2010. Safety and efficacy of INCB018424, a JAK1 and JAK2 inhibitor, in myelofibrosis. *New England Journal of Medicine* **363**: 1117-1127.

Wahba L, Amon JD, Koshland D, Vuica-Ross M. 2011. RNase H and multiple RNA biogenesis factors cooperate to prevent RNA:DNA hybrids from generating genome instability. *Mol Cell* **44**: 978-988.

Wallberg AE, Pedersen K, Lendahl U, Roeder RG. 2002. p300 and PCAF act cooperatively to mediate transcriptional activation from chromatin templates by notch intracellular domains in vitro. *Molecular and cellular biology* **22**: 7812-7819.

Wang H, Zang C, Taing L, Arnett KL, Wong YJ, Pear WS, Blacklow SC, Liu XS, Aster JC. 2014. NOTCH1-RBPJ complexes drive target gene expression through dynamic interactions with superenhancers. *Proc Natl Acad Sci U S A* **111**: 705-710.

Wang P, Bowl MR, Bender S, Peng J, Farber L, Chen J, Ali A, Zhang Z, Alberts AS, Thakker RV et al. 2008a. Parafibromin, a component of the human PAF complex, regulates growth factors and is required for embryonic development and survival in adult mice. *Mol Cell Biol* **28**: 2930-2940.

Wang PF, Tan MH, Zhang C, Morreau H, Teh BT. 2005. HRPT2, a tumor suppressor gene for hyperparathyroidism-jaw tumor syndrome. *Horm Metab Res* **37**: 380-383.

Wang Z, Zang C, Rosenfeld JA, Schones DE, Barski A, Cuddapah S, Cui K, Roh TY, Peng W, Zhang MQ et al. 2008b. Combinatorial patterns of histone acetylations and methylations in the human genome. *Nat Genet* **40**: 897-903.

Wei P, Walls M Fau - Qiu M, Qiu M Fau - Ding R, Ding R Fau - Denlinger RH, Denlinger Rh Fau - Wong A, Wong A Fau - Tsaparikos K, Tsaparikos K Fau - Jani JP, Jani Jp Fau - Hosea N, Hosea N Fau - Sands M, Sands M Fau - Randolph S et al. Evaluation of

selective gamma-secretase inhibitor PF-03084014 for its antitumor efficacy and gastrointestinal safety to guide optimal clinical trial design.
Weinstein LS, Simonds WF. 2003. HRPT2, a Marker of Parathyroid Cancer. *New England Journal of Medicine* **349**: 1691-1692.
Weng AP, Ferrando AA, Lee W, Morris JPt, Silverman LB, Sanchez-Irizarry C, Blacklow SC, Look AT, Aster JC. 2004. Activating mutations of NOTCH1 in human T cell acute lymphoblastic leukemia. *Science* **306**: 269-271.
Wolfer A, Wilson A, Nemir M, MacDonald HR, Radtke F. 2002. Inactivation of Notch1 impairs VDJbeta rearrangement and allows pre-TCR-independent survival of early alpha beta Lineage Thymocytes. *Immunity* **16**: 869-879.
Won JH, Park S, Hong S, Son S, Yu JW. Rotenone-induced Impairment of Mitochondrial Electron Transport Chain Confers a Selective Priming Signal for NLRP3 Inflammasome Activation.
Wood A, Krogan Nj Fau - Dover J, Dover J Fau - Schneider J, Schneider J Fau - Heidt J, Heidt J Fau - Boateng MA, Boateng Ma Fau - Dean K, Dean K Fau - Golshani A, Golshani A Fau - Zhang Y, Zhang Y Fau - Greenblatt JF, Greenblatt Jf Fau - Johnston M et al. Bre1, an E3 ubiquitin ligase required for recruitment and substrate selection of Rad6 at a promoter.
Wu C, Li W. 2018. Genomics and pharmacogenomics of pediatric acute lymphoblastic leukemia. *Critical Reviews in Oncology/Hematology* **126**: 100-111.
Yatim A, Benne C, Sobhian B, Laurent-Chabalier S, Deas O, Judde JG, Lelievre JD, Levy Y, Benkirane M. 2012. NOTCH1 nuclear interactome reveals key regulators of its transcriptional activity and oncogenic function. *Mol Cell* **48**: 445-458.
Yost AJ, Shevchuk OO, Gooch R, Gusscott S, You MJ, Ince TA, Aster JC, Weng AP. 2013. Defined, serum-free conditions for in vitro culture of primary human T-ALL blasts. *Leukemia* **27**: 1437-1440.
Yu M, Yang W, Ni T, Tang Z, Nakadai T, Zhu J, Roeder RG. 2015. RNA polymerase II-associated factor 1 regulates the release and phosphorylation of paused RNA polymerase II. *Science* **350**: 1383-1386.
Zenatti PP, Ribeiro D Fau - Li W, Li W Fau - Zuurbier L, Zuurbier L Fau - Silva MC, Silva Mc Fau - Paganin M, Paganin M Fau - Tritapoe J, Tritapoe J Fau - Hixon JA, Hixon Ja Fau - Silveira AB, Silveira Ab Fau - Cardoso BA, Cardoso Ba Fau - Sarmento LM et al. Oncogenic IL7R gain-of-function mutations in childhood T-cell acute lymphoblastic leukemia.
Zeng H, Xu W. 2015. Ctr9, a key subunit of PAFc, affects global estrogen signaling and drives ERalpha-positive breast tumorigenesis. *Genes Dev* **29**: 2153-2167.
Zentner GE, Tesar PJ, Scacheri PC. 2011. Epigenetic signatures distinguish multiple classes of enhancers with distinct cellular functions. *Genome Res* **21**: 1273-1283.
Zhang J, Ding L, Holmfeldt L, Wu G, Heatley SL, Payne-Turner D, Easton J, Chen X, Wang J, Rusch M. 2012. The genetic basis of early T-cell precursor acute lymphoblastic leukaemia. *Nature* **481**: 157-163.
Zheng JIE. 2012. Energy metabolism of cancer: Glycolysis versus oxidative phosphorylation. *Oncology letters* **4**: 1151-1157.
Zheng R, Li M, Wang S, Liu Y. Advances of target therapy on NOTCH1 signaling pathway in T-cell acute lymphoblastic leukemia.

Zhi X, Giroux-Leprieur E, Wislez M, Hu M, Zhang Y, Shi H, Du K, Wang L. 2015. Human RNA polymerase II associated factor 1 complex promotes tumorigenesis by activating c-MYC transcription in non-small cell lung cancer. *Biochem Biophys Res Commun* **465**: 685-690.

Zorova LD, Popkov VA, Plotnikov EY, Silachev DN, Pevzner IB, Jankauskas SS, Babenko VA, Zorov SD, Balakireva AV, Juhaszova M et al. Mitochondrial membrane potential.

Zuber J, Shi J, Wang E, Rappaport AR, Herrmann H, Sison EA, Magoon D, Qi J, Blatt K, Wunderlich M. 2011. RNAi screen identifies Brd4 as a therapeutic target in acute myeloid leukaemia. *Nature* **478**: 524-528.